UZJMCS

Tashkent State Transport University

Uzbekistan Journal of Mathematics and Computer Science

ujmcs.tstu.uz

2025

Volume: 1

Issue: 1

Online ISSN: 3093-8619

Print ISSN: 3093-8589

Tashkent 2025

TASHKENT STATE TRANSPORT UNIVERSITY

Uzbekistan Journal of Mathematics and Computer Science

2025
Volume: 1
Issue: 1

Online ISSN: 3093-8619
Print ISSN: 3093-8589

ujmcs.tstu.uz

Tashkent State Transport University
Uzbekistan Journal of Mathematics and Computer Science

Volume 1, Issue 1 May, 2025

Uzbekistan Journal of Mathematics and Computer Science is a prestigious publication established by Tashkent State Transport University (TSTU). The journal focuses on mathematics, computer sciences, and physics, and aims to disseminate cutting-edge research and applied studies in the field of transport and related fields. Located at 1 Temiryolchilar street, TSTU Printing House, Tashkent, Uzbekistan, 100167, the journal operates as a dynamic platform for both national and international academic and professional communities. Submissions and inquiries can be sent to the editorial team at ujmcs.tstu.uz.

Uzbekistan Journal of Mathematics and Computer Science publishes pioneering scientific and applied research conducted by universities, higher education institutions, research centers, and institutes in the fields of mathematics and computer science, both within the Republic of Uzbekistan and internationally. This journal serves as a vital platform for sharing primary scientific results from doctoral dissertations, including Doctor of Philosophy (PhD) and Doctor of Science (DSc) in the physics, mathematics, and computer sciences.

The journal is published twice a year and provides a wide range of high-quality research articles in various fields. These fields include, but are not limited to:

- Algebra
- Analysis
- Functional analysis and operator theory
- Geometry
- Topology
- Differential equations
- Mathematical physics
- Integral equations
- Combinatorics
- Probability theory
- Financial Mathematics
- Econometrics
- Numerical analysis
- Applied mathematics
- Mathematical and computer modeling
- Computational and discrete mathematics
- Dynamical systems
- Mathematical statistics
- Artificial intelligence
- Information Security
- Computational linguistics
- Information technologies in education
- Computational sciences and high-performance computing
- Cryptology
- Computer graphics
- Database
- Theory of algorithms
- Computer programming
- Information security
- Programming languages and compilers
- Applied Computer Science
- Computer networks
- Software development and programming

Articles are published in three languages: Russian and English, ensuring wide accessibility and facilitating cross-cultural academic exchange. **Uzbekistan Journal of Mathematics and Computer Science**, a leading publication in its field, continues to be an essential platform for sharing knowledge.

Editorial Team

Hayotov Abdullo	Computational mathematics	a.hayotov@centralasian.uz	Uzbekistan
Aripov Mirsaid	Ordinary differential equations	mirsaidaripov@mail.ru	Uzbekistan
Chilin Vladimir	Functional analysis, noncommutative integration, operator theory, theory Banach-Kantorovich space	vladimirchilin@gmail.com	Uzbekistan
Rakhmonov Zafar	Mathematical modeling, numerical methods	zraxmonov@inbox.ru	Uzbekistan
Sharipov Olimjon	Probability theory and mathematical statistics	osharipov@mail.ru	Uzbekistan
Raimova Gulnora	Probability Theory and Mathematical Statistics, Quantitative Methods in Economics, Econometrics, Financial Mathematics, Systems Analysis, Decision Making in Management	raimova27@gmail.com	Uzbekistan
Sharipov Anvarjon	Geometry and topology	asharipov@inbox.ru	Uzbekistan
Ashurov Ravshan	Mathematical Analysis, Differential Equations, Mathematical Physics	ashurovr@gmail.com	Uzbekistan
Karimov Erkin	Partial differential equations, Special functions, Direct and inverse problems	erkinjon@gmail.com	Uzbekistan
Alimov Akrom	Functional analysis. (Operator algebras and their differentiation)	alimovakrom63@yandex.ru	Uzbekistan
Azimov Jahongir	Theory of branching random processes, stochastic models with a discrete set of states, asymptotic analysis of statistical estimates	azimovjb@gmail.com	Uzbekistan
Isanov Rovshanbek	Inverse problems of equations of mathematical physics	diyora.isanova.97@bk.ru	Uzbekistan
Kasimov Shuxrat	Fuel balance of energy, solid fuels	shuxrat1812@mail.ru	Uzbekistan

Kendjaev Ravshan	Probability theory, mathematical statistics	lovsan63@mail.ru	Uzbekistan
Sharipova Lola	Probability theory, partial differential equations	lolaxon@gmail.com	Uzbekistan
Tuychiyeva Sayyora	Mathematical modeling of dynamic problems of porous media, Mathematical analysis	sayyora-tohirzoda@mail.ru	Uzbekistan
Yusupov Farrux	Dynamic systems, graph theory, problems of mathematical biology, genetics, epidemiology and ecology	farrukhyusupovchambil@mail.ru	Uzbekistan
International editors			
Aleksey Tujilin	Differential geometry, calculus of variations, graph theory and combinatorics	alexey.tuzhilin@yahoo.com	Russian Federation
Josef Mikeš	Riemannian geometry, geodesic mappings, holomorphically projective mappings, F-planar mappings	josef.mikes@upol.cz	Czech Republic
Umar Islambekov	Statistics, Machine Learning, Applied Topology, Data Science	yagol@physics.msu.ri	Russian Federation
Марат Гаязович Юмагулов	Differential equations, nonlinear oscillations, bifurcations	yum_mg@mail.ru	Russian Federation
Юрий Степанович Волков	Approximation theory, splines, numerical analysis	volkov@math.nsc.ru	Russian Federation
Fedor Sukochev	Theory noncommutative symmetric spaces, operator theory	f.sukochev@unsw.edu.au	Australia
Tursun Yuldashev	Differential equations, computational mathematics, approximation methods of optimal control	tursun.k.yuldashev@gmail.com	Kyrgyzstan
Alexander Katz	Functional analysis, operator theory	katza@stjohns.edu	USA

Semyon Litvinov	Theory noncommutative symmetric spaces, operator theory	snl2@psu.edu	USA
Nurlan Temirbekov	Computational mathematics, mathematical modeling	temirbekov@rambler.ru	Kazakhstan
Farrukh Mukhamedov	Operator algebras, Functional analysis, Dynamical systems	farrukh.m@uaeu.ac.ae	UAE
Allaberen Ashyralyev	Delay differential equations, numerical functional analysis, stochastic differential equations	aallaberen@gmail.com	Turkey
Dilmurat Azimov	Trajectory optimization, guidance, navigation and control, analytical methods of integration	azimov@hawaii.edu	USA

CONTENTS

Uzbekistan Journal of Mathematics and Computer Science
Volume 1 No. 1 Page 1–14 (2025)
DOI: https://doi.org/10.56143/ujmcs.v1i1.2
Research article

Generalized Models of the Seir Epidemiological Model and Their Discrete Analogues

Eshmamatova D.B.* Tadzhieva M.A. and Zavgorodneva S.Yu.

Abstract

The paper considers a discrete analogue of the $SEIR$ model, which, unlike SIR, includes a group of infected individuals in the incubation (latent) period. This model is based on Lotka-Volterra mappings operating in a three-dimensional simplex with degenerate skew-symmetric matrices, which correspond to mixed graphs. The models considered in this paper are intended to study the course of viral diseases transmitted by the air-capillary route without a repeated effect.

Keywords: *The SEIR model; Lotka-Volterra mapping; simplex; graph; trajectory; skew-symmetric matrix; viral diseases.*

AMS Subject Classification (2020): *Primary: 37B25 ; Secondary: 37C25; 37C27.*

1. Introduction

The history of widespread diseases that have engulfed peoples for many centuries is not only the history of innumerable disasters and severe social upheavals, accompanied by a huge number of victims carried away by these diseases, but it is also the history of the hard work of human thought, striving to know the essence of the phenomena occurring at the same time and to find measures to combat them. The scientific study of any phenomenon presupposes at least its description and explanation. The first descriptions of epidemics are given in historical writings. Among them, descriptions of the first historically proven plague (the Justinian plague, 527-565), epidemics of the plague of the XIV century (the "black death") and later times have been preserved. In the VI century A.D., an epidemic of plague and, probably, other contagious diseases, which began in the reign of Justinian, raged for 62 years. This was facilitated by strong earthquakes and volcanic eruptions and the famine and other disasters that accompanied them. According to historians, the plague epidemic shook the withering Byzantine Empire more than anything else. During the plague pandemic in the XIV century . In Europe, about 25 million people died from the plague, that is, a quarter of the entire population.

At the end of the XVII - beginning of the XVIII century. In Europe, more than 10 million people were sick with smallpox every year and about 1.5 million died from this disease alone. There are numerous historical descriptions of epidemics of syphilis, smallpox (rash diseases), typhoid fevers, cholera. It should be recognized that only smallpox, leprosy and plague have a history that almost coincides with the history of human culture, and the history of other infectious diseases is the history of three or four centuries at best, and for most a little more than 100 years. Naturally, epidemics of various contagious diseases, which often covered ancient cities and countries and often assumed the dimensions of widespread disasters, provided extensive material for observations on the conditions of their spread. This already in ancient times allowed us to draw many reasonable empirical conclusions [1]. In the writings of Hippocrates (460-377 BC), there are already

Received : *05–janvuary–2025,* ***Accepted :*** *15–february–2025*
**** Corresponding author***

generalizations regarding the signs of epidemics ("Seven Books on Epidemics"). The largest physician of ancient antiquity after Hippocrates, Claudius Galen (about 138-201) wrote that the most dangerous diseases are called pestilence. As we can see, despite the fact that the science of the epidemic originated a very long time ago, mathematical analysis about the study of diseases and their spread is about 350 years old. Modeling of infectious diseases is a tool that has been used to study the mechanisms of disease spread, predict the future development of the outbreak and evaluate strategies to combat the epidemic [2]. The first statistical studies of infectious diseases were made by John Graunt. In 1662, J. Graunt published the book "Natural and Political Observations on the Lists of the Dead" (Natural and Political Observations Made upon the Bills of Mortal), which is devoted mainly to statistics on social hygiene and statistics of diseases. The accounts he studied were lists of numbers and causes of death published weekly. Graunt's analysis of the causes of death is considered the beginning of the "theory of competing risks", which, according to Daly and Ghani [2] is "a theory that is now firmly entrenched among modern epidemiologists."

A hundred years later, in 1760, Daniel Bernoulli used mathematical methods to analyze smallpox mortality [3]. Bernoulli argued that inoculation with a live virus would reduce the mortality rate and, consequently, increase the population, regardless of the fact that the inoculation itself could be fatal. D. Bernoulli created a mathematical model to protect the practice of inoculation against smallpox [3]. Calculations based on this model have shown that universal vaccination against smallpox will increase life expectancy from 26 years 7 months to 29 years 9 months [3]. At the beginning of the 20th century, William Hamer [4] and Ronald Ross [5] applied the law of mass actions to explain epidemic behavior. In the 20s of the last century, Kermak-McKendrick (1927), as well as Reed-Frost (1928), considered epidemiological models that describe the relationship between susceptible, infected and recovered people in the population. The Kermak-McKendrick epidemic model successfully predicted the behavior of outbreaks very similar to those observed in many recorded epidemics [10].

2. Main Part

Consider a discrete analogue of the SEIR model, which, unlike the SIR model, includes a group of infected individuals in the incubation (latent) period, this group is denoted by E.

Let the quadratic stochastic Lotka-Volterra operator have the form:

$$x_k^{(n+1)} = x_k^{(n)} \left(1 + \sum_{i=1}^{m} a_{ki} x_i^{(n)}\right), \ k = \overline{1,m}, \tag{2.1}$$

moreover, the coefficients of this system satisfy the following conditions:

$$a_{ki} = -a_{ik}, \ |a_{ki}| \leq 1. \tag{2.2}$$

This mapping displays the $(m-1)$-dimensional simplex

$$S^{m-1} = \left\{ x = (x_1, ..., x_m) : \ x_i \geq 0; \ \sum_{i=1}^{m} x_i = 1 \right\} \tag{2.3}$$

into itself. Note that from (2.1) equality, that there is a one-to-one correspondence between the Lotka-Volterra operators and skew-symmetric matrices with coefficients satisfying the conditions (2.2).

Often, in the problems of population genetics and epidemiological models, there is an interest in degenerate cases that more accurately correspond to the real situation.

Therefore, we will give the necessary definitions for the further presentation of our work.

Definition 2.1 A skew-symmetric matrix is called degenerate if some coefficients of the matrix are equal to zero, i.e. $a_{ki} = 0$.

In cases where the skew-symmetric matrix is non-degenerate, we can introduce the concept of a tournament ([6],[7],[11],[12]) but since we are considering Lotka-Volterra maps with a degenerate skew-symmetric matrix, we will introduce the concept of a mixed graph. To do this, we give classical definitions from graph theory [9]:

Definition 2.2. A directed graph or digraph is a finite nonempty set of vertices and of the given set of ordered pairs of different vertices.

The definition implies that every orientation of a graph generates a directed graph.

From the name, one can understand that a mixed graph is a graph that contains both oriented and undirected edges.

Definition 2.3. An undirected graph is a graph that does not have oriented edges, and, generally speaking, it can be considered as a mixed graph. The digraph can be considered as a mixed graph, in which each symmetric pair of oriented edges is replaced by an undirected edge.

Choose an arbitrary interior point from the simplex: $x^0 \in S^{m-1}$. If $x^0 \in S^{m-1}$, then the sequence $\{x^{(n)}\} \subset S^{m-1}$, defined by the recurrent formula $x^{(n+1)} = Vx^{(n)}$, $n = 0, 1, ...$, is called a trajectory starting from the point x^0.

Let $\omega(x^0) = \{x^0, x^{(1)}, ...\}'$ the set of limit points of a given trajectory. Obviously, $\omega(x^0)$ is a nonempty closed and invariant subset of S^{m-1}, i.e. $V(\omega(x^0)) \subset \omega(x^0)$.

We know from [8] that the Lotka-Volterra mapping V is always a homeomorphism of the simplex S^{m-1}.

Since V is a homeomorphism for $|a_{ki}| \leq 1$, for any internal point of the simplex $x^0 \in S^{m-1}$, there is a negative trajectory

$$x^{(-n-1)} = V^{-1}(x^{(-n)}),\ n = 0, 1, ...$$

We donate by $\alpha(x^0) = \{x^0, x^{-1}, ..., x^{-n}, ..., \}'$ the set of limit points of the negative trajectories.

An arbitrary point of the simplex determines the state of the individual in which it is located, and its positive trajectory determines the course of the disease. The meaning of the negative trajectory is to describe the individual's medical history.

To determine the location of the set of negative trajectory $\alpha(x^0)$ and the set of positive trajectory $\omega(x^0)$, we give a theorem from [8]:

Theorem 2.4. If A is a skew-symmetric matrix, then the sets of solutions of linear inequality systems

$$P = \{x \in S^{m-1} : Ax \geq 0\} \text{ and } Q = \{x \in S^{m-1} : Ax \leq 0\}$$

are convex nonempty polyhedra.

The set P corresponds to $\alpha(x^0)$ – negative trajectory, and the set Q corresponds to $\omega(x^0)$ – positive trajectory. The epidemiological meaning of these sets lies in the set of P the epidemic of viral diseases begins, i.e. the epidemic flares up in the set of Q, the disease is on the decline.

Let the Lotka-Volterra mapping acting in a three-dimensional simplex have the form:

$$V : \begin{cases} x_1' = x_1(1 - a_{12}x_2 + a_{13}x_3 + a_{14}x_4), \\ x_2' = x_2(1 + a_{21}x_1 + a_{23}x_3 + a_{24}x_4), \\ x_3' = x_3(1 + a_{31}x_1 + a_{32}x_2 + a_{34}x_4), \\ x_4' = x_4(1 + a_{41}x_1 + a_{42}x_2 + a_{43}x_3). \end{cases}$$

where the coefficients a_{ki} satisfy the conditions (2.2).

If the skew-symmetric matrix is in the general position, then as we indicated above we will get the non-degenerate case. For such cases, the concept of a tournament corresponds. But we are interested in degenerate cases of mappings, since they correspond to the course of viral diseases. For degenerate cases, we have introduced the concept of a mixed graph.

The total number of mixed graphs corresponding to Lotka-Volterra mappings operating in the three-dimensional simplex S^3 is 42 cases. Among them, those that describe the course of viral diseases that do not have a repeat effect are four cases. Viral diseases that do not have a repeated effect are measles, chickenpox, rubella, scarlet fever, mumps, whooping cough and others.

Let us move on to the description of these four models (See Figure 1).

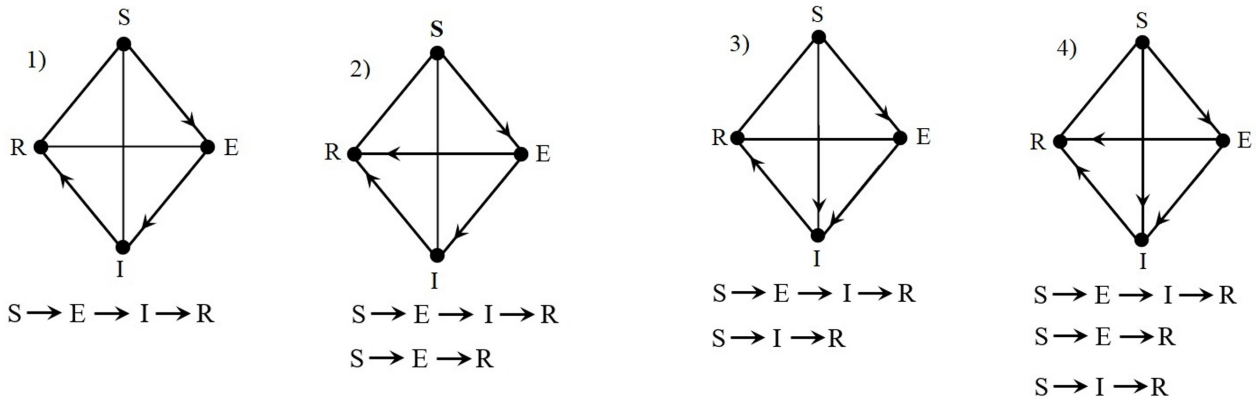

Figure 1. Discrete SEIR models.

Let us turn to the consideration of the first case. Here, as shown in Figure 1, there is only one transition from groups to groups, i.e.

$$V_1 : \begin{cases} S' = S(1 - aE), \\ E' = E(1 + aS - dI), \\ I' = I(1 + dE - fR), \\ R' = R(1 + fI). \end{cases} \tag{2.4}$$

Theorem 2.5. If the course of the disease is described by model 1, then the set P and Q correspond to the following

$$P = \left\{ \frac{d}{a+d} \le S \le 1 \right\} \quad \text{or} \quad P = \left\{ 0 \le I \le \frac{a}{a+d} \right\}$$

$$Q = \left\{ 0 \le E \le \frac{f}{f+d} \right\} \quad \text{or} \quad Q = \left\{ \frac{d}{f+d} \le R \le 1 \right\}.$$

The meaning of the theorem in epidemiology lies in the fact that an individual passes all stages over time, that is, from a susceptible class to a latent one, from a latent to an open form of the disease, and only then recovers.This path is typical for diseases such as chicken pox, the incubation period of which is 3-5 days, at this stage it is not possible to identify the disease, with scarlet fever it ranges from 1 to 12 days, more often 2-7 days. The incubation period for measles (the period when a person is contagious to others, but does not have symptoms of the disease) averages 9-11 days, the maximum incubation period is 21 days, the signs of the disease appear gradually, not immediately. There is a very long incubation period for mumps, the time from infection to the onset of the first symptoms, which usually takes 12 to 19 days.

Now let us move on to the case describing diseases that pass from the susceptible to the latent and then recover. One of the features of infectious diseases is the presence of an incubation period, that is, the period from the time of infection to the appearance of the first signs. The duration of this period depends on the method of infection and the type of pathogen and can last from several hours to several years (the latter is rare). This model also includes a generalized complete transition of individuals from each category. As an

example of such viral diseases, we can cite COVID-19. Despite all the epidemic danger, most patients suffer from coronavirus infection in a mild form, that is, they recover from a latent period when the disease does not manifest itself clearly. At the moment, it is recorded that the mild form (there is no viral pneumonia or pneumonia passes in mild form) is 81 percent of cases.

$$V_2 : \begin{cases} S' = S(1 - aE), \\ E' = E(1 + aS - dI - eR), \\ I' = I(1 + dE - fR), \\ R' = R(1 + eE + fI). \end{cases} \tag{2.5}$$

Theorem 2.6. If the epidemiological model describes diseases in which there are two transitions

$$S \to E \to R$$

$$S \to E \to I \to R$$

then the following conditions are met for each of them:

1) $S \to E \to R$ This transition corresponds to those individuals for whom the disease does not show itself clearly, i.e., the individual is in the latent period (the disease passes in a mild form), the situation occurs on the edge Γ_{SER} of the graph. Then there is a neutral point $N_1(\frac{e}{a+e}, 0, \frac{a}{a+e})$ on the edge of Γ_{SR}. Then we get

$$P = \left\{ \frac{e}{a+e} \le S \le 1 \right\} \text{ or } P = \left\{ 0 \le R \le \frac{a}{a+e} \right\}$$

$$Q = \left\{ 0 \le S \le \frac{e}{a+e} \right\} \text{ or } Q = \left\{ \frac{a}{a+e} \le R \le 1 \right\}.$$

If the starting point lies to the left of the curve connecting the vertex E and the neutral point N_1, then the disease progresses, but up to a certain time, and as soon as the trajectory crosses this curve, then the epidemic is on the decline in the set Q.

2) $S \to E \to I \to R$. This situation occurs for those individuals who completely go through all stages of the disease. Here the picture corresponds to the entire graph, the onset of the disease on the edge Γ_{SI}

$$P = \left\{ \frac{d}{a+d} \le S \le 1 \right\} \text{ or } P = \left\{ 0 \le I \le \frac{a}{a+d} \right\}$$

the end of the disease on the edge

$$Q = \left\{ 0 \le S \le \frac{e}{a+e} \right\} \text{ or } Q = \left\{ \frac{a}{a+e} \le R \le 1 \right\}.$$

Let us move on to the third model, it describes diseases that either immediately show themselves clearly, ignoring the latent period, or go from latent to open form and only then go to recovery. As the situation around the world has shown since November 2019, this is an infection called COVID-19. In most cases, as the COVID-19 clinic shows, individuals who have chronic diseases, the disease progresses immediately, affecting the vulnerable organs of the patient.

$$V_3 : \begin{cases} S' = S(1 - aE - bI), \\ E' = E(1 + aS - dI), \\ I' = I(1 + bS + dE - fR), \\ R' = R(1 + fI). \end{cases} \tag{2.6}$$

Theorem 2.7. If the epidemiological model describes diseases in which there are the following transitions

$$S \to I \to R,$$

$$S \to E \to I \to R,$$

then the following conditions are met for each of them:

1) $S \to I \to R$

In this transition, the disease progresses immediately, the situation occurs on the edge Γ_{SIR} of the graph. Then there is a neutral point $N_2(\frac{f}{b+f}, 0, \frac{b}{b+f})$ on the edge of Γ_{SR}. Then we get

$$P = \left\{ \frac{f}{b+f} \le S \le 1 \right\} \quad \text{or} \quad P = \left\{ 0 \le R \le \frac{b}{b+f} \right\}$$

$$Q = \left\{ 0 \le S \le \frac{b}{b+f} \right\} \quad \text{or} \quad Q = \left\{ \frac{f}{b+f} \le R \le 1 \right\}.$$

If the starting point lies to the left of the curve connecting the vertex I and the neutral point N_2, then the disease progresses, but up to a certain time, and as soon as the trajectory crosses this curve, then the epidemic is on the decline in the set Q.

2) $S \to E \to I \to R$. This situation occurs for those individuals who completely go through all stages of the disease. Here the picture corresponds to the entire graph, the onset of the disease on the edge Γ_{SR}.

$$P = \left\{ \frac{f}{b+f} \le S \le 1 \right\} \quad \text{or} \quad P = \left\{ 0 \le R \le \frac{b}{b+f} \right\}$$

the end of the disease on the edge Γ_{RE}.

$$Q = \left\{ 0 \le E \le \frac{f}{f+d} \right\} \quad \text{or} \quad Q = \left\{ \frac{d}{d+f} \le R \le 1 \right\}.$$

Finally, let us move on to the last model, which includes all three possible transitions, and for this model we obtain the following theorem:

In the model, there are three transitions from a state to a state of individuals in the population:

$$V_4 : \begin{cases} S' = S(1 - aE - bI), \\ E' = E(1 + aS - dI - eR), \\ I' = I(1 + bS + dE - fR), \\ R' = R(1 + eE + fI). \end{cases} \tag{2.7}$$

1) $S \to E \to R$; 2) $S \to I \to R$; 3) $S \to E \to I \to R$.

Theorem 2.8. If there are three transitions in the epidemiological situation

$$1) S \to E \to R,\ 2) S \to I \to R,\ 3) S \to E \to I \to R.$$

then the following conditions are satisfied for each of them:

1) $S \to I \to R$;

This corresponds to the situation on the verge Γ_{SIR}. Here there is a neutral point $N_1(\frac{f}{f+b}, 0, \frac{b}{f+b})$ on the edge Γ_{SR}, then we get

$$P = \left\{ \frac{f}{f+b} \le S \le 1 \right\} \text{ and } Q = \left\{ 0 \le S \le \frac{f}{f+b} \right\},$$

or

$$P = \left\{0 \le R \le \frac{b}{f+b}\right\} \text{ and } Q = \left\{\frac{b}{f+b} \le R \le 1\right\},$$

If the starting point lies to the left of the curve connecting the vertex I and the neutral point N_1, then the disease progresses, but up to a certain time, and as soon as the trajectory crosses this curve, then the epidemic is on the decline in the set Q.

2) $S \to E \to R$;

This transition corresponds to those individuals, for which the disease does not manifest itself explicitly, i.e., this situation is on the face Γ_{SER}. Then on the same edge Γ_{SR}, there is a neutral point $N_2\left(\frac{e}{a+e}; 0; \frac{a}{a+e}\right)$. At the same time, either

$$P = \left\{\frac{e}{a+e} \le S \le 1\right\} \text{ and } Q = \left\{0 \le S \le \frac{e}{a+e}\right\},$$

or

$$P = \left\{0 \le R \le \frac{a}{a+e}\right\} \text{ and } Q = \left\{\frac{a}{a+e} \le R \le 1\right\},$$

If the starting point lies to the left of the curve (straight line) connecting the vertex E and neutral point N_2, then the disease progresses, but up to a certain time, and as soon as the trajectory crosses this curve, then the epidemic is on the decline in the set Q.

3) $S \to E \to I \to R$. This situation occurs for those individuals who completely go through all stages of the disease.

If $eb < af$, then

$$P = \left\{\frac{f}{f+b} \le S \le 1\right\} \text{ and } Q = \left\{0 \le S \le \frac{e}{a+e}\right\},$$

or

$$P = \left\{0 \le R \le \frac{b}{f+b}\right\} \text{ and } Q = \left\{\frac{a}{a+e} \le R \le 1\right\}.$$

If $eb > af$, then

$$P = \left\{\frac{e}{a+e} \le S \le 1\right\} \text{ and } Q = \left\{0 \le S \le \frac{f}{f+b}\right\},$$

or

$$P = \left\{0 \le R \le \frac{a}{a+e}\right\} \text{ and } Q = \left\{\frac{b}{f+b} \le R \le 1\right\}.$$

Corollary 1. If the epidemiological situation is described by a discrete dynamic system (3), then for any transition from a group to a group (i.e., for any course of the disease), the disease begins and ends at the edge Γ_{SR}. The boundaries of the beginning and end of the disease depend on the coefficients of transition a, b, e, f from groups to groups. The boundaries of the beginning and end of the disease depend on the coefficients of transition from groups to groups S, E, I, R.

Theorem 2.9 The set of limit points of the positive trajectory $\omega^+(x^0) \subset Q$ and the set of limit points of the negative trajectory $\omega^-(x^0) \subset P$. That is, the medical history begins in the set P, and ends in the set Q.

In other words, any trajectory in this case converges for an arbitrary initial point but converges to a point belonging to the set Q, and the whole situation depends on the initial point.

Theorems 2.5 - 2.9 are proved using Theorem 2.4.

3. Numerical analysis

In order to verify the compliance of the mathematical description of the above-analyzed models, for diseases transmitted by the air-capillary route, we have compiled a package of application programs in the Python

programming language 10. For each model, in accordance with the numerical analysis of the data, a phase portrait of the course of the disease was obtained.

For the first model described by mapping V_1 (see Figure 1, Example 1), as well as, according to the Theorem 2.5, the location of individuals and the phase portrait looks as follows:

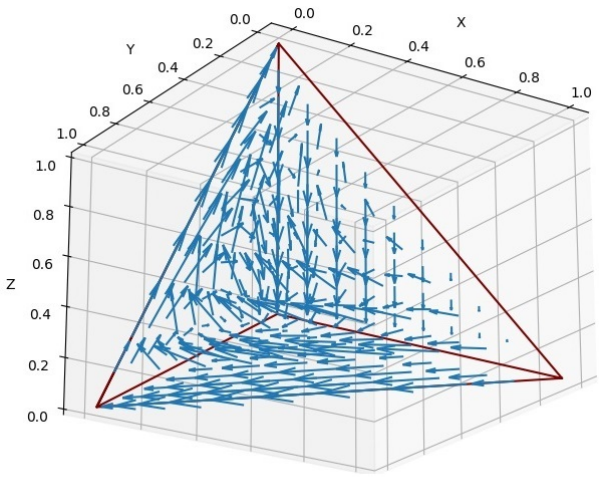

Figure 2. Phase portrait of trajectories of internal mapping points V_1.

The trajectory of the inner points of the first model is shown in Table 1.

$S^{(i)}$	$E^{(i)}$	$I^{(i)}$	$R^{(i)}$
0.7	**0.1**	**0.1**	**0.1**
0.6300000000000001	0.16000000000000003	0.1	0.11000000000000001
0.5292000000000001	0.24480000000000005	0.10500000000000001	0.12100000000000002
0.3996518400000001	0.3486441600000001	0.11799900000000002	0.13370500000000002
0.2603155599507456	0.4468407778134146	0.14336160594084005	0.14948205629500003
0.1439959526654199	0.4991005735915551 3	0.18599142979823496	0.1709120439447903
0.07212749009524641	0.4781406068663161	0.24703168367061717	0.20270021936782062
0.03764040820936109	0.39451180960672466	0.3150741863452577	0.25277359583865683
0.01629405005874072 5	0.18901208182541437	0.34269707426417556	0.4519967938516696
0.013214277735770625	0.12731796670623402	0.25257298287657115	0.6068947726814244
0.011531862762960851	0.0968433030542703	0.1314448384729987	0.7601799957097704
0.010415079082627178	0.08523053440744374	0.044252654053683324	0.860101732456246
0.009527396326519074	0.08234653980960868	0.009962546990266543	0.898163516873606
0.008742848205635452	0.08231070665815321	0.001834932020809267	0.9071115131154023
0.008023218191624631	0.08287930212086154	0.0003214786102515538	0.9087760010772625
0.007358259467139381	0.08351761692248237	5.5970487259704123e-05	0.9090681531231187

Table 1. The trajectory of internal points in the entire simplex for mapping V_1.

Let us move on to the second model described by the mapping V_2 (see Figure 1, Example 2), and also, according to Theorem 2.6, the location of individuals and the phase portrait describes Figure 3.

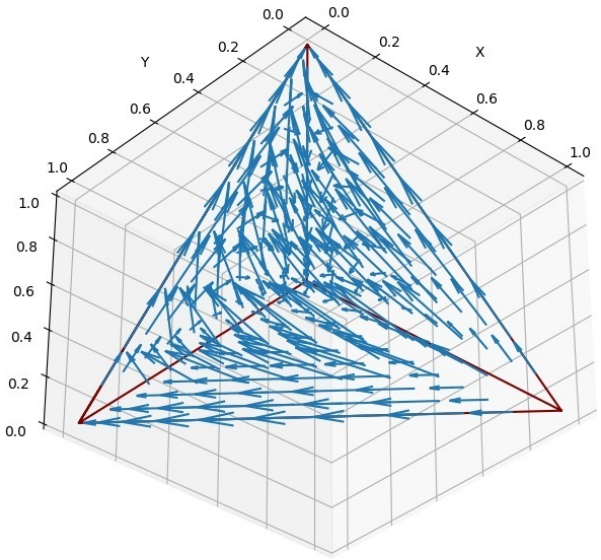

Figure 3. Phase portrait of trajectories of internal mapping points V_2.

The values of the complete transition of individuals from groups to groups $S \to E \to I \to R$ are given in Table 2 (mapping V_2).

$S^{(t)}$	$E^{(t)}$	$I^{(t)}$	$R^{(t)}$
0.7	**0.1**	**0.1**	**0.1**
0.6300000000000001	0.15000000000000002	0.1	0.12000000000000002
0.5355000000000001	0.21150000000000002	0.10299999999999998	0.15000000000000002
0.4222417500000001	0.2712487500000001	0.10933449999999999	0.19717500000000002
0.3077092031146875	0.3026409781471876	0.11743331641937498	0.27221650231875
0.21458378889916688	0.2778423900849278	0.1210061635162295	0.3865676574996759
0.15496331611794276	0.19643733929055335	0 0.10784973602909471	0 0.5407496085624093
0.12452273461209315	0.09946879127925114	0.07071574867654648	0.7052927254321093
0.11213660871344128	0.03466629223585898	0.027874455606756318	0.8253226434439435
0.10824924826544295	0.008976472713378626	0.005835340244806634	0.8769389387763717
0.10727755184214445	0.002023969908971026	0.0007704839356076375	0.8899279943132767
0.10706042530530788	0.0004383495278655796 3	8.6368148442748 22e-05	0.8924148570183837
0.107013495418422 2	9.405192407991973e-05	9.329789036363018e-06	0.8928831228684613
0.10700343059327558	2.0138496057663705e-05	1.0002553504814046e-06	0.8929754306553161

Table 2. Transition values of individuals S→E→I→R

In Table 3, we present the trajectory of the inner points on the SER face, that is, the transition $S \to E \to R$.

$S^{(t)}$	$E^{(t)}$	$I^{(t)}$	$R^{(t)}$
0.7	**0.2**	**0.0**	**0.1**
0.56	0.32000000000000006	0.0	0.12
0.3808	0.4608000000000001	0.0	0.1584
0.20532736	0.5632819200000001	0.0	0.23139072000000002
0.08967017043066877	0.548600900537549	0.0	0.36172892903178244
0.04047703418104839	0.3993492205698504	0.0	0.5601737452491015
0.024312562129867522	0.19180874407210863	0.0	0.783878693798024
0.019649200122562525	0.04611731831712962	0.0	0.9342334815603079
0.018743031705833326	0.0039391438822218 53	0.0	0.97731782441 1945
0.018669200207155002	0.0001631798518814918	0.0	0.9811676199409637
0.01866615376983045	6.119502313158958e-06	0.0	0.9813277267278566
0.018666039542259278	2.2849259065307614e-07	0.0	0.9813337319651503
0.018666035277207546	8.530155673351109e-09	0.0	0.981333956192637
0.018666035117983 36	3.184484462012411e-10	0.0	0.9813339645635684
0.018666035112039188	1.1888339861528531e-11	0.0	0.9813339648760726
0.01866603511181728	4.438163386996236e-13	0.0	0.9813339648877389

Table 3. The trajectory of the inner points, on the SER edge, that is, the transition S→E→R.

As we pointed out above, the third model describes diseases that either immediately manifest themselves vividly, ignoring the latent period, or move from a hidden form to an open one and only then proceed to recovery. For such a course of the disease, the phase portrait is shown in Figure 3, the numerical analysis of the transition $S \to I \to R$ in Table 4, and the complete transition $S \to E \to I \to R$ in Table 5.

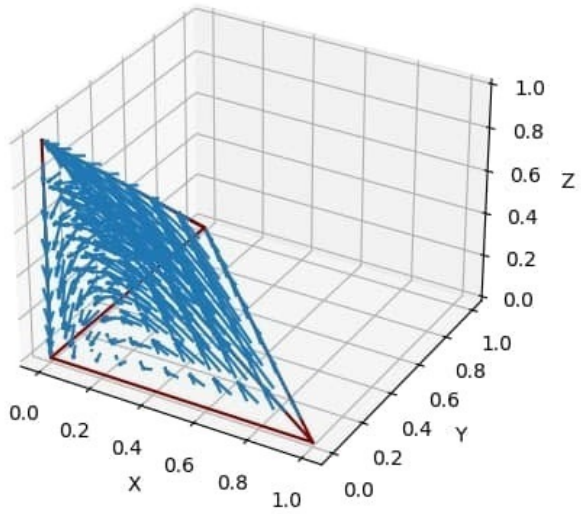

Figure 4. Phase portrait of trajectories of internal mapping points V3.

$S^{(t)}$	$E^{(t)}$	$I^{(t)}$	$R^{(t)}$
0.7	**0.0**	**0.2**	**0.1**
0.56	0.0	0.32000000000000006	0.11000000000000001
0.3808	0.0	0.4640000000000001	0.12210000000000003
0.20410879999999998	0.0	0.5840368	0.13700841000000005
0.08490174959615998	0.0	0.623225897054352	0.15577971441072816
0.0319887805426092	0.0	0.579052913851406	0.1800470338326162
0.013465583958858184	0.0	0.49331935086407785	0.21246396822453942
0.006822750821268525	0.0	0.3951495971151317	0.25760490601825753
0.004126743583027333 4	0.0	0.296053129525377 1	0.3239651936229328
0.002905008230523 3237	0.0	0.20136395544851707	0.42891864030207716

Table 4. Trajectories of internal points of the operator V3, on the SIR edge.

$S^{(t)}$	$E^{(t)}$	$I^{(t)}$	$R^{(t)}$
0.6	**0.2**	**0.1**	**0.1**
0.4200000000000001	0.30000000000000004	0.17	0.11000000000000001
0.22260000000000002	0.3750000000000001	0.27370000000000005	0.12210000000000003
0.07819937999999997	0.35583750000000003	0.40384435	0.13700841000000005
0.01879273033274699	0.2399608079876 2504	0.5237976193986446	0.15577971441072816
0.0044396241675139034	0.11877942676967133	0.5777350632228913	0.1800470338326162
0.0013473616047193016	0.05068372314900657	0.5449035449319701	0.21246396822453942
0.0005448901874473319	0.02313427203731753	0.4574830980050661	0.25760490601825753
0.00028300649859449374	0.012563339233420406	0.3504660240312798	0.323965193622 9328
0.0001802668296099624	0.008163871190374476	0.24142943840975728	0.42891864030207716
0.0001352734349964888 8	0.006194344028809603	0.13989037251432845	0.612889840300 6597
0.0001155120535892101 9	0.005328652865331848	0.055038436989306924	0.9885237966444279

Table 5. Trajectories of internal points of the operator V3, in the entire simplex.

Let us move on to the numerical analysis of the latest model, which includes all transitions simultaneously. This model describes those viral diseases, the course of which may be different for each individual. A separate numerical analysis is made for each transition and a phase portrait of the trajectory of internal points is shown. This model corresponds to the V_4 mapping.

For the transition $S \to E \to R$:

$S^{(i)}$	$E^{(i)}$	$I^{(i)}$	$R^{(i)}$
0.1	**0.8**	**0.0**	**0.1**
0.019999999999999997	0.8	0.0	0.18000000000000002
0.003999999999999998	0.672	0.0	0.32400000000000007
0.0013119999999999994	0.45696	0.0	0.5417280000000002
0.0007124684799999997	0.21001150463999987	0.0	0.7892760268800003
0.0005628419025066261	0.044404085236143385	0.0	0.9550330728613502
0.0005378494226932487	0.002021707745285429	0.0	0.9974404428320215
0.0005367620483495925	6.262050894659341e-06	0.0	0.999456975900756
0.0005367586871183274	6.761675811579 46e-09	0.0	0.9994632345512061
0.0005367586834889392	7.258822182944388e-12	0.0	0.9994632413092526
0.0005367586834850429	7.792471729883707e-15	0.0	0.9994632413165075
0.0005367586834850388	8.365353733711145e-18	0.0	0.9994632413165153
0.0005367586834850388	8.980352513983743e-21	0.0	0.9994632413165153
0.0005367586834850388	9.64056438527156e-24	0.0	0.9994632413165153
0.0005367586834850388	1.0349313294978596e-26	0.0	0.9994632413165153
0.0005367586834850388	1.111016755836994e-29	0.0	0.9994632413165153

Table 6. The trajectory of internal points for mapping V_4 on the SER edge.

Phase portrait on this face:

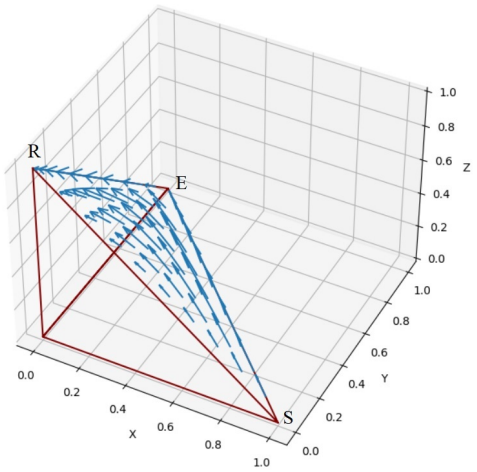

Figure 5. Phase portrait of trajectories of internal V_4 mapping points on the edge Γ_{SER}.

The values of the transition $S \to I \to R$ are shown in Table 7, and the phase portrait on the SIR edge is shown in the Figure 6.

$S^{(i)}$	$E^{(i)}$	$I^{(i)}$	$R^{(i)}$
0.2	**0.0**	**0.4**	**0.4**
0.12	0.0	0.32	0.5599999999999999
0.08159999999999999	0.0	0.17920000000000005	0.7392
0.06697727999999999	0.0	0.06135808	0.87166464
0.06286768269557759	0.0	0.011984008590131197	0.9251483087142912
0.06211427584611215	0.0	0.0016504301608192273	0.9362352939930687
0.06201176057183828	0.0	0.00020775446826347914	0.9377804849598982
0.06199887735149459	0.0	2.5809602606452324e-05	0.9379753130458989
0.06199727185108106	0.0	3.2009989085632098e-06	0.9379995218159832
0.0619970787318915	0.0	3.969166796008565e-07	0.9380025243514288
0.06199705412421687	0.0	4.921550681328109e-08	0.9380028966602761
0.06199705107300043	0.0	6.102435301473628e-09	0.9380029428245641
0.06199705069466743	0.0	7.566660233499998e-10	0.9380029485486663
0.06199705064775637	0.0	9.382212418966837e-11	0.9380029492584213
0.06199705064139666	0.0	1.1633389979336518e-11	0.9380029493464267
0.06199705064121843	0.0	1.442471735508057e-12	0.9380029493573389

Table 7. The trajectory of internal points for mapping V_4 on the SIR edge.

The values of the transition from groups to groups $S \to E \to I \to R$ are given in the Table 8.

The phase portrait of the trajectories of the interior points in the entire simplex of the V_4 mapping is shown in the Figure 7.

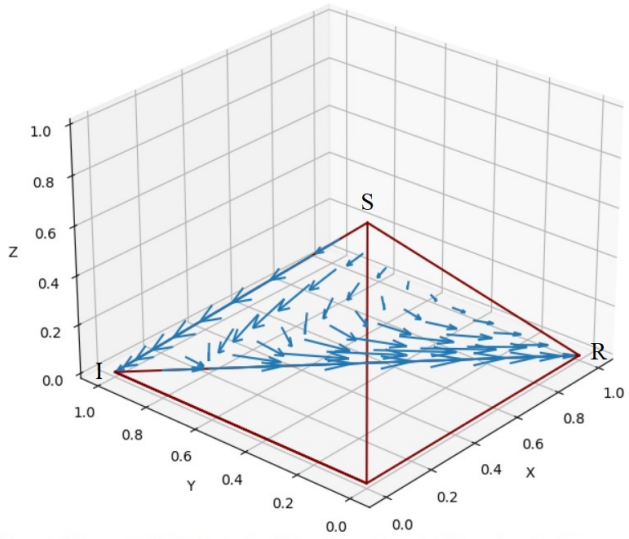

Figure 6. Phase portrait of trajectories of internal mapping points V_4, on the edge Γ_{SIR}.

$S^{(t)}$	$E^{(t)}$	$I^{(t)}$	$R^{(t)}$
0.2	**0.2**	**0.1**	**0.5**
0.14	0.11999999999999998	0.09	0.65
0.11060000000000002	0.047999999999999994	0.0549	0.7865
0.09921926000000002	0.012921600000000004	0.020428290000000005	0.86743085
0.09591030859311862	0.002731110926592001	0.004999007050182902	0.8963595734301064
0.09516891059250494	0.0005313423504363043	0.0010112083747259434	0.9032885386823327
0.09502210772045758	0.0001014168699787353	0.00019456833685570248	0.9046819070727079
0.09499398258225009	1.9283974869098355e-05	3.7053908788534226e-05	0.904949679534092
0.0949886308223112	3.6640950173501116e-06	7.042598817572789e-06	0.9050006624838537
0.09498761380812318	6.961081633941756e-07	1.338034845924733e-06	0.9050103520488675
0.09498742058973257	1.3224379135291078e-07	2.541971275842274e-07	0.9050121929693485
0.09498738388270647	2.5123010747659895e-08	4.829119078925327e-08	0.905012542703092
0.09498737690928352	4.772738763520 33e-09	9.17411251378296e-09	0.9050126091438652
0.0949873755845087	9.066998944191418e-10	1.7428499380453792e-09	0.9050126217659415
0.09498737533283491	1.7225008764935555e-10	3.310974895031178e-10	0.9050126241638174

Table 8. The trajectory of the internal mapping points V_4 throughout the simplex, i.e. the complete transition of individuals from groups to groups.

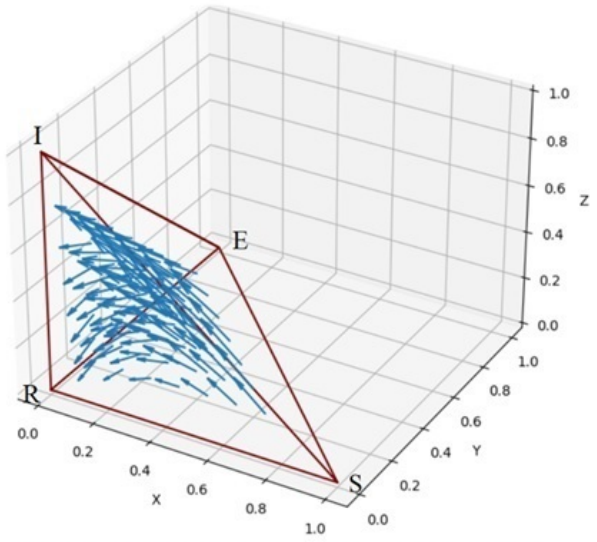

Figure 7. Phase portrait of trajectories of internal mapping points V_4.

4. Conclusion

The paper identifies a class of mixed graphs described by Lotka-Volterra mappings with degenerate skew-symmetric matrices, presented as discrete analogues of the $SEIR$ model of viral diseases transmitted by the air capillary route. If we compare the results of the previously studied continuous models and the discrete models proposed by us, then in the continuous case when an individual becomes ill, either absolutely recovers or dies [4], since the solution of differential equations is either unique or tends to infinity. Finding the set P and Q gives us the opportunity to determine the history of the epidemiological situation and its decline. In other words, the set P corresponds to the history of the disease, i.e. it consists of a set of limit points of the negative trajectory, the set Q corresponds to the end of the epidemiological situation, i.e. the set of limit points of the positive trajectory. In the work, a specific focus of the disease is shown in each model, a numerical analysis is made and a phase portrait is constructed. That is, the initial state of the population is shown, and specifically the end of the epidemiological situation. All these models are designed to study viral diseases that do not have a repeat effect, i.e. an individual who has recovered receives temporary or permanent immunity.

Acknowledgements

We, the authors of the paper Generalized models of the $SEIR$ epidemiological model and their discrete analogues would like to thank the Tashkent State Transport University for the opportunity to publish our work.

References

[1] https://www.hmong.press/wiki/ Mathematical modelling in epidemiology.
[2] Daly, D.J., Ghani, J.: *Epidemic modeling: an introduction. New York: Cambridge University* Press.(2005).
[3] Murray, J.D.: *Mathematical biology. Third Edition.* Springer.p.776. (2009).
[4] Hammer, W.: *Epidemiology is old and new* . London: Kegan Paul. (1928)
[5] Ross, R.: *The prevention of malaria.* New York: Dutton. (2010)
[6] Ganikhodzhaev, R.N.: *Quadratic stochastic operators, Lyapunov function and tournaments*, Acad. Sci. Sb. Math., 76(2), pp.489-506, (1993)
[7] Ganikhodzhaev, R.N., Tadzieva, M.A., Eshmamatova, D.B.: *Dynamical Proporties of Quadratic Homeomorphisms of a Finite-Dimensional Simplex*. Journal of Mathematical Sciences — 245 — (3). — P. — 398-402, (2024)
[8] Ganikhodzhaev, R.N., Eshmamatova, D.B.: *Quadratic automorphisms of a simplex and the asymptotic behavior of their trajectories*. Vladikavkaz. Mat. Zh., Volume 8, Number 2, 12-28, (2006)
[9] Harary, F., Palmer, E.M.: *Graphical enumeration. Academic Press New York and London*. (1973)
[10] Kermack, W.O. and McKendrick, A.G.: *A contribution to the mathematical theory of epidemics*, Proc. R. Soc. Lond, 115, 700-721. (1927)
[11] Eshmamatova, D.B., Ganikhodzhaev, R.N.: *Tournaments of Volterra type transversal operators acting in the simplex* S^{m-1}. AIP Conference Proceedings 2365, 060009, https:doi.org/10.1063/5.0057303. (2021)
[12] Ganikhodzhaev, R.N., Tadzhieva, M.A.: *Stability of fixed points of discrete dynamic systems of Volterra type.* AIP Conference Proceedings, V. 2365. P. 060005-1 – 060005-7. https://doi.org/10.1063/5.0057979. (Scopus. IF=0.7). (2021)
[13] Ganikhodzhaev, R.N.: *A chart of fixed points and Lyapunov functions for a class of discrete dynamical systems*, Math. Notes, 56 (5-6), pp.1125-1131, (1994)
[14] Kuznetsov, Y.A.: *Elements of applied bifurcation theory. Second edition.* NewYork 10027, p 592, (1998)
[15] Murray, Y. D.: *On a necessary condition for the ergodicity of quadratic operators defined on a two-dimensional simplex*, Russ. Marh. Surv 59. 13. p.571-573, (2004)
[16] Ulam, S.: *A collection of mathematical problems.Interscience.* New-York, 150 p.Graph Theory. Addison-Wesley.1969. p.274. (1960)
[17] Volterra, V.: *Theorie mathematique de la lutte pour la vie*. Paris, p.290, (1931)

Affiliations

First Author
Address: Eshmamatova, D.B.: Doctor of physical and mathematical sciences, head of the department of higher mathematics, Tashkent State Transport University, Institute of Mathematics named after V.I. Romanovsky

Academy of Sciences of the Republic of Uzbekistan, Senior Researcher. Tashkent, Uzbekistan.
E-MAIL: 24dil@mail.ru
ORCID ID: 0000-0002-1096-2751

Second Author
Address: Tadzhieva, M.A.: Doctor of physical and mathematical sciences, head of the department of higher mathematics, Tashkent State Transport University, Institute of Mathematics named after V.I. Romanovsky Academy of Sciences of the Republic of Uzbekistan, Senior Researcher. Tashkent, Uzbekistan.
E-MAIL: mohbonut@mail.ru
ORCID ID: 0000-0001-9232-3365

Third Author
Address: Zavgorodneva, S.Yu.: Assistant of the department of higher mathematics, Tashkent State Transport University, Tashkent, Uzbekistan.
E-MAIL: zavgorodnevasveta22@gmail.com
ORCID ID: 0009-0002-7852-7403

Uzbekistan Journal of Mathematics and Computer Science
Volume 1 No. 1 Page 15–19 (2025)
DOI: https://doi.org/10.56143/ujmcs.v1i1.4/
Research article

Mathematical description of the transitional part of the railway line plan

A.Artykbaev*, M.Toshmatova and M.Ergashaliev

Abstract

The most complex part of a railway track plan is its transition curve. The transition curve is the section of the track plan that connects the circular arc portion of the railway layout to the straight section of the track. It serves to provide a smooth transition from the straight section to the circular arc of a given radius. The radius of the circular section is determined based on the angle between the connecting straight segments of the railway. A mathematical model of the railway, depending on the angle and radius of curvature, is provided in [1]. In this article, we determine the optimal method for defining the length of the transition curve. This length is computed under the assumption that the transition section is a clothoid.

Keywords: *Mathematical model, curvature, osculating circle, tangent line, monotonic function, coordinate system, clothoid, arc length.*

AMS Subject Classification (2020): *Primary: 53A17; 53A04; Secondary: 90B20; 93C15; 65D17; 68U07.*

1. Introduction

A railway track plan is a diagram that represents the movement of the center of the railway track. The railway plan consists mainly of straight sections and a curved line that connects two straight segments intersecting at a certain angle. The curved section is often chosen as an arc of a circle.

However, for technical reasons, and to ensure the safety and comfort of train movement during the transition from the straight section to the circular arc, a connecting curve is known as the transition curve is introduced.

1.1. ***Problem Statement***

It is known [1] that a railway consists of straight sections and a curved section that connects two differently directed straight segments. The need for curved sections on the railway is associated with the need to provide an accessible route between two points connected by the railway [2] [3]. Evidently, in straight sections of the railway, the path can be considered as two parallel lines, the distance between which is a constant value equal to the width of the track gauge [4],[5].

The complexity of designing and constructing a railway is primarily associated with the curved section of the track. Even in the simplest case, where both straight sections lie in the same plane and form an angle at the intersection of the directions defined by these tracks, they are connected by a single curve. This curve consists of three parts: the transition section, the arc of a circle with a given radius, and the entry section.

Received : *30–januuary–2025,* ***Accepted :*** *17–february–25*
**** Corresponding author***

In general terms, the entry section connects the straight part of the track to the curved section. Clearly, this section is also itself a curve.

In the previous work [6], we proposed considering the railway as two curves. Specifically, the inner part of the curved section of the track is treated as a planar curve, while the outer part of the track is regarded as a spatial curve [7],[8].

However, it should be noted that even when considering the railway as two parallel curves, both have a transition section. When defining the transition section of the railway plan, two fundamentally important problems arise. First, an analytical function must be chosen that satisfies the geometric requirements of the transition section. Second, the appropriate length of the transition section must be determined.

In this article, we address these two problems in a general formulation. By "general formulation," we mean the following: we consider a circle of a given radius, where its arc forms the main curved section of the railway, while the equation of the transition section is treated as an unknown function with a natural parameter.

Within this framework, we determine the conditions that the analytical formula of the transition curve must satisfy and compute the optimal length of the transition section.

2. Mathematical Description of the Transition Section

Following the principles outlined above, we consider the road as two parallel curves. In the curved section of the road, the inner path is considered a flat curve.

Let there be two straight lines l_1 and l_2 the straight parts of the road describe two lines that touch a point D. From point D, we will set aside the segments $AB = BD$ along the rays l_1, l_2. We consider the curve under study to be part of the junction points on the road A and B.

For the mathematical description of the curve's graph, we introduce the Cartesian coordinate system on the plane in the following way: Through points A and B, we draw a straight line, which we will take as the x-axis. The midpoint of the AB segment is chosen as the origin $O(0,0)$ of the coordinates. We choose the direction of the x-axis and the y-axis so that the rays reflecting the straight section of the road lie in the half-plane $y > 0$ (Figure 1).

With this choice for a circle of the coordinate system, with its center at point $O(0,0)$ and radius $R = O'A$, l_1 va l_2 the points will lie on the tangent.

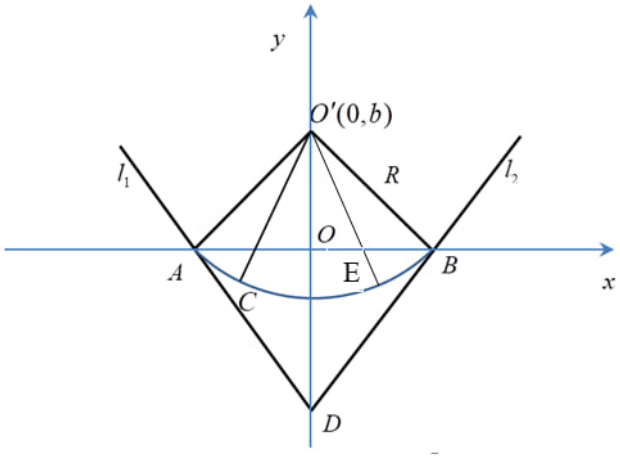

Fig.1: Moving from straight line to curvature section.

However, the curved section of the road cannot consist of a single arc of a circle. This is because, at point A, the road is a straight line on the left side, while on the right side, it is an arc of a circle. However, the circular

arc has a curvature equal to the reciprocal of its radius, that is, $k = \frac{1}{R}$.
A sharp change in curvature from zero to $\frac{1}{R}$, at point A, a sharp change in curvature from zero will result in the appearance of a sudden centrifugal force, which may lead to unexpected technical problems and, consequently, we will lose the comfort of the movement of train [9],[10].

Therefore, at point A, the transition section of the curve begins, ensuring a smooth transition of the train from the straight section to the curvature section.

Let us assume that the transition section of the track extends up to point C on the arc AB. To describe the analytical form of the transition section, we introduce a new Cartesian coordinate system as follows.

Let us assume point A as the origin of the coordinates, with the OX-axis directed along the straight line, and the ordinate axis OY directed along segment AO'.
Then, the equation of the circle with its center at point O and radius R is expressed as:

$$X^2 + (Y - R)^2 = R^2$$

or in parametric form, when the parameter is the arc length of the circle, it is given by the equation.

$$\begin{cases} X = R\cos\frac{s}{R} \\ Y = R(1 + \sin\frac{s}{R}) \end{cases} \tag{2.1}$$

Let us assume that in this coordinate system, the equation of the transition section is given in parametric form.

$$\begin{cases} X = X(s) \\ Y = Y(s) \end{cases} \tag{2.2}$$

Furthermore $X(0) = Y(0) = 0$, and the curvature of the curve for small values s was less than $\frac{1}{R}$, continuously and monotonically increasing, proportional to the arc length s. Moreover, at the point O, the curve $\overline{\gamma}$ intersects the circle at the point O.
It can be proved that for the curve $\overline{\gamma}$ to intersect the circle, its curvature at the point of intersection must be greater than the curvature of the circle, that is, greater than $\frac{1}{R}$.

Since the curvature of the curve $\overline{\gamma}$ changes continuously and monotonically in $[0, X_0]$, there exists at least one point $X_1 \in [0, X_0]$ - where the curvature of the curve $\overline{\gamma}$ takes the value $R(s_1) = \frac{1}{R}$.

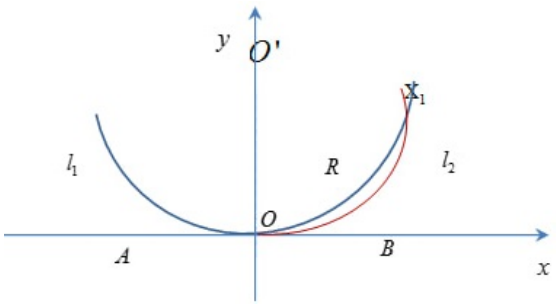

Fig.2: Parallel tangents between circle and a curve

Therefore, at point $\{X(s_1), Y(s_1)\}$, the curvature of the curve $\overline{\gamma}$ is equal to the curvature of the circle, the tangent circle of the curve $\overline{\gamma}$ is equal to the circle (1). However, the centers of these circles do not coincide. Consider the normal $\overline{l}$ to the curve $\overline{\gamma}$ at point $\{X(s_1), Y(s_1)\}$, and draw the radius $O'K$ of the circle (1), parallel to $\overline{l}$.

Let's parallelly move the arc of the circle AB to in the direction of the radius AK until it touches point $\{X(s_1), Y(s_1)\}$. Then, from this point, we replace the curve $\overline{\gamma}$ with the arc of the translated circle.

Thus, we obtain a line consisting of a part of the straight line l_1 up to point A, after point A the arc of the curve $\overline{\gamma}$, and after point $\{X(s_1), Y(s_1)\}$ – the arc of the circle with radius R, but with the center moved in the direction of the radius AK.

Thus, the constructed curve meets all the technical requirements for the transition section of the railway. We have presented the theoretical part of the construction of the curve section for the railway track plan, for the inner rail, when the entire track belongs to one horizontal plane.

Also, the conditions imposed on the equation of the transitional part were determined. Next, we move on to the numerical computation of this task, when a specific type of transition section is chosen.

Method for calculating the length of the transition section

In this part of the work, we will present the method for calculating the length of the transition section for a specifically given curve

There are various methods for constructing the transition section [11]. However, among them, a widely used method is the curve called the clothoid [12],[13].

A clothoid is a mathematical function widely used in the design of curvature sections of railways and highways. This equation ensures a linear change in curvature (from zero curvature to the maximum).

The equation of the clothoid in parametric form is expressed as follows:

$$x = \int_0^s \cos \tfrac{mt^2}{2} dt, \qquad y = \int_0^s \sin \tfrac{mt^2}{2} dt$$

Where: s is the arclength (distance along the clothoid);

m is the curvature parameter, i.e., $\frac{1}{R(s)}$, where $R(s)$ is the radius of curvature of the clothoid;

t is the integration variable.

Since its curvature is inversely proportional to the arc length.

$$k = \frac{m}{s}, \qquad s = \frac{m}{R}$$

Where: m is the proportionality coefficient. But for the point $\{X(s_1), Y(s_1)\}$, the curvature must be equal to the curvature of the circle, that is, $\frac{1}{R}$.

From the fact that the curvature of the clothoid is proportional to the arc length, it follows that.

$$ms_1 = \frac{1}{R}$$

Thus, the length of the clothoid can be determined using the formula,

$$s_1 = \frac{1}{mR}$$

The arc length is inversely proportional to the radius of the curve and the coefficient of the clotoid. There is a technical requirement that the length of the passing section should not be less than the length of the two carriages. Therefore, $mR = \frac{1}{50m}$, since the length of two carriages can be considered as 50 meters[14],[15].

To determine the distance at which the arc of the circle is parallelly moved, we construct the equation of the tangent at the point $\{X(s_1), Y(s_1)\}$, which has the form:

$$Y - Y(s_1) = \tan \frac{1}{2mR^2}(X - X(s_1))$$

Let's find the distance from the point $O'(O, R)$ to the tangent to the clothoid.

$$d = |Y(s_1) - \tan \frac{1}{2mR^2} X(s_1) - R| \cos \frac{1}{2mR^2}$$

Subtracting the radius from this distance, we get δ, which must be parallel to the section of the circle's arc.

$$\delta = d - R$$

Since the transition section must symmetrically rise when transitioning to the arc of the circle, it must descend to the point (Fig. 1). It is symmetric with respect to the bisector of the angle formed by the straight sections of the considered road.
After obtaining the equation of the curve for the inner rail, the equation for the outer rail is determined relative to the inner one. At the same time, the spatial nature of the curve representing the outer section is taken into account. The transition curve of the outer section will be analogous to the transition curve of the inner section.

References

[1] Kochetkov V.V, *"Railway Geometry: Fundamentals of Design"*. Moscow: Transport, (2015), pp. 56–61.
[2] Profillidis, V. A: *"Railway Management and Engineering."*, CRC Press, (2016), pp. 112–118.
[3] Yakunin A.N., *"Fundamentals of Railway Design."* St. Petersburg: Polytechnika, (2014).
[4] Esveld.C: *"Modern Railway Track."* . MRT-Productions, (2001), pp. 33–40.
[5] Hansen.I.A,Pachl.J: *"Railway Timetable and Traffic: Analysis, Modelling, Simulation"*., Eurailpress, (2014), pp. 205–213.
[6] Artykbaev, A., Toshmatova, M. M: *Geometric Approach to Define a Railway Plan Model*. Bulletin of the Karaganda University. Mathematics Series, No. 3(115), (2024), pp. 26–33.
[7] Atabekov, G.V: *Design of Railway Curves and Transition Sections*. Moscow: Transport, (1987), pp. 45–52.
[8] Wickens. A. H: *"Fundamentals of Rail Vehicle Dynamics"*, CRC Press, (2003), pp. 78–85.
[9] Vuchic.V. R, L.: *"Urban Transit Systems and Technology"*. Wiley, (2007), pp. 131–137.
[10] Anokhin A. N., *"Fundamentals of Railway Route Alignment and Design"*. Moscow: Transport, (2008), pp. 92–99.
[11] Lugovenko V.N *"Railway Geometry and Mathematical Modeling"* St. Petersburg: Energoatomizdat, (2013), pp. 66–72.
[12] Popov,N.P., Usoltsev,A.O., Glebov,V V. *Clothoid and Railways*.CyberLeninka, [Online]
[13] Bertolazzi,E., Frego, M. *Fast and Accurate Approximation of Clothoid Curves*. arXiv, 2012.
[14] Gross, J., Eberhardt, C. *"Mathematical Modeling of Railway Systems"*. Springer, (2019), pp. 149–156.
[15] Truong,T.V., Lam,M.N. *Geometric Design of Railway Tracks* Elsevier, (2015),pp. 215–222.

Affiliations

A.Artikbaev
Address: Tashkent state transport university, Proff. Dept. of Higher mathematics, Tashkent-Uzbekistan.
e-mail: aartykbaev@mail.ru
ORCID ID:0000-0001-6228-8749

M.Toshmatova
Address: Tashkent state transport university, Dept. of Higher mathematics, Tashkent-Uzbekistan.
e-mail: toshmatova_mm@mail.ru
ORCID ID: 0009-0006-2781-9325

M.Ergashaliev
Address: Tashkent state transport university, Dept. of Higher mathematics, Tashkent-Uzbekistan.
e-mail: magrurbekergashaliyev@gmail.com
ORCID ID: 0009-0007-4372-4657

Uzbekistan Journal of Mathematics and Computer Science
Volume 1 No. 1 Page 20–32 (2025)
DOI: https://doi.org/10.56143/ujmcs.v1i1.7
Research article

UZJMCS

On a $(\omega, c)-$periodic solution for an impulsive system of second-order differential equation with product of two nonlinear functions and mixed maxima

T. K. Yuldashev*, T. A. Abduvahobov

Abstract

Existence and uniqueness of $(\omega, c)-$periodic solution of boundary value problem for an impulsive system of ordinary differential equations with a nonlinear function under the sign of the second-order differential, product of two nonlinear functions and mixed maxima are investigated. This problem is reduced to the investigation of $(\omega, c)-$periodic solvability of the system of nonlinear functional-integral equations. The method of contracted mapping is used in the proof of unique solvability of nonlinear functional-integral equations in the space $BD([0, \omega], \mathbb{R}^n)$.

Keywords: *impulsive system of differential equations; a nonlinear function under the sign of the second-order differential; product of two nonlinear functions; $(\omega, c)-$periodic solution, mixed maxima; contracted mapping, existence and uniqueness.*

AMS Subject Classification (2020): *Primary: 34K14, 34K45, Secondary: 34C27.*

1. Problem statement. Problem Statement

Differential equations, the solution of which is functions with first kind discontinuities at times, are called differential equations with impulsive effects. One can see a lot of publications of studying on differential equations with impulsive effects, describing many natural and practical processes (for examples, [1]–[7]). Some problems with impulsive effects appear in biophysics at micro- and nano-scales [8]–[11]. The interest in the study of nonlocal problems for the impulsive differential equations is only increasing [12]–[34]. In the works [35]–[37], the periodic solutions of impulsive differential equations are studied. $(\omega, c)-$periodic solutions of the differential equations are studied in the works [38]–[43].

Definition 1.1. A continuous function $f(t) : \mathbb{R} \to \mathbb{X}$ is $(\omega, c)-$periodic, if there exists a real number $c \in (0, 1) \cup (1, \infty)$, that $f(t + \omega) = c \cdot f(t)$ for all $t \in \mathbb{R}$, where $0 < \omega < \infty$, $\mathbb{X} \in \mathbb{R}^n$ is closed set.

On the interval $\Omega \equiv [0, \omega] \setminus \{t_i\}$ for $i = 1, 2, ..., p$ we consider the questions of existence of the $(\omega, c)-$periodic solutions of the nonlinear impulsive system of second-order differential equations with mixed maxima

$$\frac{d^2}{dt^2}[x(t) + H(x(t))] =$$

Received : *05–januuary–2025,* ***Accepted :*** *17–february–2025*
*** Corresponding author***

This research is supported by the Ministry of Higher Education, Science and Innovative development of the Republic of Uzbekistan (Grant F-FA-2021-424).

$$= g\left(t, x(t), \max\left\{x(\tau)\middle|\tau \in \left[\delta_1(t)\hat{]}\delta_2(t)\right]\right\}\right) f\left(t, x(t), \max\left\{x(\tau)\middle|\tau \in \left[\delta_1(t)\hat{]}\delta_2(t)\right]\right\}\right), \tag{1.1}$$

where $\left[\delta_1(t)\hat{]}\delta_2(t)\right] = [\min\{\delta_1(t); \delta_2(t)\}, \ \max\{\delta_1(t); \delta_2(t)\}]$, $\delta_\kappa(t) \in C[\delta_0, h]$, $0 < \delta_0 = \min\limits_{0\le t\le\omega} \delta_\kappa(t)$, $\delta_0 < h = \max\limits_{0\le t\le\omega} \delta_\kappa(t) < \omega$, $\kappa = 1, 2$, $H(x) \in C^1(\mathbb{R}^n, \mathbb{R}^n)$, $g(t, x, y) \in C([0, \omega] \times \mathbb{X} \times \mathbb{X}, \mathbb{R}^n)$, $f(t, x, y) \in C\left([0, \omega] \times \mathbb{X} \times \mathbb{X}, \mathbb{R}^n\right)$.

The differential equation (1.1) we study with following $(\omega, c)-$periodic conditions

$$x(\omega) = c \cdot x(0), \quad H(x(0)) = c \cdot H(x(\omega)), \quad c \in (0, 1) \cup (1, \infty), \tag{1.2}$$

$$x'(\omega) = c \cdot x'(0), \quad H'(x(0)) = c \cdot H'(x(\omega)), \quad c \in (0, 1) \cup (1, \infty), \tag{1.3}$$

We assume that on the interval

$$I_1 = [0, t_1] \cup [t_2, t_3] \cup \ldots \cup [t_{p-3}, t_{p-2}] \cup [t_{p-1}, t_p]$$

there holds inequality $\delta_1(t) < \delta_2(t)$ and the equation (1.1) is accepting the form

$$\frac{d^2}{dt^2}[x(t) + H(x(t))] =$$

$$= g\left(t, x(t), \max\left\{x(\tau)\middle|\tau \in [\delta_1(t), \delta_2(t)]\right\}\right) f\left(t, x(t), \max\left\{x(\tau)\middle|\tau \in [\delta_1(t), \delta_2(t)]\right\}\right).$$

On another interval

$$I_2 = [t_1, t_2] \cup [t_3, t_4] \cup \ldots \cup [t_{p-2}, t_{p-1}] \cup [t_p, t_{p+1}]$$

there holds inequality $\delta_1(t) > \delta_2(t)$ and the equation (1.1) takes the form

$$\frac{d^2}{dt^2}[x(t) + H(x(t))] =$$

$$= g\left(t, x(t), \max\left\{x(\tau)\middle|\tau \in [\delta_2(t), \delta_1(t)]\right\}\right) f\left(t, x(t), \max\left\{x(\tau)\middle|\tau \in [\delta_2(t), \delta_1(t)]\right\}\right).$$

If we put $\delta_1(t_i) = \delta_2(t_i)$, $i = 1, 2, \ldots, p$, then there is no impulsive effect for the equation (1.1). So, we suppose that $\delta_1\left(t_i^+\right) \neq \delta_2\left(t_i^-\right)$, $\delta_2\left(t_i^+\right) \neq \delta_1\left(t_i^-\right)$, $i = 1, 2, \ldots, p$. Consequently, the problem (1.1)–(1.3) we study with conditions of nonlinear impulsive effects

$$x\left(t_i^+\right) - x\left(t_i^-\right) = F_{1,i}\left(x\left(t_i\right)\right), \qquad i = 1, 2, ..., p, \tag{1.4}$$

$$H\left(x\left(t_i^+\right)\right) - H\left(x\left(t_i^-\right)\right) = F_{2,i}\left(x\left(t_i\right)\right), \qquad i = 1, 2, ..., p, \tag{1.5}$$

$$x'\left(t_i^+\right) - x'\left(t_i^-\right) = G_{1,i}\left(x\left(t_i\right)\right), \qquad i = 1, 2, ..., p, \tag{1.6}$$

$$H'\left(x\left(t_i^+\right)\right) - H'\left(x\left(t_i^-\right)\right) = G_{2,i}\left(x\left(t_i\right)\right), \qquad i = 1, 2, ..., p, \tag{1.7}$$

where $0 = t_0 < t_1 < ... < t_p < t_{p+1} = \omega$, $x\left(t_i^+\right)$ and $x\left(t_i^-\right)$ right and left-hand side limits, $F_{\kappa,i}(x) \in C\left(\mathbb{X}, \mathbb{R}^n\right)$, $G_{\kappa,i}(x) \in C\left(\mathbb{X}, \mathbb{R}^n\right)$, $F_{\kappa,i} = F_{\kappa,i+p}$, $G_{\kappa,i} = G_{\kappa,i+p}$, $\kappa = 1, 2$, $t_{i+p} = t_i + \omega$.

In general, the solutions of differential equations with maxima have properties different from the solutions of differential equations without maxima. If we consider the equation

$$x'(t) = f\left(t, x(t), \max\left\{x(\tau)\middle|\tau \in [h_1(t), h_2(t)]\right\}\right),$$

then the increasing solutions coincide with the increasing solutions of the equation

$$x'(t) = f\left(t, x(t), x\left[h_2(t)\right]\right).$$

The decreasing solutions coincide with the decreasing solutions of the equation

$$x'(t) = f\left(t, x(t), x\left[h_1(t)\right]\right).$$

Periodic solutions of differential equations behave differently from periodic solutions of differential equations without maxima. If we consider the function $\max\left\{\sin\tau \middle| \tau \in [t-h(t), t]\right\}$, the properties of this function differ from the properties of the functions $\sin t$ and $\sin(t-h(t))$. For example, the function $\max\left\{\sin\tau \middle| \tau \in [t-\pi, t]\right\}$ is not negative on the axis $(-\infty, \infty)$. The function $\max\left\{\sin\tau \middle| \tau \in [t-2\pi, t]\right\}$ is constant on the axis $(-\infty, \infty)$ and equal to 1.

If we consider $(2\pi, c)-$periodic function $e^t \sin t$, this function has resonance on the interval $(0, \infty)$, where $c = e^{2\pi}$. The function $\max\left\{e^\tau \sin\tau \middle| \tau \in [t-\pi, t]\right\} = e^t \max\left\{\sin\tau \middle| \tau \in [t-\pi, t]\right\}$ has positive resonance on the interval $(0, \infty)$.

Therefore, the study differential equations with maxima is relevant and differential equations with maxima have specific singularities. In the case of differential equations with mixed maxima, the presence of impulse effects is not fictitious. In addition, differential equations with product of two nonlinear functions appear in solving nonlinear partial differential equations of parabolic and hyperbolic types (see, [44]). We note that this paper is further development of the works [45]–[47].

We recall that by $C\left([0, \omega], \mathbb{R}^n\right)$ is denoted the Banach space with continuous vector functions $x(t)$ on the segment $[0, \omega]$ and this space is equipped with the norm

$$\| x(t) \|_{C[0,\omega]} = \sqrt{\sum_{j=1}^{n} \max_{0 \le t \le \omega} \left| x_j(t) \right|}.$$

By $PC\left([0, \omega], \mathbb{R}^n\right)$ is denoted the following linear vector space

$$PC\left([0, \omega], \mathbb{R}^n\right) = \left\{x : [0, \omega] \to \mathbb{R}^n;\ x(t) \in C\left((t_i, t_{i+1}], \mathbb{R}^n\right),\ \ i = 1, ..., p\right\},$$

where limits $x\left(t_i^+\right)$ and $x\left(t_i^-\right)$ $(i = 0, 1, ..., p)$ exist and bounded; $x\left(t_i^-\right) = x\left(t_i\right)$. Note, that the linear vector space $PC\left([0, \omega], \mathbb{R}^n\right)$ is Banach space, if we equip it with the norm

$$\| x(t) \|_{PC[0,\omega]} = \max\left\{\| x(t) \|_{C(t_i, t_{i+1}]},\ i = 1, 2, ..., p\right\}.$$

We use also the vector space $BD\left([0, \omega], \mathbb{R}^n\right)$, which is Banach space with the following norm

$$\| x(t) \|_{BD[0,\omega]} = \| x(t) \|_{PC[0,\omega]} + h \cdot \| x'(t) \|_{PC[0,\omega]},$$

where $0 < h = \text{const}$.

Problem 1. *To find the $(\omega, c)-$periodic function $x(t) \in BD\left([0, \omega], \mathbb{R}^n\right)$, which for all $t \in \Omega$ satisfies the system of differential equations (1.1), $(\omega, c)-$periodic condition (1.2), (1.3) and for $t = t_i$, $i = 1, 2, ..., p$ satisfies the nonlinear limit conditions (1.4)–(1.7).*

2. Reduction to functional-integral equation

Let the function $x(t) \in BD\left([0, \omega], \mathbb{R}^n\right)$ is a solution of the $(\omega, c)-$periodic boundary value problem (1.1)–(1.7). Then, after integration on the intervals $(0, t_1]$, $(t_1, t_2]$, ..., $\left(t_p, t_{p+1}\right]$ we have:

$$\int_0^{t_1} g(s, x, y) f(s, x, y) ds = \int_0^{t_1} \frac{d^2}{dt^2}\left[x(s) + H(x(s))\right] ds =$$

$$= x'\left(t_1^-\right) - x'\left(0^+\right) + H'\left(x\left(t_1^-\right)\right) - H'\left(x\left(0^+\right)\right), \tag{2.1}$$

$$\int_{t_1}^{t_2} g(s,x,y)f(s,x,y)ds = \int_{t_1}^{t_2} \frac{d^2}{dt^2}\left[x(s) + H(x(s))\right]ds =$$

$$= x\left(t_2^-\right) - x\left(t_1^+\right) + H'\left(x\left(t_2^-\right)\right) - H'\left(x\left(t_1^+\right)\right), \tag{2.2}$$

$$\int_{t_2}^{t_3} g(s,x,y)f(s,x,y)ds = \int_{t_2}^{t_3} \frac{d^2}{dt^2}\left[x(s) + H(x(s))\right]ds =$$

$$= x\left(t_3^-\right) - x\left(t_2^+\right) + H'\left(x\left(t_3^-\right)\right) - H'\left(x\left(t_2^+\right)\right), \tag{2.3}$$

$$\vdots$$

$$\int_{t_p}^{\omega} g(s,x,y)f(s,x,y)ds = \int_{t_p}^{t_{p+1}} \frac{d^2}{dt^2}\left[x(s) + H(x(s))\right]ds =$$

$$= x\left(t_{p+1}^-\right) - x\left(t_p^+\right) + H'\left(x\left(t_{p+1}^-\right)\right) - H'\left(x\left(t_p^+\right)\right). \tag{2.4}$$

From the formulas (2.1)–(2.4), by virtue of the following properties

$$x'(0^+) = x'(0), \quad x'\left(t_{p+1}^-\right) = x'(t), \quad H'\left(x\left(0^+\right)\right) = H'(x(0)), \quad H'\left(x\left(t_{p+1}^-\right)\right) = H'(x(t)),$$

on the interval $(0, \omega]$ we have

$$\int_0^t g(s,x,y)f(s,x,y)ds =$$

$$= -x'(0) - \left[x'\left(t_1^+\right) - x'\left(t_1\right)\right] - \left[x'\left(t_2^+\right) - x'\left(t_2\right)\right] - \ldots - \left[x'\left(t_p^+\right) - x'\left(t_p\right)\right] + x'(t) -$$

$$-H'(x(0)) - \left[H'\left(x\left(t_1^+\right)\right) - H'\left(x\left(t_1\right)\right)\right] - \left[H'\left(x\left(t_1^+\right)\right) - H'\left(x\left(t_1\right)\right)\right] - \ldots -$$

$$- \left[H'\left(x\left(t_p^+\right)\right) - H'\left(x\left(t_p\right)\right)\right] + H'(x(t)).$$

Hence, taking into account the impulsive conditions (1.6), (1.7) in the last equality, we obtain

$$\frac{d}{dt}\left[x(t) + H(x(t))\right] = x'(0) + H'(x(0)) + \sum_{0<t_i<t} G_{1,i}(x(t_i)) +$$

$$+ \sum_{0<t_i<t} G_{2,i}(x(t_i)) + \int_0^t g(s,x,y)f(s,x,y)ds. \tag{2.5}$$

From (2.5) for $t = \omega$ we have

$$x'(\omega) + H'(x(\omega)) = x'(0) + H'(x(0)) + \sum_{0<t_i<\omega} G_{1,i}(x(t_i)) +$$

$$+ \sum_{0<t_i<\omega} G_{2,i}\left(x\left(t_i\right)\right) + \int_0^{\omega} g(s,x,y)f(s,x,y)ds. \tag{2.6}$$

Let the function $x(t) \in BD([0,\omega],\mathbb{R}^n)$ in (2.5), satisfies the boundary value conditions in (1.3). Then, applying the conditions in (1.3) to (2.6), we have

$$x'(0)+H'(x(0))=\frac{1}{c-1}\sum_{0<t_i<\omega}\left[G_{1,i}(x(t_i))+G_{2,i}(x(t_i))\right]+\frac{1}{c-1}\int_0^{\omega} g(s,x,y)f(s,x,y)ds. \tag{2.7}$$

Substituting (2.7) into (2.5), we obtain that

$$\frac{d}{dt}\left[x(t)+H(x(t))\right]=\frac{1}{c-1}\sum_{0<t_i<\omega}\left[G_{1,i}(x(t_i))+G_{2,i}(x(t_i))\right]+\sum_{0<t_i<t}\left[G_{1,i}(x(t_i))+G_{2,i}(x(t_i))\right]+$$

$$+\frac{1}{c-1}\int_0^{\omega} g(s,x,y)f(s,x,y)ds+\int_0^{t} g(s,x,y)f(s,x,y)ds. \tag{2.8}$$

We denote the right-hand side of the equation (2.8) by $a(s,x)$ and after integration on the intervals $(0,t_1]$, $(t_1,t_2]$, $\ldots$, $(t_p,t_{p+1}]$, taking into account

$$x(0^+)=x(0),\quad x(t_{p+1}^-)=x(t),\quad H(x(0^+))=H(x(0)),\quad H(x(t_{p+1}^-))=H(x(t)),$$

we have

$$\int_0^{t} a(s,x)ds=-x(0)-\left[x\left(t_1^+\right)-x\left(t_1\right)\right]-\left[x\left(t_2^+\right)-x\left(t_2\right)\right]-\ldots-\left[x\left(t_p^+\right)-x\left(t_p\right)\right]+x(t)-$$

$$-H(x(0))-\left[H\left(x\left(t_1^+\right)\right)-H\left(x\left(t_1\right)\right)\right]-\left[H\left(x\left(t_1^+\right)\right)-H\left(x\left(t_1\right)\right)\right]-\ldots-$$
$$-\left[H(x(t_p^+))-H(x(t_p))\right]+H(x(t)).$$

Hence, taking into account the impulsive conditions (1.4), (1.5) in the last equality, we obtain

$$x(t)+H(x(t))=x(0)+H(x(0))+\sum_{0<t_i<t}F_{1,i}(x(t_i))+\sum_{0<t_i<t}F_{2,i}(x(t_i))+\int_0^{t} a(s,x)ds. \tag{2.9}$$

From (2.9) for $t=\omega$ we have

$$x(\omega)+H(x(\omega))=x(0)+H(x(0))+\sum_{0<t_i<\omega}F_{1,i}(x(t_i))+\sum_{0<t_i<\omega}F_{2,i}\left(x\left(t_i\right)\right)+\int_0^{\omega} a(s,x)ds.$$

Hence, by virtue of conditions in (1.2), we obtain

$$x(t)+H(x(t))=\frac{1}{\nu}\sum_{0<t_i<\omega}\left[F_{1,i}(x(t_i))+F_{2,i}(x(t_i))\right]+$$

$$+\sum_{0<t_i<t}\left[F_{1,i}(x(t_i))+F_{2,i}(x(t_i))\right]+\frac{\omega}{\nu}\sum_{0<t_i<\omega}\left[G_{1,i}(x(t_i))+G_{2,i}(x(t_i))\right]+$$

$$+\frac{1}{\nu}\int_0^{\omega}\sum_{0<t_i<s}\left[G_{1,i}(x(t_i))+G_{2,i}(x(t_i))\right]ds+$$

$$+\frac{\omega(1+\nu)}{\nu^2}\int_0^{\omega} g(s,x,y)f(s,x,y)ds-\frac{1}{\nu}\int_0^{\omega} s\cdot g(s,x,y)f(s,x,y)ds+$$

$$+\frac{t}{\nu}\sum_{0<t_i<\omega}\left[G_{1,i}(x(t_i))+G_{2,i}(x(t_i))\right]+\int_0^{t}\sum_{0<t_i<s}\left[G_{1,i}(x(t_i))+G_{2,i}(x(t_i))\right]ds+$$

$$+\frac{t}{\nu}\int_0^{\omega} g(s,x,y)f(s,x,y)ds+\int_0^{t}(t-s)g(s,x,y)f(s,x,y)ds, \tag{2.10}$$

where $\nu = c-1$.

The equation (2.10) we rewrite in the complete form

$$x(t)=J(t;x)\equiv -H(x(t))+\frac{1}{\nu}\sum_{0<t_i<\omega}\left[F_{1,i}(x(t_i))+F_{2,i}(x(t_i))\right]+$$

$$+\sum_{0<t_i<t}\left[F_{1,i}(x(t_i))+F_{2,i}(x(t_i))\right]+\frac{\omega+t}{\nu}\sum_{0<t_i<\omega}\left[G_{1,i}(x(t_i))+G_{2,i}(x(t_i))\right]+$$

$$+\frac{1}{\nu}\int_0^{\omega}\sum_{0<t_i<s}\left[G_{1,i}(x(t_i))+G_{2,i}(x(t_i))\right]ds+$$

$$+\int_0^{\omega}\frac{\omega+\nu(\omega-s)}{\nu^2}g\left(s,x(s),\max\left\{x(\tau)\middle|\tau\in\left[\delta_1(s)\hat{|}\delta_2(s)\right]\right\}\right)\times$$

$$\times f\left(s,x(s),\max\left\{x(\tau)\middle|\tau\in\left[\delta_1(s)\hat{|}\delta_2(s)\right]\right\}\right)ds+$$

$$+\frac{t}{\nu}\int_0^{\omega} g\left(s,x(s),\max\left\{x(\tau)\middle|\tau\in\left[\delta_1(s)\hat{|}\delta_2(s)\right]\right\}\right)f\left(s,x(s),\max\left\{x(\tau)\middle|\tau\in\left[\delta_1(s)\hat{|}\delta_2(s)\right]\right\}\right)ds+$$

$$+\int_0^{t}(t-s)g\left(s,x(s),\max\left\{x(\tau)\middle|\tau\in\left[\delta_1(s)\hat{|}\delta_2(s)\right]\right\}\right)f\left(s,x(s),\max\left\{x(\tau)\middle|\tau\in\left[\delta_1(s)\hat{|}\delta_2(s)\right]\right\}\right)ds+$$

$$+\int_0^{t}\sum_{0<t_i<s}\left[G_{1,i}(x(t_i))+G_{2,i}(x(t_i))\right]ds. \tag{2.11}$$

3. Main Results

Lemma 3.1. *Assume that there exist some positive quantities, such that for all $t\in[0,\omega]$ are fulfilled the following conditions:*

$$\|\,g(t,x,y)\,\|_{C[0,\omega]}\le M_g<\infty,\quad \|\,f(t,x,y)\,\|_{C[0,\omega]}\le M_f<\infty,\quad \|\,H(t,x)\,\|_{C[0,\omega]}\le M_H<\infty;$$

$$\max_{1\le i\le p}\left\|\,F_{\kappa,i}\left(x(t_i)\right)\right\|_{C[0,\omega]}\le M_{F_{\kappa,i}}<\infty,\quad \max_{1\le i\le p}\left\|\,G_{\kappa,i}\left(x(t_i)\right)\right\|_{C[0,\omega]}\le M_{G_{\kappa,i}}<\infty,\ \ \kappa=1,2.$$

Then for the equation (2.11) *is true the following estimate*

$$\| J(t;x) \|_{C[0,\omega]} \leq M_H + p\frac{1+|\nu|}{|\nu|}\max_{1\leq i\leq p}\left[M_{F_{1,i}} + M_{F_{2,i}}\right] +$$

$$+p\frac{\omega(3+|\nu|)}{|\nu|}\max_{1\leq i\leq p}\left(M_{G_{1,i}} + M_{G_{2,i}}\right) + \frac{\omega^2(2+3|\nu|+\nu^2)}{2\nu^2}M_g M_f. \tag{3.1}$$

Proof. From the equation (2.11) we obtain

$$\| J(t;x) \|_{C[0,\omega]} \leq \| H(x) \|_{C[0,\omega]} + \frac{1}{|\nu|}\sum_{0<t_i<\omega}\left[\left\| F_{1,i}(x)\right\|_{C[0,\omega]} + \left\| F_{2,i}(x)\right\|_{C[0,\omega]}\right] +$$

$$+\sum_{0<t_i<t}\left[\left\| F_{1,i}(x)\right\|_{C[0,\omega]} + \left\| F_{2,i}(x)\right\|_{C[0,\omega]}\right] + \frac{\omega+t}{|\nu|}\sum_{0<t_i<\omega}\left[\left\| G_{1,i}(x)\right\|_{C[0,\omega]} + \left\| G_{2,i}(x)\right\|_{C[0,\omega]}\right] +$$

$$+\frac{1}{|\nu|}\int_0^\omega\sum_{0<t_i<s}\left[\left\| G_{1,i}(x)\right\|_{C[0,\omega]} + \left\| G_{2,i}(x)\right\|_{C[0,\omega]}\right]ds+$$

$$+\int_0^\omega\frac{\omega+\nu(\omega-s)}{\nu^2}\| g(s,x,y) \|_{C[0,\omega]}\| f(s,x,y) \|_{C[0,\omega]}\,ds+$$

$$+\frac{t}{\nu}\int_0^\omega\| g(s,x,y) \|_{C[0,\omega]}\| f(s,x,y) \|_{C[0,\omega]}\,ds+$$

$$+\int_0^t(t-s)\| g(s,x,y) \|_{C[0,\omega]}\| f(s,x,y) \|_{C[0,\omega]}\,ds+$$

$$+\int_0^t\sum_{0<t_i<s}\left[\left\| G_{1,i}(x)\right\|_{C[0,\omega]} + \left\| G_{2,i}(x)\right\|_{C[0,\omega]}\right]ds \leq$$

$$\leq \| H(x) \|_{C[0,\omega]} + p\frac{1+|\nu|}{|\nu|}\max_{1\leq i\leq p}\left[\left\| F_{1,i}(x)\right\|_{C[0,\omega]} + \left\| F_{2,i}(x)\right\|_{C[0,\omega]}\right] +$$

$$+p\frac{\omega(3+|\nu|)}{|\nu|}\max_{1\leq i\leq p}\left[\left\| G_{1,i}(x)\right\|_{C[0,\omega]} + \left\| G_{2,i}(x)\right\|_{C[0,\omega]}\right] +$$

$$+\frac{\omega^2(2+3|\nu|+\nu^2)}{2\nu^2}\| g(t,x,y) \|_{C[0,\omega]}\| f(t,x,y) \|_{C[0,\omega]}. \tag{3.2}$$

From the estimate (3.2) follows (3.1). Lemma 3.1 is proved. □

Lemma 3.2. *For the difference of two functions with maxima there holds the following estimate*

$$\left\|\max\left\{x(\tau)\middle|\tau\in\left[\lambda_1(s)\hat{]}\lambda_2(s)\right]\right\} - \max\left\{y(\tau)\middle|\tau\in\left[\lambda_1(s)\hat{]}\lambda_2(s)\right]\right\}\right\|_{PC[0,\omega]} \leq$$

$$\leq \| x(t)-y(t) \|_{PC[0,\omega]} + h\| x'(t)-y'(t) \|_{PC[0,\omega]} = \| x(t)-y(t) \|_{BD[0,\omega]}, \tag{3.3}$$

where $h = \max\limits_{0\leq t\leq\omega}|\lambda_2(t)-\lambda_1(t)|$.

Proof. For definiteness, we assume that $\lambda_1(t) < \lambda_2(t)$. It is obvious that there the following relation

$$\max\left\{x(\tau)\middle|\tau \in [\lambda_1(t), \lambda_2(t)]\right\} = \max\left\{[x(\tau) - y(\tau) + y(\tau)]\middle|\tau \in [\lambda_1(t), \lambda_2(t)]\right\} \leq$$

$$\leq \max\left\{[x(\tau) - y(\tau)]\middle|\tau \in [\lambda_1(t), \lambda_2(t)]\right\} + \max\left\{y(\tau)\middle|\tau \in [\lambda_1(t), \lambda_2(t)]\right\}$$

is true. Hence, we obtain that

$$\max\left\{x(\tau)\middle|\tau \in [\lambda_1(t), \lambda_2(t)]\right\} - \max\left\{y(\tau)\middle|\tau \in [\lambda_1(t), \lambda_2(t)]\right\} \leq$$

$$\leq \max\left\{[x(\tau) - y(\tau)]\middle|\tau \in [\lambda_1(t), \lambda_2(t)]\right\}. \tag{3.4}$$

We fix the variable t and denote by s_1 and s_2 the points of the segment $[\lambda_1(t), \lambda_2(t)]$, on which the maximums of the functions $x(t)$ and $y(t)$ are reached:

$$\max\left\{x(\tau)\middle|\tau \in [\lambda_1(t), \lambda_2(t)]\right\} = x(s_1), \max\left\{y(\tau)\middle|\tau \in [\lambda_1(t), \lambda_2(t)]\right\} = y(s_1),$$

$$\max\left\{[x(\tau) - y(\tau)]\middle|\tau \in [\lambda_1(t), \lambda_2(t)]\right\} = x(s_2) - y(s_2).$$

Then the inequality (3.4) we can rewrite in the form

$$\max\left\{x(\tau)\middle|\tau \in [\lambda_1(t), \lambda_2(t)]\right\} - \max\left\{y(\tau)\middle|\tau \in [\lambda_1(t), \lambda_2(t)]\right\} \leq x(s_2) - y(s_2). \tag{3.5}$$

Subtracting $x(s_1) - y(s_1)$ from both sides of the estimate (3.5), we obtain

$$\max\left\{x(\tau)\middle|\tau \in \left[\lambda_1(t), \lambda_2(t)\right]\right\} - \max\left\{y(\tau)\middle|\tau \in \left[\lambda_1(t), \lambda_2(t)\right]\right\} - x(s_1) + y(s_1) \leq$$

$$\leq x(s_2) - y(s_2) - x(s_1) + y(s_1), \quad s_1, s_2 \in \left[\lambda_1(t), \lambda_2(t)\right]. \tag{3.6}$$

We consider separately the right-hand side of (3.6) and apply the Lagrange's Mean-value theorem:

$$x(s_2) - y(s_2) - x(s_1) + y(s_1) = [x(s_2) - x(s_1)] - [y(s_2) - y(s_1)] =$$

$$= (s_2 - s_1)x'(\bar{s}) - (s_2 - s_1)y'(\bar{\bar{s}}) = (s_2 - s_1)[x'(\bar{s}) - y'(\bar{\bar{s}})] \leq$$

$$\leq h_0 \cdot |\, x'(\bar{s}) - y'(\bar{\bar{s}})\,|, \quad h_0 = |\, s_2 - s_1\,|, \quad \bar{s}, \bar{\bar{s}} \in (s_1, s_2). \tag{3.7}$$

From the inequalities (3.6) and (3.7) we have

$$\max\left\{x(\tau)\middle|\tau \in [\lambda_1(t), \lambda_2(t)]\right\} - \max\left\{y(\tau)\middle|\tau \in [\lambda_1(t), \lambda_2(t)]\right\} - x(s_1) + y(s_1) \leq h_0 \cdot |\, x'(\bar{s}) - y'(\bar{\bar{s}})\,|$$

or

$$\max\left\{x(\tau)\middle|\tau \in [\lambda_1(t), \lambda_2(t)]\right\} - \max\left\{y(\tau)\middle|\tau \in [\lambda_1(t), \lambda_2(t)]\right\} \leq$$

$$\leq [x(s_1) - y(s_1)] + h_0 \cdot |\, x'(\bar{s}) - y'(\bar{\bar{s}})\,|.$$

Hence, we obtain that

$$\left|\max\left\{x(\tau)\middle|\tau \in [\lambda_1(t), \lambda_2(t)]\right\} - \max\left\{y(\tau)\middle|\tau \in [\lambda_1(t), \lambda_2(t)]\right\}\right| \leq$$

$$\leq |\, x(s_1) - y(s_1)\,| + h_0 \cdot |\, x'(\bar{s}) - y'(\bar{\bar{s}})\,|. \tag{3.8}$$

Proceeding in (3.8) to the norm in the space of continuous functions $C[0, T]$, for

$$h = \max_{0 \leq t \leq T} |\, \lambda_2(t) - \lambda_1(t)\,| \geq h_0$$

we arrive at (3.3). The case $\lambda_1(t) > \lambda_2(t)$ is proved similarly. The Lemma 3.2 is proved. □

Theorem 3.1. *Assume that the conditions of the Lemma 3.1 are fulfilled and there exist some positive quantities, such that for all $t \in \Omega$ are fulfilled the following conditions:*
1). $\| H(x_1) - H(x_2) \| \le L_0 \| x_1 - x_2 \|$, $\| H'(x) \| \le M_{H'}$, $\| H'(x_1) - H'(x_2) \| \le \bar{L}_0 \| x_1 - x_2 \|$;
2). $\| g(t, x_1, y_1) - g(t, x_2, y_2) \| \le L_1 [\| x_1 - x_2 \| + \| y_1 - y_2 \|]$;
3). $\| f(t, x_1, y_1) - f(t, x_2, y_2) \| \le L_2 [\| x_1 - x_2 \| + \| y_1 - y_2 \|]$;
4). $\left\| F_{\kappa,i}(t, x_1) - F_{\kappa,i}(t, x_2) \right\| \le L_{3,\kappa,i} \| x_1 - x_2 \|$;
5). $\left\| G_{\kappa,i}(t, x_1) - G_{\kappa,i}(t, x_2) \right\| \le L_{4,\kappa,i} \| x_1 - x_2 \|$;
6). *The radius of the inscribed ball in $\mathbb{X}$ is greater than*

$$M_H + p\frac{1+|\nu|}{|\nu|} \max_{1\le i\le p} \left[M_{F_{1,i}} + M_{F_{2,i}}\right] +$$

$$+p\frac{\omega(3+|\nu|)}{|\nu|} \max_{1\le i\le p} \left[M_{G_{1,i}} + M_{G_{2,i}}\right] + \frac{\omega^2(2+3|\nu|+\nu^2)}{2\nu^2} M_g M_f;$$

7). $\rho < 1$, *where $\rho = \beta_1 + h\beta_2$ and β_1, β_2 are defined from (3.13), (3.16) below.*
Then the problem (1.1)–(1.7) has a unique $(\omega, c)-$periodic solution for all $t \in [0, \omega]$.

Proof. The theorem we proof by the fixed-point method. According to the theorem condition, we have

$$f(t+\omega, x(t+\omega), y(t+\omega)) = f(t+\omega,\, c\,x(t),\, c\,y(t)) = c\,f(t, x(t), y(t)).$$

We differentiate the equation (2.11):

$$x'(t) = J(t; x') \equiv -H'(x(t)) + \frac{1}{\nu} \sum_{0<t_i<\omega} \left[G_{1,i}(x(t_i)) + G_{2,i}(x(t_i))\right] +$$

$$+\frac{1}{\nu}\int_0^{\omega} g\left(s, x(s), \max\left\{x(\tau)\middle|\tau \in \left[\delta_1(s)\hat{|}\delta_2(s)\right]\right\}\right) f\left(s, x(s), \max\left\{x(\tau)\middle|\tau \in \left[\delta_1(s)\hat{|}\delta_2(s)\right]\right\}\right) ds+$$

$$+\int_0^{t} g\left(s, x(s), \max\left\{x(\tau)\middle|\tau \in \left[\delta_1(s)\hat{|}\delta_2(s)\right]\right\}\right) f\left(s, x(s), \max\left\{x(\tau)\middle|\tau \in \left[\delta_1(s)\hat{|}\delta_2(s)\right]\right\}\right) ds+$$

$$+ \sum_{0<t_i<t} \left[G_{1,i}(x(t_i)) + G_{2,i}(x(t_i))\right]. \tag{3.9}$$

For the difference of two operators in (2.11), to obtain estimate, we use the following approach:

$$\| g(x)f(x) - g(y)f(y) \| \le \| g(x)f(x) - g(y)f(x) \| + \| g(y)f(x) - g(y)f(y) \| \le$$

$$\le \| f(x) \| \| g(x) - g(y) \| + \| g(y) \| \| f(x) - f(y) \|.$$

Consequently, by virtue of conditions of theorem, from (2.11) we have

$$\|J(t;x) - J(t;y)\|_{PC[0,\omega]} \le L_0 \| x(t) - y(t) \|_{PC[0,\omega]} +$$

$$+p\frac{1+|\nu|}{|\nu|} \max_{1\le i\le p} \left[L_{3,1,i} \| x(t_i) - y(t_i) \|_{C[t_i,t_{i+1}]} + L_{3,2,i} \| x(t_i) - y(t_i) \|_{C[t_i,t_{i+1}]}\right] +$$

$$+p\frac{\omega(3+|\nu|)}{|\nu|} \max_{1\le i\le p} \left[L_{4,1,i} \| x(t_i) - y(t_i) \|_{C[t_i,t_{i+1}]} + L_{4,2,i} \| x(t_i) - y(t_i) \|_{C[t_i,t_{i+1}]}\right] +$$

$$+\frac{\omega^2(2+3|\nu|+\nu^2)}{2\nu^2} \left[L_1 \left\| f\left(t, x(t), \max\left\{x(\tau)\middle|\tau \in \left[\delta_1(t)\hat{|}\delta_2(t)\right]\right\}\right) \right\|_{C[0,\omega]} \times$$

$$\times \Big(\| x(t) - y(t) \|_{PC[0,\omega]} + \Big\| \max \{x(\tau) | \tau \in [\delta_1(t) \hat{]} \delta_2(t)]\} -$$
$$- \max \{y(\tau) | \tau \in [\delta_1(t) \hat{]} \delta_2(t)]\} \Big\|_{PC[0,\omega]} +$$
$$+ L_2 \Big\| g \Big(t, y(t), \max \{y(\tau) | \tau \in [\delta_1(t) \hat{]} \delta_2(t)]\} \Big) \Big\|_{C[0,\omega]} \times$$
$$\times \Big(\| x(t) - y(t) \|_{PC[0,\omega]} + \Big\| \max \{x(\tau) | \tau \in [\delta_1(t) \hat{]} \delta_2(t)]\} -$$
$$- \max \{y(\tau) | \tau \in [\delta_1(t) \hat{]} \delta_2(t)]\} \Big\|_{PC[0,\omega]} \Big]. \tag{3.10}$$

Appling Lemma 3.2 (inequality (3.3)) to the inequality (3.10), we obtain that

$$\|J(t;x) - J(t;y)\|_{PC[0,\omega]} \le L_0 \| x(t) - y(t) \|_{PC[0,\omega]} +$$
$$+ p \frac{1 + |\nu|}{|\nu|} \max_{1 \le i \le p} \left[L_{3,1,i} + L_{3,2,i} \right] \| x(t) - y(t) \|_{PC[0,\omega]} +$$
$$+ p \frac{\omega(3 + |\nu|)}{|\nu|} \max_{1 \le i \le p} \left[L_{4,1,i} + L_{4,2,i} \right] \| x(t) - y(t) \|_{PC[0,\omega]} +$$
$$+ \frac{\omega^2(2 + 3|\nu| + \nu^2)}{2\nu^2} \Big[L_1 M_f \Big(2 \| x(t) - y(t) \|_{PC[0,\omega]} + h \| x'(t) - y'(t) \|_{PC[0,\omega]} \Big) +$$
$$+ L_2 M_g \Big(2 \| x(t) - y(t) \|_{PC[0,\omega]} + h \| x'(t) - y'(t) \|_{PC[0,\omega]} \Big) \Big]. \tag{3.11}$$

The estimate (3.11) we rewrite as

$$\|J(t;x) - J(t;y)\|_{PC[0,\omega]} \le \beta_1 \| x(t) - y(t) \|_{PC[0,\omega]} + \gamma_1 h \| x'(t) - y'(t) \|_{PC[0,\omega]}, \tag{3.12}$$

where

$$\beta_1 = L_0 + p \max_{1 \le i \le p} \left(\frac{1 + |\nu|}{|\nu|} \left[L_{3,1,i} + L_{3,2,i} \right] + \frac{\omega(3 + |\nu|)}{|\nu|} \left[L_{4,1,i} + L_{4,2,i} \right] \right) +$$
$$+ 2 \frac{\omega^2(2 + 3|\nu| + \nu^2)}{2\nu^2} \left(M_f L_1 + M_g L_2 \right), \tag{3.13}$$
$$\gamma_1 = \frac{\omega^2(2 + 3|\nu| + \nu^2)}{2\nu^2} \left(M_f L_1 + M_g L_2 \right).$$

Since $\beta_1 > \gamma_1$, then from (3.12) we have

$$\|J(t;x) - J(t;y)\|_{PC[0,\omega]} \le \beta_1 \left[\| x(t) - y(t) \|_{PC[0,\omega]} + h \| x'(t) - y'(t) \|_{PC[0,\omega]} \right]. \tag{3.14}$$

Now for the difference of two operators in (3.9), similarly, we have estimate

$$\|J(t;x') - J(t;y')\| \le \left[\bar{L}_0 + p \frac{1 + |\nu|}{|\nu|} \max_{1 \le i \le p} \left(L_{4,1,i} + L_{4,2,i} \right) + 2 \left(M_f L_1 + M_g L_2 \right) \right] \times$$
$$\times \| x(t) - y(t) \|_{PC[0,\omega]} + h \left(M_f L_1 + M_g L_2 \right) \| x'(t) - y'(t) \|_{PC[0,\omega]} =$$
$$= \beta_2 \| x(t) - y(t) \|_{PC[0,\omega]} + \gamma_2 h \| x'(t) - y'(t) \|_{PC[0,\omega]} \le$$
$$\le \beta_2 \left[\| x(t) - y(t) \|_{PC[0,\omega]} + h \| x'(t) - y'(t) \|_{PC[0,\omega]} \right], \tag{3.15}$$

where

$$\beta_2 = \bar{L}_0 + p \frac{1 + |\nu|}{|\nu|} \max_{1 \le i \le p} \left(L_{4,1,i} + L_{4,2,i} \right) + 2 \left(M_f L_1 + M_g L_2 \right) > \gamma_2 = M_f L_1 + M_g L_2. \tag{3.16}$$

We multiply both sides of (3.15) to h term by term. Then, adding the estimates (3.14) and (3.15) term by term, we obtain that

$$\|J(t;x) - J(t;y)\|_{BD[0,\omega]} \leq \rho \cdot \| x(t) - y(t) \|_{BD[0,\omega]}, \tag{3.17}$$

where $\rho = \beta_1 + h\beta_2$.

According to the last condition of the theorem $\rho < 1$, so right-hand side of (2.11) as an operator is contraction mapping. From the estimates (3.1) and (3.17) implies that there exists a unique fixed point $x(t)$, satisfying equation (1.1), $(\omega, c)-$periodic conditions (1.2), (1.3) and impulsive conditions (1.4)–(1.7). The theorem is proved. □

Conclusion

Existence and uniqueness of $(\omega, c)-$periodic solution of impulsive system of ordinary differential equations (1.1) with a nonlinear function under the sign of the second-order differential, a product of two nonlinear functions and mixed maxima are investigated. The equation (1.1) is studied under the periodic conditions (1.2) and (1.3) and impulsive conditions (1.4)–(1.7). The problem (1.1)–(1.7) is reduced to the investigation of solvability of the system of nonlinear functional-integral equations (2.11). The method of contracted mapping is used in the proof of unique solvability of nonlinear functional-integral equations in the space $BD([0, \omega], \mathbb{R}^n)$.

Funding

This research is supported by the Ministry of Higher Education, Science and Innovative development of the Republic of Uzbekistan (Grant F-FA-2021-424).

Availability of data and materials

Not applicable.
Not applicable.

Competing interests

The authors declare that they have no competing interests.
The authors declare that they have no competing interests.

Author's contributions

All authors contributed equally to the writing of this paper. All authors read and approved the final manuscript.
All authors contributed equally to the writing of this paper. All authors read and approved the final manuscript.

References

[1] Bainov, D. D., Simeonov, P. S.: Impulsive differential equations: Periodic solutions and applications. New York, NY, USA, Wiley. (1993)
[2] Benchohra, M., Henderson, J., Ntouyas, S. K.: Impulsive differential equations and inclusions. Contemporary mathematics and its application, New York, Hindawi Publishing Corporation. (2006).
[3] Halanay, A., Veksler, D.: Qualitative theory of impulsive systems. Moscow, Mir. (1971) (Russian).
[4] Lakshmikantham, V., Bainov, D. D., Simeonov, P. S.: Theory of impulsive differential equations. Singapore, World Scientific. (1989).
[5] Perestyk, N. A., Plotnikov, V. A., Samoilenko, A. M., Skripnik, N. V.: Differential equations with impulse effect: multivalued right-hand sides with discontinuities. DeGruyter Stud. **40**, Mathematics, Berlin, Walter de Gruter Co. (2011).
[6] Samoilenko, A. M., Perestyk, N. A.: Impulsive differential equations. Singapore, World Sci. (1995).
[7] Stamova, I., Stamov, G.: Impulsive biological models. In: Applied impulsive mathematical models, CMS Books in Mathematics, Springer, Cham. (2016).

[8] Catlla, J., Schaeffer, D. G., Witelski, Th. P., Monson, E. E., Lin, A. L.: *On spiking models for synaptic activity and impulsive differential equations*. SIAM Review. **50** (3), 553–569 (2008).

[9] Choi, S. K., Koo, N.: *A note on linear impulsive fractional differential equations*, J. Chungcheong Math. Soc. **28**, 583–590 (2015).

[10] Fedorov, E. G., Popov, I. Yu.: *Analysis of the limiting behavior of a biological neurons system with delay*. J. Phys. Conf. Ser. **2086** (012109), (2021).

[11] Fedorov, E. G., Popov, I. Yu.: *Hopf bifurcations in a network of Fitzhigh-Nagumo biological neurons*. International J. of Nonlinear Sciences and Numerical Simulation (2021). https://doi.org/10.1515/ijnsns-2021-0188.

[12] Fedorov, E. G.: *Properties of an oriented ring of neurons with the FitzHugh-Nagumo model*. Nanosystems: Phys. Chem. Math. **12** (5), 553–562 (2021).

[13] Anguraj, A., Arjunan, M. M.: *Existence and uniqueness of mild and classical solutions of impulsive evolution equations*. Elect. J. Differ. Equat. **2005** (111), 1–8 (2005).

[14] Ashyralyev, A., Sharifov, Ya. A.: *Existence and uniqueness of solutions for nonlinear impulsive differential equations with two–point and integral boundary conditions*. Adv. in Difference Equat. **2013** (173) (2013).

[15] Ashyralyev, A., Sharifov, Ya. A.: *Optimal control problems for impulsive systems with integral boundary conditions*. Elect. J. Differ. Equat. **2013** (80), 1–11 (2013).

[16] Bai, Ch., Yang, D.: *Existence of solutions for second-order nonlinear impulsive differential equations with periodic boundary value conditions*. Boundary Value Problems (Hindawi Publishing Corporation) **2007** (41589), 1–13 (2007).

[17] Bin, L., Xinzhi, L., Xiaoxin, L.: *Robust global exponential stability of uncertain impulsive systems*. Acta Mathematika Scientia. **25** (1), 161–169 (2005).

[18] Dhayal, R., Malik, M., Abbas, S.: *Solvability and optimal controls of non-instantaneous impulsive stochastic fractional differentialequation of order*. Stochastics. **93** 780–802 (2020).

[19] Dhayal, R., Malik, M., Abbas, S., Debbouche, A.: *Optimal controls for second-order stochastic differential equations driven by mixed-fractional Brownian motion with impulses*. Math. Methods Appl. Sci. **43**, 4107–4124 (2020).

[20] Fayziyev, A. K., Abdullozhonova, A. N., Yuldashev, T. K.: *Inverse problem for Whitham type multi-dimensional differential equation with impulse effects*. Lobachevskii J. Math. **44** (2), 570–579 (2023).

[21] Feckan, M., Wang, J. R.: *Periodic impulsive fractional differential equations*. Adv. Nonlinear Anal. **8**, 482–496 (2019).

[22] Guechi, S., Dhayal, R., Debbouche, A., Malik, M.: *Analysis and optimal control of ϕ-Hilfer fractional semilinear equations involving nonlocal impulsive conditions*. Symmetry. **13** (2084), (2021).

[23] Ji, Sh., Wen, Sh.: *Nonlocal cauchy problem for impulsive differential equations in Banach spaces*. Intern. J. Nonlinear Science. **10** (1), 88–95 (2010).

[24] Kao, Y., Li, H.: *Asymptotic multistability and local S-asymptotic ω-periodicity for the nonautonomous fractionalorder neural networks with impulses*. Sci. China Inform. Sci. **64**, 1–13 (2021).

[25] Li, M., Han, M.: *Existence for neutral impulsive functional differential equations with nonlocal conditions*, Indagationes Mathematcae **20** (3), 435–451 (2009).

[26] Mardanov, M. J., Sharifov, Ya. A., Molaei Habib, H.: *Existence and uniqueness of solutions for first-order nonlinear differential equations with two-point and integral boundary conditions*. Elect. J. Differen. Equat. **2014** (259), 1–8 (2014).

[27] Sharifov, Ya. A.: *Optimal control problem for systems with impulsive actions under nonlocal boundary conditions*. Vestnik Sam. Gos. Tekhn. Universiteta. Seria: Fiz.-Mat. Nauki. **33** (4), 34–45 (2013) (in Russian)

[28] Sharifov, Ya. A.: *Optimal control for systems with impulsive actions under nonlocal boundary conditions*, Russian Math. (Izv. VUZ). **57** (2), 65–72 (2013).

[29] Sharifov, Ya. A., Mammadova, N. B.: *Optimal control problem described by impulsive differential equations with nonlocal boundary conditions*. Differen. equat. **50** (3), 403–411 (2014).

[30] Sharifov, Ya. A.: *Conditions optimality in problems control with systems impulsive differential equations with nonlocal boundary conditions*. Ukrainain Math. Journ. **64** (6), 836–847 (2012).

[31] Yuldashev, T. K., Fayziyev, A. K.: *On a nonlinear impulsive system of integro-differential equations with degenerate kernel and maxima*. Nanosystems: Phys. Chem. Math. **13** (1), 36–44 (2022).

[32] Yuldashev, T. K., Fayziyev, A. K.: *Integral condition with nonlinear kernel for an impulsive system of differential equations with maxima and redefinition vector*. Lobachevskii J. Math. **43** (8), 2332–2340 (2022).

[33] Yuldashev, T. K., Fayziyev, A. K.: *Inverse problem for a second order impulsive system of integro-differential equations with two redefinition vectors and mixed maxima*. Nanosystems: Phys. Chem. Math. **14** (1), 13–21 (2023).

[34] Wang, J. R., Feckan, M., Zhou, Y.: *A survey on impulsive fractional differential equations*. Frac. Calc. Appl. Anal. **19**, 806–831 (2016).

[35] Yuldashev, T. K.: *Periodic solutions for an impulsive system of nonlinear differential equations with maxima*. Nanosystems: Phys. Chem. Math. **13** (2), 135–141 (2022).

[36] Yuldashev, T. K.: *Periodic solutions for an impulsive system of integro-differential equations with maxima*. Vestnik Sam. Gos. Tekhn. Universiteta. Ser. Fiz.-Mat. Nauki. **26** (2), 368–379 (2022).

[37] Yuldashev, T. K., Sulaimonov, F. U.: *Periodic solutions of second order impulsive system for an integro-differential equations with maxima*. Lobachevskii J. Math. **43** (12), 3674–3685 (2022).

[38] Alvarez, E., Castillo, S., Pinto, M.: *(ω, c)-pseudo periodic functions, first order Cauchy problem and Lasota Wazewska model with ergodic and unbounded oscillating production of red cells*. Bound. Value Probl. **2019**, 1–20 (2019).

[39] Alvarez, E., Gomez, A., Pinto, M.: *$(\omega, c)-$periodic functions and mild solutions to abstract fractional integrodifferential equations*. Electron. J. Qual. Theory Differ. Equat. **16**, 1–8 (2018).

[40] Alvarez, E., Diaz, S., Lizama, C.: *On the existence and uniqueness of (N, λ)-periodic solutions to a class of Volterra difference equations*. Adv. Differ. Equ. **2019**, 1–12 (2019).

[41] Agaoglou, M., Feckan, M., Panagiotidou, A. P.: *Existence and uniqueness of (ω, c)-periodic solutions of semilinear evolution equations*. Int. J. Dyn. Sys. Diff. Equ. no. 10, 149–166 (2020).

[42] Khalladi, M. T., Rahmani, A.: (ω, c)-*pseudo almost periodic distributions*. Nonauton. Dyn. Syst. no. 7, 237–248 (2020).
[43] Khalladi, M. T., Kostic, M., Pinto, M., Rahmani, A., Velinov, D.: *On semi-c-periodic functions*. J. Math. **2021**, 1–5 (2021).
[44] Yuldashev, T. K.: *Nonlinear optimal control of thermal processes in a nonlinear Inverse problem*. Lobachevskii J. Math. **41** (1), 124–136 (2020).
[45] Yuldashev, T. K., Mamedov, Kh. R., Abduvahobov, T. A.: *On a periodic solution for an impulsive system of differential equations with Gerasimov–Caputo fractional operator and maxima*. Journal of Contemporary Applied Mathematics. **13** (1), 111–122 (2023).
[46] Yuldashev, T. K., Mamedov, Kh. R., Abduvahobov, T. A.: (ω, c)-*periodic solution for an impulsive system of differential equations with the quadrate of Gerasimov–Caputo fractional operator and maxima*. Journal of Contemporary Applied Mathematics. **13** (2), 65–79 (2023).
[47] Yuldashev, T. K., Abduvahobov, T. A.: *Periodic solutions for an impulsive system of fractional order integro-differential equations with maxima*. Lobachevskii J. Math. **44** (10), 4401–4409 (2023).

Affiliations

Yuldashev Tursun Kamaldinovich
Address: Tashkent State Transport University, Dept. of Higher Mathematics, 100169, Tashkent, Uzbekistan.
e-mail: tursun.k.yuldashev@gmail.com
ORCID ID: https://orcid.org/0000-0002-9346-5362

Abduvahobov Tohirjon Akbarali ogli
Address: Tashkent State University of Economics, Dept. of Higher and Applied Mathematics, 100069, Tashkent, Uzbekistan.
e-mail: tohirjonabduvahopov2603@gmail.com
ORCID ID: https://orcid.org/0009-0000-2128-2762

Uzbekistan Journal of Mathematics and Computer Science
Volume 1 No. 1 Page 33–40 (2025)
DOI: https://doi.org/10.56143/ujmcs.v1i1.8
Research article

The problem of studying a depth-velocity seismic model of the geological medium

Akram Begmatov*, Vladimir Bogdanov and Yuriy Volkov

Abstract

A review of the algorithm for numerical solution of the inverse kinematic problem of seismics, consisting in studying the depth-velocity model of the geological medium, is given. The algorithm is based on the eikonal equation and the technology of smoothing multidimensional splines.

Keywords: *inverse kinematic problem of seismics; eikonal equation; approximation; splines.*

AMS Subject Classification (2020): *Primary: 35R30 ; Secondary: 65M99; 86A15; 65D07.*

The study of the structure and condition of the interior of the Earth is of fundamental importance. Changes in the internal structure of the Earth are usually accompanied by global catastrophes or local cataclysms. Seismic activity of natural or man-made origin requires an understanding of the cause-and-effect relationships that occur as a result of these events. It is necessary to assess the possible consequences, forecast the development of events in time and energy characteristics. Depth study of the earth's crust cannot be carried out otherwise than using indirect information about the elastic and plastic characteristics of the medium. Disturbances caused by the natural removal of excess stress in the medium at great depths or by artificial sources on the surface of the Earth generate waves, the front and propagation velocity of which are determined by these characteristics. Thus, there is a problem of determining the propagation velocity of seismic waves inside the Earth using information available for observation about the movement of seismic wave fronts that appear on the surface as a result of earthquakes or artificial sources. The inverse kinematic problem of seismics (IKPS), the research of which was initiated by G. Gerglotz [1] and E. Wiechert [2] in 1907, plays an important role both in the theory of inverse problems of mathematical physics [3] and in practical geophysics [4]. Understanding that direct measurement of the physical parameters of the consequences of seismic events is possible only in a very shallow near-surface layer, for example, by drilling, therefore, practically the only way to study the internal structure of the Earth are methods based on solving certain inverse problems.

The inverse kinematic problem of seismics with internal sources allows in some cases to reconstruct the velocity field in the area of earthquake foci. Such a problem can be solved, for example, by an iterative method. At the first stage, the coordinates of earthquake foci located compactly are specified using a fairly simple model of the medium. At the second stage of the study, the obtained coordinates of the foci and travel times are used to construct and refine the model of the medium. One of the approaches to reconstructing the depth-velocity model of the medium from seismological data can be represented by two groups: a differential method that uses the inversion principle when the wave propagates along the rays from the detector to the source [5, 6] and an integral tomographic method — reconstructing the velocity along the source-detector rays [7]. In the tomography method, the velocity is assumed to be constant in the selected three-dimensional blocks, while the total residual is minimized. In this case, the velocity is determined in the area of passage of seismic rays.

Received : *15–desember–2024,* ***Accepted :*** *24–march–2025*
**** Corresponding author***

The differential method, in which the velocity is determined in the area of concentration of earthquake foci, was developed in the 1980s at the Novosibirsk Computing Center [8]. This technique was first tested on data from the Kamchatka region. The velocity field [9] was reconstructed in the focal area of the Kronotsky earthquake of 1997 for a long period of time: before the earthquake, during the development of the aftershock process and in the following years. The algorithm for solving the IKPS with internal sources was based on the ideas of wave front inversion and their approximations by plane or spherical wave fronts. It turned out that even if the hypocenters of earthquakes are known with a large error, the velocity of the medium determined as a result of the algorithm was restored stably.

In this paper, we review the algorithm in which the onset times and hypocenters of earthquakes are considered to be known. For comparative analysis of different methods, the mentioned technique was studied in [10, 11].

The issues concerning surface waves require special consideration and are not discussed here.

Following [12], we consider the equations of wave propagation in an isotropic elastic medium

$$\frac{\partial^2 u_i^p}{\partial t^2} = v_p^2 \Delta u_i^p, \quad \frac{\partial^2 u_i^s}{\partial t^2} = v_s^2 \Delta u_i^s, \quad i = 1, 2, 3,$$

where Δ is the Laplace operator, u^p, u^s are the displacement vectors in longitudinal and transverse directions, v_p is the propagation velocity of the longitudinal wave (the wave of compression), v_s is the propagation velocity of the transverse wave (the share wave), and

$$v_p^2 = \frac{\lambda + 2\mu}{\rho}, \quad v_s^2 = \frac{\mu}{\rho}. \tag{1}$$

Both these waves propagate in the elastic medium. The wave of compression leads to a relative change in volume equal to $\operatorname{div} u^p$. The shear wave is characterized by the relation $\operatorname{div} u^s = 0$. In other words, the vector field u^s of displacements in the transverse direction is solenoidal.

Such expressions of the parameters of an elastic medium as the Young modulus (the elasticity coefficient) E and the Poisson coefficient (the deformation) σ are related to the kinematic parameters as follows

$$E = \frac{\mu(3\lambda + 2\mu)}{\lambda + \mu} = \rho \frac{v_s^2(3\kappa - 1)}{\kappa - 1}, \quad \sigma = \frac{\lambda}{2(\lambda + \mu)} = \frac{\kappa - 2}{2(\kappa - 1)}, \tag{2}$$

where $\kappa = \left(\frac{v_p}{v_s}\right)^2$. For example, for mountain rocks we have $\sqrt{\kappa} \approx \sqrt{3} \approx 1.73$.

The eikonal equation, which plays a significant role in the IKPS, is an approximation of the general formulation.

The propagation of monochromatic waves in an elastic medium is described by the Helmholtz equation

$$\Delta u(x) + k_0^2 n^2(x) u(x) = 0, \tag{3}$$

where $x \in \mathbb{R}^3$, $k_0 = \omega/c$ is the wave number, ω is the frequency, c is certain characteristic value of the wave propagation velocity in the medium, and $n(x)$ is the coefficient of refraction. In an inhomogeneous medium whose properties change slightly with respect to wavelength, the wave front also has a little change with distance or stays «almost flat». The solution of (3) is sought in the form of a plane wave

$$u(x) = a(x)\, \mathrm{e}^{\mathrm{i}k_0 \psi(x)}, \tag{4}$$

where the amplitude $a(x)$ and the wave vector $k(x) = k_0 \nabla\psi(x)$, $k = (k_1, k_2, k_3)$, also slightly vary with respect to the wavelength.

Representing the field $u(x)$ as the series

$$u(x) = \sum_{j=0}^{\infty} \frac{a_j(x)}{(ik_0)^j} e^{ik_0\psi(x)}, \tag{5}$$

and inserting (5) into (3), we obtain the infinite system of equations

$$\begin{aligned} &\langle \nabla\psi, \nabla\psi\rangle = n^2, \quad 2\langle \nabla a_0, \nabla\psi\rangle + a_0\Delta\psi = 0, \\ &2\langle \nabla a_j, \nabla\psi\rangle + a_j\Delta\psi = -\Delta a_{j-1}, \quad j = 1, 2, \dots \end{aligned} \tag{6}$$

The function ψ is called the eikonal, and the first equation of (6) is the eikonal equation. The equations connecting the amplitudes $a_0, a_1, \dots$ are the transport equations of zero, first, second, etc. orders of approximation.

The formulation of the IKPS is given in [4]. Let D be a half-space $x^3 > 0$ of $\mathbb{R}^3$ with boundary ∂D being the coordinate plane OXY. The domain D is filled by an elastic medium in which waves propagate with velocity $v(x) = 1/n(x)$, $x = (x^1, x^2, x^3)$. The velocity v is the velocity v_p of longitudinal or v_s of transverse waves. Let $\tau(x_0, x)$ be the time it takes for which the wave arrives at point x from point x_0. The function $\tau(x, x_0)$ $(= \tau(x_0, x))$ satisfies the eikonal equation and the condition at infinity

$$| \nabla_x \tau(x, x_0) | = \frac{1}{v(x)} \equiv n(x), \quad \tau(x, x_0) = O(|x - x_0|), \quad x \to \infty. \tag{7}$$

The problem of determining the velocity $v(x)$ for $x \in D$ is posed if the function $\tau(x, x_0)$ is known, satisfying (7) for $x \in \partial D$, $x_0 \in B$ for some set B, $B \subset \overline{D}$.

Usually in the inverse kinematic problem of seismics it is assumed that the subset B belongs to the boundary ∂D, $B \subset \partial D$. If B is a domain, $B \subset D$, then we speak of an inverse kinematic problem of seismics with internal sources.

Let us describe an algorithm for numerically solving the IKPS with internal sources, based on multivariate spline approximation. We consider the problem with one receiver. Let the receiver be located at a point $x_0 = (x_0^1, x_0^2, 0)$ on the Earth's surface, recording incoming signals from certain points $x_i = (x_i^1, x_i^2, x_i^3)$, $i = 1, \dots, n$, called disturbance sources. The sources in some way, generally speaking chaotically, fill a certain region inside the Earth (focal zone). The times $\tau(x_i, x_0)$ of wave arrival from source x_i to receiver x_0 are assumed to be known. If the location of the receiver is fixed and the hodograph is discretely known, then we assume that we know the values t_i of a sufficiently smooth function $T(x)$ at the points $x = x_i$, i.e. $t_i = \tau(x_i, x_0) = T(x_i)$.

The eikonal equation relates the gradient of the function $T(x)$ to the function $v(x)$ of the signal propagation velocity at the point x.

In a real problem, the sources of disturbances are located at the hypocenters of earthquakes, i.e. chaotically, and the data on the hodographs contain significant errors. In such cases, difference methods do not give acceptable results. Global spline approximation methods based on radial basis functions have proven to be «good» methods for such a problem [13, 14].

Splines of this type can be obtained as a result of minimization of some functional $J(f)$ on the set of functions f from some space (the condition of minimality of the norm) under the condition of interpolation of a given set of values or their smoothing [15, 16]. As a result, the spline is represented as

$$s(x) = \sum_{i=1}^{n} \lambda_i R(x, x_i) + \pi(x). \tag{8}$$

Here x_i, $i = 1, \ldots, n$, are the spline support nodes, points in the space (generally multidimensional, but we are only interested in $\mathbb{R}^3$) where the data are given;

$R(x, y) = \phi(|x - y|)$ is the radial basis function, ϕ is a function of one variable, $|x - y|$ is the Euclidean distance between points x and y in space;

$\lambda_i \in \mathbb{R}$ are the spline coefficients;

$\pi \in \mathcal{P}$, where $\mathcal{P}$ is a given finite-dimensional space of functions in the multidimensional space under consideration, called the spline trend. Usually $\mathcal{P}$ is the space of algebraic polynomials of some degree.

The coefficients λ_i, $i = 1, \ldots, n$, of the interpolation spline $s(x)$ are determined from the interpolation conditions

$$s(x_i) = t_i, \quad i = 1, \ldots, n, \tag{9}$$

and from the conditions for the annulment of the spline trend

$$\sum_{i=1}^{n} \lambda_i \pi(P_i) = 0 \quad \forall \pi \in \mathcal{P}.$$

Choosing some basis $u_j \in \mathcal{P}$, $j = 1, \ldots, k$, $k = \dim \mathcal{P}$, and writing the function π from the trend $\mathcal{P}$ in the form

$$\pi(x) = \sum_{j=1}^{k} \mu_j u_j(x),$$

we obtain the system of linear equations

$$\begin{pmatrix} \boldsymbol{B} & \boldsymbol{C} \\ \boldsymbol{C}^T & \boldsymbol{O} \end{pmatrix} \begin{pmatrix} \boldsymbol{\lambda} \\ \boldsymbol{\mu} \end{pmatrix} = \begin{pmatrix} \boldsymbol{t} \\ \boldsymbol{0} \end{pmatrix}. \tag{10}$$

Here $\boldsymbol{B}$ is a symmetric matrix of size $(n \times n)$ with coefficients $b_{ij} = R(x_i, x_j)$, $\boldsymbol{C}$ is a matrix of size $(n \times k)$ with coefficients $c_{ij} = u_j(x_i)$, $\boldsymbol{O}$ is the null matrix, $\boldsymbol{\lambda} = (\lambda_1, \ldots, \lambda_n)^T$ and $\boldsymbol{\mu} = (\mu_1, \ldots, \mu_k)^T$ are vectors of unknowns spline coefficients, $\boldsymbol{t} = (t_1, \ldots, t_n)^T$ are the given values of the function, $\boldsymbol{0}$ is the column of zeros. For the unique solvability of the problem of determining the coefficients of a spline, it is also necessary to satisfy the conditions $n \geq k$ and $\operatorname{rank} \boldsymbol{C} = k$. These conditions will also be sufficient if the function $R(x, y)$ is conditionally positive definite (see [17]), therefore it serves as a reproducing kernel of some function space.

The condition for the minimum norm for a spline also allows us to formulate the problem of constructing a smoothing spline $s_\alpha(x)$, as a result of minimizing the functional

$$J_\alpha(f) = \alpha J(f) + \sum_{i=1}^{n} (f(x_i) - t_i)^2, \tag{11}$$

where $\alpha > 0$ is a parameter of smoothing that can be varied. Assuming that the system of equations (10) has a unique solution ($n \geq k$ and $\operatorname{rank} \boldsymbol{C} = k$), the smoothing spline $s_\alpha(x)$ is also uniquely determined, its coefficients satisfy the system of equations

$$\begin{pmatrix} \boldsymbol{B} + \alpha \boldsymbol{I} & \boldsymbol{C} \\ \boldsymbol{C}^T & \boldsymbol{O} \end{pmatrix} \begin{pmatrix} \boldsymbol{\lambda} \\ \boldsymbol{\mu} \end{pmatrix} = \begin{pmatrix} \boldsymbol{t} \\ \boldsymbol{0} \end{pmatrix}. \tag{12}$$

Here $\boldsymbol{I}$ is the identity matrix. It is obvious that when $\alpha \to 0$ the smoothing spline s_α tends to the interpolation one, and for $\alpha \to \infty$ in the limit we obtain a function from the trend $\mathcal{P}$ that minimizes the functional

$$\sum_{i=1}^{n} (f(x_i) - t_i)^2.$$

The radial basis function is considered as

$$\phi(r) = \begin{cases} (-1)^{m/2+1} r^m \ln r, & m \text{ is even}, \\ (-1)^{(m+1)/2} r^m, & m \text{ is odd}, \end{cases} \tag{13}$$

leading to D^m-splines or natural (thin plate) splines, which are sometimes called polyharmonic or pseudo-polynomial splines (see, for example, [14, 15]).

The practical construction of an interpolation spline is reduced to solving the system of equations (10). The questions of existence and uniqueness of general splines were studied in [18]. Note that the restrictions on the initial data that ensure the existence and uniqueness of the splines under consideration are not burdensome and, in essence, are reduced to the question of the existence in the set of points with data of a set of k points for which the interpolation polynomial $\pi(x)$ exists and is unique.

If the initial data have an error, then, as a rule, interpolation splines do not give an acceptable result. In such cases, it is necessary to construct smoothing splines, i.e. instead of the system of equations (10), it is necessary to solve the system (12) with changes in the matrix only in the entries of the main diagonal of the first block.

Note that although the complexities and difficulties of constructing interpolation and smoothing splines with radial basis functions are similar, the non-zero smoothing parameter α improves the conditionality of the system of equations. The smoothing parameter regulates the level of data smoothing. The value $\alpha = 0$ corresponds to an interpolation spline, i.e. $s(x) = s_0(x)$. With increasing α, the behavior of the spline becomes smoother, oscillations decrease or even disappear, but at the same time, generally speaking, the deviation from the initial data increases, as already noted, in the limit at $\alpha \to \infty$ the spline tends to some element of the trend. We add that the degree of smoothing, generally speaking, can be adjusted at each point; to do this, in the minimized functional (11), the corresponding weights must be added to each term, what does not lead to any complications in the calculations.

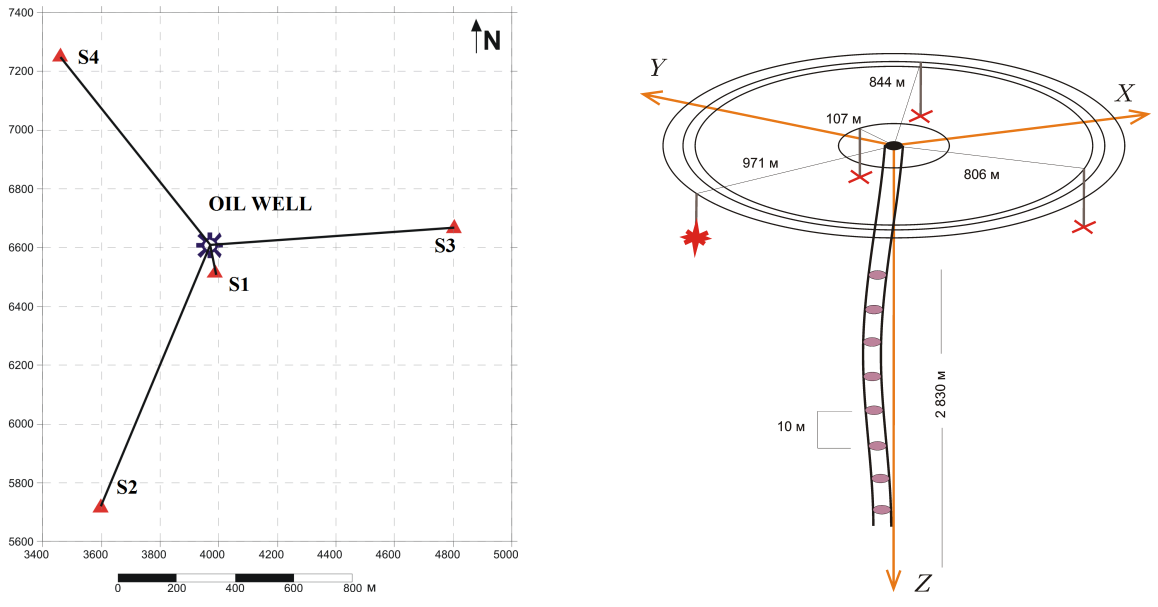

a) b)

Fig.1. Well is in the center, disturbance sources S2, S3, S4 uniformly along the azimuth, S1 – near the well.

The presented technology allows [19] to solve the problem of vertical seismic profiling for technologically acceptable depths, about 3000 m. Drilling wells is an expensive procedure. However, if a single drilling in

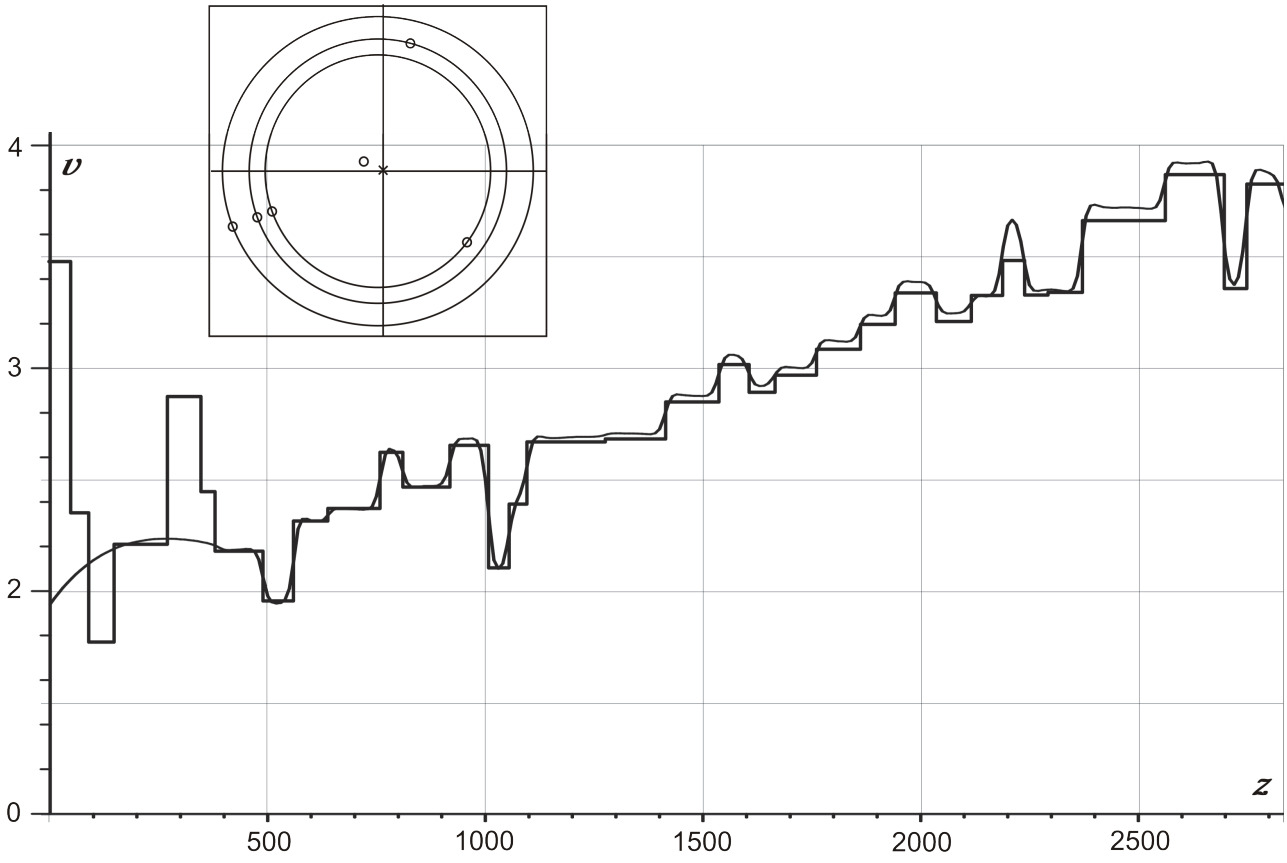

Fig.2. Piecewise constant function of the velocity of longitudinal waves characterizes the stratification of the medium near the well. Smooth function is the solution by the presented method of the IKPS with an inner source.

rocks is economically available or one of the wells of oil and gas fields can be temporarily decommissioned, then the study of the wellbore area can be carried out using logging. The well is used as a line of detectors, and the disturbance sources are located on the daylight surface with different azimuthal values. Assuming that the studied medium has a structure close to a layered one, the problem of determining the velocity characteristic in the studied area can be reduced to IKPS with internal sources. We demonstrate the method on a real problem. When studying the layered structure near the well, detectors are located inside the well, and disturbance sources are uniformly along azimuths around the well. Data on the arrival times of longitudinal waves are the initial information for the problem of describing the medium. Usually it is required to determine the velocity structure of the medium near the well. We assume local horizontal homogeneity of the studied area. Based on the principle of reversibility applied in seismology problems, we can theoretically consider the sources as detectors and vice versa. We now consider that in places S1,S2,S3,S4 the wells are located in which disturbances are produced, and one detector is located at the well site. The sketch in plan (a) and in isometric view (b) is given in Fig.1. According to the initial information on the wave travel times we construct a new hodograph function of three spatial variables. Thus we have 3D IKPS with an inner source and travel times of seismic waves from fictitious sources to a single detector. The solution to the problem using real data is shown in Fig.2. The assumption of horizontal homogeneity allows us to “multiply” the data by adding new fictitious wells at one of the azimuths. The top left square in Fig.2 shows the layout of fictitious wells. The initial information about the front travel times is also duplicated accordingly. The depth given in meters

is plotted horizontally, and the values of the longitudinal wave velocity in kilometers per second are plotted vertically. The piecewise constant function is the real layering of the medium.

The dynamics of the change in the state of the medium in the presence of time-dependent data can be described by moving to a spline approximation of a function of four variables, or by using averaging methods over short time intervals.

A problem that arises in close connection with the seismic and seismological problem under consideration is the problem of determining the velocity characteristics of the medium located in the entire region between the focal zone and seismic receivers. In modern terminology, this is a seismic tomography problem. From a tomographic point of view, it is often characterized as a problem with limitations on "viewing angles" and is highly ill-posed.

In conclusion, we note that the frequently used information about layer thicknesses of the initial segment in the data for our method is excessive and is not used, which simplifies data collection and calculations when solving the problem. Moreover, it is possible to use a priori information in various options at the data preparation stage. The mathematical tools allows applying various smoothing procedures, focusing attention on the details of interest.

Funding

The work of second and third authors was carried out as part of a state assignment for the Sobolev Institute of Mathematics, Siberian Branch, Russian Academy of Sciences (project No. FWNF-2022-0015).

Availability of data and materials

Not applicable.

Competing interests

The authors declare that they have no competing interests.

Author's contributions

All authors contributed equally to the writing of this paper. All authors read and approved the final manuscript.

References

[1] Herglotz, G.: *Über das Benndorfsche Problem der Fortpflanzungsgeschwindigkeit der Erdbebenstrahlen.* Physik. Zeitshrift. **8** (5), 145-147 (1907).
[2] Wiechert, E. *Über Erdbebenwellen. I. Theoretisches über die Ausbreitung der Erdbebenwellen.* Nachr. Ges. Wiss. Göttingen, Math.-Phys. Kl. **4**, 415-529 (1907).
[3] Romanov, V. G.: Inverse problems of mathematical physics. Nauka, Moscow (1984). [Russian]
[4] Goldin, S. V.: Geometric seismics. IPGG SB RAS, Novosibirsk (2017). [Russian]
[5] Pivovarova, N. B., Pivovarov, V. G.: *Methodical aspects of reconstruction of three-dimensional high-speed medium*. Vestnik Otdelenia nauk o Zemle RAN **1**, 21 (2003).
[6] Slavina, L. B., Pivovarova, N. B.: The dynamics of seismic velocity fields during periods of increased seismic and volcanic activity in kamchatka. IFZ RAS, Moscow (2009). [Russian]
[7] Gobarenko, V., Yegorova, T., Stifenson, R.: *The structure of the Kerch peninsula and north-eastern part of the Black sea crust according to the results of local seismic tomography*. Geofizicheskij zhurnal **36** (2), 38-59 (2014).
[8] Anikonov, Yu. E., Pivovarova, N. B., Slavina, L. B.: *Three-dimensional velocity field of the Kamchatka focal zone.* In: Mathematical problems of geophysics **5** (1). Vychislitel'nyj Tsentr SO AN SSSR, Novosibirsk, 92-117 (1974). [Russian]
[9] Slavina, L. B., Pivovarova, N. B., Levina, V. I.: *A study in the velocity structure of December 5, 1997, M w = 7.8 Kronotskii rupture zone, Kamchatka*. J. Volcanol. Seismol. **1** (4), 254-262 (2007).
[10] Anikonov, Yu. E., Bogdanov, V. V., Derevtsov, E. Yu., Miroshnichenko, V.L., Sapozhnikova, N. A.: *Numerical solution of an inverse kinematic seismic problem with internal sources.* Sib. Zh. Ind. Mat. **9** (4), 3-26 (2006).

[11] Anikonov, Yu. E., Bogdanov, V. V., Derevtsov, E. Yu., Miroshnichenko, V. L., Pivovarova, N. B., Slavina, L. B.: *Some approaches to a numerical solution for the multidimensional inverse kinematic problem of seismics with inner sources.* J. Inv. Ill-Posed Problems textbf17 (3), 209-238 (2009).
[12] Anikonov, Yu. E., Bogdanov, V. V., Volkov, Yu. S., Derevtsov, E. Yu.: *On the determination of the velocity and elastic parameters of a medium in the focal zone from earthquake hodographs.* J. Appl. Ind. Math. **15** (4), 569-585 (2021).
[13] Wendland, H.: Scattered data approximation. Cambridge, Cambridge University Press (2005).
[14] Rozhenko, A. I.: Theory and algorithms of variational spline approximation. ICM&MG SB RAS, Novosibirsk (2005). [Russian]
[15] Ignatov, M. I., Pevny, A. B.: Natural splines of many variables. Nauka, Leningrad (1991). [Russian]
[16] Schaback, R.: *Native Hilbert spaces for radial basis functions I.* In: New developments in approximation theory (ISNM, 132). Basel, Birkhäuser, 255-282 (1999).
[17] Rozhenko, A. I.: *Comparison of radial basis functions.* Numer. Analysis Appl. **11** (3), 220-235 (2018).
[18] Rozhenko, A. I., Shaidorov T. S.: *On spline approximation with a reproducing kernel method.* Numer. Analysis Appl. **6** (4), 314-323 (2013).
[19] Bogdanov, V. V., Karsten, W. V., Miroshnichenko, V. L., Volkov, Yu. S.: *Application of splines for determining the velocity characteristic of a medium from a vertical seismic survey.* Central European J. Math. **11** (4), 779-786 (2013).

Affiliations

Akram Begmatov
Address: Tashkent state transport university, 1 Temiryolchilar Street, Mirobod District, Tashkent, Uzbekistan.
e-mail: akrambegmatov@mail.ru
ORCID ID: 0000-0002-2813-7653

Vladimir Bogdanov
Address: Sobolev Institute of Mathematics, 4 Acad. Koptyug avenue, 630090, Novosibirsk, Russia.
e-mail: bogdanov@math.nsc.ru

Yuriy Volkov
Address: Sobolev Institute of Mathematics, 4 Acad. Koptyug avenue, 630090, Novosibirsk, Russia.
e-mail: volkov@math.nsc.ru
ORCID ID: 0000-0002-7298-8578

Uzbekistan Journal of Mathematics and Computer Science
Volume 1 No. 1 Page 41–49 (2025)
DOI: https://doi.org/10.56143/ujmcs.v1i1.9
Research article

UZJMCS

Periodic Solution of the Keller-Segel Model With Logistic Sensitivity

Takhirov Jozil Ostonovich* **Anvarjonov Bunyodbek Baxodirovich**

Abstract

Mathematical modeling of chemotaxis (the movement of biological cells in response to chemical gradients) has evolved into a modern discipline, aspects of which include its mechanistic basis, modeling of specific systems, and the mathematical behavior of the underlying equations. In this paper, we consider in detail the periodic variant of the Keller-Segel model. The global existence and uniqueness of the classical solutions of this system are proved by the contraction mapping principle together with L_p estimates and Schauder estimates of parabolic equations.

Keywords: *Reaction–diffusion-taxis system; Chemotaxis; haptotaxis; Schauder estimates; Global existence.*

AMS Subject Classification (2020): *Primary: 35B40; 35B65. Secondary: 35K57; 35Q92.*

1. Introduction

Theoretical and mathematical modeling of chemotaxis goes back to the well-known works of Keller and Segel [1, 2]. The review article by Horstmann [3] gives a detailed introduction to the mathematics of the Keller-Segel (KS) model of chemotaxis. In its original form, this model consists of four coupled reaction-advection-diffusion equations. They can be reduced under quasi-steady-state conditions to a model for two unknown functions u and v, which will form the basis of our study in this paper. The general form of the model is: his is an example of a numbered second-level heading.

$$\begin{aligned} u_t &= \nabla(k_1(u,v)\nabla u - k_2(u,v)u\nabla v) + k_3(u,v), \\ v_t &= D\Delta v + k_4(u,v) - k_5(u,v)v, \end{aligned} \tag{1.1}$$

where u denotes the density of cells (or organisms) in a given region $Q \subset R_n$, and v describes the concentration of the chemical signal. Cell dynamics follow from population kinetics and motion, the latter including a diffusive flux modeling undirected (random) cell migration and an advective flux with a velocity dependent on the signal gradient modeling the contribution of chemotaxis. $k_1(u,v)$ describes the cell diffusivity (sometimes also called motility), while $k_2(u,v)$ is the chemotactic sensitivity; both functions may depend on the levels of u and v. k_3 describes cell growth and death, while k_4 and k_5 are kinetic functions describing the production and degradation of the chemical signal. A key property of the above equations is their ability to induce spatial patterning when the chemical signal acts as an autoattractant, i.e. when cells both produce and migrate up chemical signal gradients.

Received : *03–february–2025,* ***Accepted :*** *25–march–2025*
*** Corresponding author***

Although several additional approaches have been developed (e.g., stochastic and discrete approaches, [4, 5, 6], it is the deterministic continuum Keller–Segel model that has become the predominant method for representing chemotactic behavior in biological systems at the population level. Much effort has been devoted to explaining their origins in the mechanistic/microscopic description of the motion. Horstmann's review [3] discusses five methods in detail, and we refer to this work for further details in this important area. As mentioned above, Keller–Segel type equations have become widely used in chemotaxis models as a result of their ability to capture key phenomena, their intuitive nature, and their relative tractability (analytically and numerically) compared to discrete/individual approaches.

In addition to their use in models of biological systems, a large body of work has appeared on the mathematical properties of the Keller-Segel equations (1.1) and, in particular, on the conditions under which specializations or variations (1.1) either lead to a finite time explosion or have globally existing solutions.

Each of the variations is introduced in a form that includes one additional parameter that, under an appropriate limit, reduces the system to a minimal form. In many cases, this modification orders the problem in such a way that solutions exist globally in time.

Mathematical modeling of chemotaxis (the movement of biological cells in response to chemical gradients) has become a modern discipline, aspects of which include its mechanistic basis, modeling of specific systems, and the mathematical behavior of the basic equations. Currently, there are mathematical models (or a class of models) of these processes that are two [7] or three-component [8, 9] systems of parabolic equations of the reaction-diffusion type, and they are studied from the point of view of wave regimes [7] or global solvability [8, 9]. In [10] a two-component model constructed in [11] was investigated:

$$\begin{aligned} u_t - d_1\Delta u + \nabla(u\chi(u)\nabla v) = -au + bg(v)u, \quad (x,t) \in Q_T, \\ v_t - d_2\Delta v = k(v) - g(v)u, \quad (x,t) \in Q_T. \end{aligned} \tag{1.2}$$

with initial boundary conditions

$$\frac{\partial u}{\partial \nu} = \frac{\partial v}{\partial \nu} = 0 \text{ on } S_T, \tag{1.3}$$

$$u(x,0) = u_0(x), v(x,0) = v_0(x), x \in \Omega. \tag{1.4}$$

In this paper, we consider the one-dimensional (flat) case of system (1.2) with periodic boundary conditions.

In the domain $D = \{(x,t) : 0 < t \leqslant T, -l < x < l\}$, it is required to find a solution $(u(x,t), v(x,t))$ to the problem

$$u_t - d_1 u_{xx} + (u\chi(u)v_x)_x = -au + bg(v)u, \quad (x,t) \in D, \tag{1.5}$$

$$v_t - d_2 v_{xx} = k(v) - g(v)u, \quad (x,t) \in D, \tag{1.6}$$

$$u(-l,t) = u(l,t), u_x(-l,t) = u_x(l,t), \quad 0 \leqslant t \leqslant T, \tag{1.7}$$

$$v(-l,t) = v(l,t), v_x(-l,t) = v_x(l,t), \quad 0 \leqslant t \leqslant T, \tag{1.8}$$

$$u(x,0) = u_0(x), v(x,0) = v_0(x), \quad -l \leqslant x \leqslant l. \tag{1.9}$$

Throughout this work, the following constraints are assumed to hold:

1) $\chi(u) \in C'([0,\infty]), \chi(u) \equiv 0$ for $u \geqslant u_m$ - positive constant, $\chi'(u)$ - Lipschitz continuous;

2) $u_0(x) \geqslant 0, 0 \leqslant v_0(x) \leqslant K, u_0(x), v_0(x) \in C^{2+\alpha}(-l \leqslant x \leqslant l), 0 < \alpha < 1;$

3) At the corner points $(0,-l),(0,l)$ the first-order compatibility conditions are satisfied:
$u_0(-l)=u_0(l), u_0'(-l)=u_0'(l), v_0(-l)=v_0(l), v_0'(-l)=v_0'(l)$.

Throughout this work, we use ideas and methods, as well as the notations of functional spaces and norms from the works. [10, 13].

$C_{x,t}^{m+\alpha,\beta}(D)$ (m - a positive integer, $0<\alpha<1, 0<\beta<1$) - Banach space of functions $u(x,t)$ with a finite norm

$$\|u\|_{C_{x,t}^{m+\alpha,\beta}(D)}=\sum_{|l|=0}\left[\sup_D|\partial_x^l u|+<D_x^l u>_{x,D}^{(\alpha)}+<D_x^l u>_{D,t}^{(\beta)}\right],$$

where

$$<w>_{x,D}^{(\alpha)}=\sup_{(x,t),(y,t)\in D}\frac{|w(x,t)-w(y,t)|}{|x-y|^{\alpha}},$$
$$<w>_{D,t}^{(\beta)}=\sup_{(x,t),(\tau,t)\in D}\frac{|w(x,t)-w(x,\tau)|}{|t-\tau|^{\beta}}.$$

$C_{x,t}^{2+\alpha,1+\beta}(D)$ - function space $u(t,x)$ with a norm $\|u\|_{C_{x,t}^{2+\alpha,\beta}(D)}+\|u_t\|_{C_{x,t}^{\alpha,\beta}(D)}$.

2. Local solvability of the problem

First, let us consider the following nonlinear problem for the parabolic equation.

$$u_t-d_1u_{xx}+(c(u)v_x)_x=f(x,t)u,\quad (x,t)\in D, \tag{2.1}$$
$$u(-l,t)=u(l,t), u_x(-l,t)=u_x(l,t),\quad 0\leqslant t\leqslant T, \tag{2.2}$$
$$u(x,0)=u_0(x)\geqslant 0,\quad -l\leqslant x\leqslant l, \tag{2.3}$$

where $c(u)=u\chi(u)$.

Next, through A_0 we denote constants that do not depend on T, and through A we denote constants that depend on T.

Lemma 2.1. *Let $v(x,t)\in C^{2+\alpha,1+\frac{\alpha}{2}}(D), f(x,t)\in C^{\alpha,\frac{\alpha}{2}}(D)$ and*

$$\|v\|_{C^{2+\alpha,1+\frac{\alpha}{2}}(D)}, \|f\|_{C^{2+\alpha,1+\frac{\alpha}{2}}(D)}\leqslant A_0. \tag{2.4}$$

Then there exists a unique nonnegative solution. $u(x,t)\in C^{2+\alpha,1+\frac{\alpha}{2}}(D)$ of the problem. (1.9)-(2.2) for small T, depending on $\|u_0\|_{C^{2+\alpha}(-l\leqslant x\leqslant l)}$.

Proof. The lemma is proved using the fixed-point principle [13, 14]. We introduce the Banach space. X of functions. $u(x,t)$ with a norm

$$\|u\|_{C^{2+\alpha,\frac{\alpha}{2}}(D)},(0<T<1)$$

and the set

$$X_B=\left\{u\in X: u(x,0)=u_0(x), \|u\|_{C^{2+\alpha,\frac{\alpha}{2}}(D)}\leqslant B\right\},$$

where $B=\|u_0\|_{C^{2+\alpha}(-l\leqslant x\leqslant l)}+\|v_0\|_{C^{2+\alpha}(-l\leqslant x\leqslant l)}+1$.

For each $u\in X_B$ we define the mapping $\tilde{u}=Fu$, where $\tilde{u}$ satisfies the conditions.

$$\tilde{u}_t-d_1\Delta\tilde{u}-f\tilde{u}=-c'(u)u_xv_x-c(u)\Delta v,(x,t)\in D, \tag{2.5}$$

$$\tilde{u}(-l,t)=\tilde{u}(l,t),\tilde{u}_x(-l,t)=\tilde{u}_x(l,t),0\leqslant t\leqslant T, \tag{2.6}$$

$$\tilde{u}(x,0)=u_0(x),-l\leqslant x\leqslant l. \tag{2.7}$$

By virtue of the conditions 1)-3) and $u(x,t)\in X_B$, we have

$$f_1(x,t)=-c'(u)u_xv_x-c(u)v_{xx}\in C^{\alpha,\frac{\alpha}{2}}(D). \tag{2.8}$$

Taking the conditions into account 2) and (2.4) and the theory of parabolic equations [13], as well as the results on periodic solutions of quasilinear parabolic equations [15] we conclude that there exists a unique solution $\tilde{u}(x,t)$ of the problem. (2.5)-(2.7) and the estimate holds

$$\|\tilde{u}\|_{C^{2+\alpha,1+\frac{\alpha}{2}}(D)}\leqslant\|u_0(x)\|_{C^{2+\alpha}(-l\leqslant x\leqslant l)}+M_1(B)\leqslant B+M_1(B)=M_2(B). \tag{2.9}$$

In this section, constants depending on B are denoted by $M_j=M_j(B)$, $j=3,4$.

Next, as in the work [10] it is proved that the transformation F maps the set X_B into itself and is a contraction.

Here, the nonnegativity of the function can be established $u(t,x)$. We rewrite (2.1) in the form of

$$u_t-d_1\Delta u+c'(u)u_xv_x+(\chi(u)v_{xx}-f)u=0,(x,t)\in D. \tag{2.10}$$

From the problem (2.10), (2.2), (2.3) by the maximum principle [13] we have

$$u(x,t)\geqslant 0,(x,t)\in\bar{D}.$$

This concludes the proof of Lemma 2.1. □

Now, we proceed to prove the local unique solvability of the problem (1.5)-(1.9). For convenience, we introduce the notation $U=(u,v)$.

Theorem 2.1. *Suppose that conditions 1)-3) are satisfied. Then, there exists a unique solution* $U(x,t)\in C^{2+\alpha,1+\frac{\alpha}{2}}(D)$ *of the problem.* (1.5)-(1.9) *for small.* $T>0$, *depending on* $\|U_0\|_{C^{2+\alpha}}=\|u_0\|_{C^{2+\alpha}}+\|v_0\|_{C^{2+\alpha}}$. *Moreover*

$$u(x,t)\geqslant 0,v(x,t)\geqslant 0.$$

Proof. We apply the fixed-point principle again. Let us introduce the Banach space Y of functions $U(x,t)$ with a norm $\|U\|_{C^{\alpha,\frac{\alpha}{2}}(D)}$ and a subset

$$Y_B=\left\{U\in Y:u\geqslant 0,v\geqslant 0,U(x,0)=(u_0(x),v_0(x)),\|U\|_{C^{\alpha,\frac{\alpha}{2}}(D)}\leqslant B\right\}.$$

For $U\in Y_B$ we define the corresponding function $\tilde{U}=GU$, where $\tilde{U}(x,t)$ satisfies the following conditions

$$\tilde{v}_t-d_2\tilde{v}_{xx}=\left(r-\frac{r}{K}v-\frac{b_1u}{1+b_2v}\right)\tilde{v},\quad (x,t)\in D, \tag{2.11}$$

$$\begin{gathered}\tilde{v}(-l,t)=\tilde{v}(l,t),\tilde{v}_x(-l,t)=\tilde{v}_x(l,t),\quad 0\leqslant t\leqslant T,\\ \tilde{v}(x,0)=v_0(x),\quad -l\leqslant x\leqslant l,\end{gathered} \tag{2.12}$$

$$\tilde{u}_t-d_1\tilde{u}_{xx}+(c(\tilde{u})\tilde{v}_x)_x=(-a+bg(v))\tilde{u},\quad (x,t)\in D, \tag{2.13}$$

$$\begin{gathered}\tilde{u}(-l,t)=\tilde{u}(l,t),\tilde{u}_x(-l,t)=\tilde{u}_x(l,t),\quad 0\leqslant t\leqslant T,\\ \tilde{u}(x,0)=u_0(x),\quad -l\leqslant x\leqslant l.\end{gathered} \tag{2.14}$$

First, let us consider the problem (2.11)-(2.12). Since $(u,v)\in Y_B$, then, due to conditions 1)-3), the expression in parentheses on the right-hand side (2.11) (the coefficient in front of $\tilde{v}$) satisfies the Hölder condition. Then,

by the theory of linear parabolic equations [13, 15] there exists a unique solution to the problem (2.11)-(2.13) and the estimate holds

$$\|\tilde{v}\|_{C^{2+\alpha,1+\frac{\alpha}{2}}(D)} \leqslant \|v_0(x)\|_{C^{2+\alpha}(-l\leqslant x\leqslant l)} + M_3(B) \leqslant B + M_3(B) = M_4(B). \tag{2.15}$$

In turn, by the maximum principle $\tilde{v}(x,t) \geqslant 0, (x,t) \in \bar{D}$.

Similarly, it is proved that, taking into account (2.15) the problem (2.13),(2.14) has a unique solution $\tilde{u}(x,t)$ and the estimates hold

$$\|\tilde{u}\|_{C^{2+\alpha,1+\frac{\alpha}{2}}(D)} \leqslant M_5(B), \tilde{u}(x,t) \geqslant 0, (x,t) \in D. \tag{2.16}$$

From (2.15) and (2.16) we conclude that

$$\|\tilde{U}\|_{C^{2+\alpha,1+\frac{\alpha}{2}}(D)} \leqslant M_6(B). \tag{2.17}$$

For $\tilde{U}(x,t)$ using the definition of Hölder continuity, it can be established that

$$\|\tilde{U}(x,t) - \tilde{U}(x,0)\|_{C^{2,\frac{\alpha}{2}}(D)} \leqslant A_0 \max(T^{\frac{\alpha}{2}}, T^{1-\frac{\alpha}{2}})\|\tilde{U}\|_{C^{2+\alpha,1+\frac{\alpha}{2}}(D)}. \tag{2.18}$$

By combining (2.17) and (2.18) we conclude that if T is sufficiently small, then

$$\|\tilde{U}\|_{C^{\alpha,\frac{\alpha}{2}}(D)} \leqslant \|\tilde{U}(x,0)\|_{C^{\alpha,\frac{\alpha}{2}}(D)} + A_0 \max(T^{\frac{\alpha}{2}}, T^{1-\frac{\alpha}{2}})M_6(B) \leqslant \|U_0(X)\|_{C^{2+\alpha}(D)} + 1 \equiv B. \tag{2.19}$$

Then, due to the nonnegativity u, v and (2.19) we have that $\tilde{U} \in Y_B$. Therefore, G maps Y_B into itself.

Next, as in the work [10] it can be proved that the operator is a contraction G. Using the theory of parabolic equations, it can be established that $U(x,t) \in C^{2+\alpha,1+\frac{\alpha}{2}}(D)$.

Theorem 2.1 is proved. □

3. Global solvability of the problem

It is known that, thanks to results on linear problems and fixed-point theorems for completely continuous mappings, the question of the solvability of problems reduces to the issue of a priori boundedness of Hölder norms (the classical solvability case) for all possible solutions of these problems. Depending on the method used to establish a priori estimates, sometimes the following are applied L_p estimates and embedding theorems [13].

Therefore, we proceed to obtain a priori estimates.

Lemma 3.1. *Let the pair of functions $(u,v) \in C^{2,1}(D)$ be the solution to the problem (1.5)-(1.9). Then*

$$u(x,t) \geqslant 0, 0 \leqslant v(x,t) \leqslant K, \quad (x,t) \in D. \tag{3.1}$$

Proof. From (1.5), (1.7), (1.9) we have

$$u_t - d_1 u_{xx} + c'(u)v_x u_x + [\chi(u)v_{xx} + a - bg(v)]u = 0, \quad (x,t) \in D, \tag{3.2}$$

$$u(-l,t) = u(l,t), u_x(-l,t) = u_x(l,t), \quad 0 \leqslant t \leqslant T, \tag{3.3}$$

$$u(x,0) = u_0(x) \geqslant 0, \quad -l \leqslant x \leqslant l. \tag{3.4}$$

It is clear that $\underline{u}(x,t) \equiv 0$ is a lower solution [14] of the problem (3.2)-(3.4). Therefore, by the maximum principle $u(x,t) \geqslant 0$ in $\bar{D}$.

Similarly $v(x,t) \geqslant 0$ in $\bar{D}$.

From (1.6), (1.8), (1.9) taking into account the inequalities $u(x,t) \geqslant 0, v(x,t) \geqslant 0$, we have

$$v_t - d_2 v_{xx} = k(v) - g(v)u \leqslant k(v), \quad (x,t) \in D, \tag{3.5}$$

$$v(-l,t) = v(l,t), v_x(-l,t) = v_x(l,t), \quad 0 \leqslant t \leqslant T, \tag{3.6}$$

$$v(x,0) = v_0(x) \geqslant 0, \quad -l \leqslant x \leqslant l. \tag{3.7}$$

Let $\bar{v}(t)$ be the solution to the problem

$$\bar{v}'(t) = r\bar{v}(t)\left(1 - \frac{\bar{v}(t)}{K}\right), \bar{v}(0) = \max_{-l\leqslant x\leqslant l} v_0(x) \leqslant K, \tag{3.8}$$

which has the form

$$\bar{v}(t) = Ke^{Kt}\left(e^{Kt} - 1 + \frac{K}{\bar{v}(0)}\right)^{-1}, \quad 0 \leqslant \bar{v}(t) \leqslant K.$$

It can be established that $\bar{v}(t)$ is the upper solution [14] of the problem (3.5)-(3.7). Therefore, by the maximum principle

$$v(x,t) \leqslant \bar{v}(t) \leqslant K. \tag{3.9}$$

Lemma 3.1 is proved. □

Lemma 3.2. *Let a pair of functions $(u,v) \in C^{2,1}(D)$ are solutions to the problem (1.5)-(1.9). Then*

$$\|u\|_{L^{p+1}(D)} \leqslant A, \quad p > 1. \tag{3.10}$$

Proof. Multiplying (1.5) by u^p and integrating over D_t, taking into account the conditions (1.7), (1.9) and inequalities $u(x,t) \geqslant 0, 0 \leqslant g(v) \leqslant \frac{b_1}{b_2}$, we find

$$\frac{1}{1+p}\int_{-l}^{l} u^{p+1}(x,t)dx - \frac{1}{1+p}\int_{-l}^{l} u_0^{p+1}(x)dx + pd_1\int_0^t dt\int_{-l}^{l} u^{p-1}u_x^2(x,t)dx \leqslant$$

$$\leqslant p\int_0^t dt\int_{-l}^{l} u^{p-1}\chi(u)u_x v_x dx + \frac{bb_1}{b_2}\int_0^t dt\int_{-l}^{l} u^{p+1}dx. \tag{3.11}$$

Taking assumption 1) into account, we transform the first term on the right-hand side (3.11)

$$J = \left|p\int_0^t dt\int_{-l}^{l} u^{p-1}\chi(u)u_x v_x dx\right| = \left|\int_0^t dt\int_{-l}^{l} u^{\frac{p-1}{2}}\chi(u)u^{\frac{p-1}{2}}u_x v_x dx\right| \leqslant$$

$$\leqslant u_m^{\frac{p-1}{2}}\max_{0\leqslant u\leqslant u_m}\chi(u)\int_0^t dt\int_{-l}^{l}\left|u^{\frac{p-1}{2}}u_x v_x\right|dx \leqslant \varepsilon\int_0^t dt\int_{-l}^{l} u^{p-1}u_x^2 dx + \frac{1}{2\varepsilon}A_0\int_0^t dt\int_{-l}^{l} u_x^2 dx. \tag{3.12}$$

Next, by multiplying (1.6) by v and integrating over D_t, taking into account (1.8), (1.9) and inequalities $u \geqslant 0, v \geqslant 0, k(v) \leqslant rv$, we find

$$\frac{1}{2}\int_{-l}^{l} v^2(x,t)dx - \frac{1}{2}\int_{-l}^{l} u_0^2(x)dx + d_2\int_0^t dt\int_{-l}^{l} v_x^2 dx \leqslant r_1\int_0^t dt\int_{-l}^{l} v^2(x,t)dx. \tag{3.13}$$

Hence, taking into account (3.1) and (1.3) we have

$$\int_0^t dt \int_{-l}^{l} u_x^2(x,t)dx \leqslant A. \tag{3.14}$$

Now, combining (3.11), (3.12) and (3.14), we obtain

$$\int_{-l}^{l} u^{p+1}(x,t)dx + p(p+1)(d_1-\varepsilon)\int_0^t \int_{-l}^{l} u^{p-1}u_x^2 dxdt \leqslant A + A_0 \int_0^t dt \int_{-l}^{l} u^{p+1}(x,t)dx. \tag{3.15}$$

Choosing $0 < \varepsilon < d_1$ from (3.14) we find

$$\int_{-l}^{l} u^{p+1}(x,t)dx \leqslant A + A_0 \int_0^t dt \int_{-l}^{l} u^{p+1}(x,t)dx. \tag{3.16}$$

Hence, by the Bellman–Gronwall inequality, we have

$$\int_0^t dt \int_{-l}^{l} u^{p+1}(x,t)dx \leqslant A.$$

Lemma 3.2 is proved. □

Lemma 3.3. *Let a pair of functions $(u,v) \in C^{2,1}(D)$ are solutions to the problem (1.5)-(1.9). Then the following inequality holds*

$$\|u,v\|_{W_p^{2,1}(D)} \leqslant A, \quad p > 3. \tag{3.17}$$

Proof. We rewrite the equation (1.6) in the form

$$v_t - d_2 v_{xx} - \left(r - \frac{r}{K}v - \frac{b_1 u}{1+b_2 v}\right)v = 0. \tag{3.18}$$

By virtue of (3.1) and (3.10) we have

$$\left\| r - \frac{r}{K}v - \frac{b_1 u}{1+b_2 v} \right\|_{L^p(D)} \leqslant A.$$

For the function $v(t,x)$ we have the following problem

$$\begin{gathered} v_t - d_2 v_{xx} - c_1(x,t)v = 0, \quad D, \\ v(-l,t) = v(l,t), v_x(-l,t) = v_x(l,t), \quad 0 \leq t \leq T, \\ v(x,0) = v_0(x) \geqslant 0, \quad 0 \leqslant x \leqslant l, \end{gathered} \tag{3.19}$$

where $c_1(x,t) \subset L_p(D), v_0(x) \in C^{2+\alpha}(-l \leqslant x \leqslant l)$.

According to Theorem 9.1 ([13], Chapter IV) for the solution of problem (3.19) the following inequality holds

$$\|v\|_{W_p^{2,1}(D)} \leqslant A. \tag{3.20}$$

Taking (3.20) into account and applying the Sobolev embedding theorem ([13], Lemma 3.3, Chapter II), we obtain

$$\|v_x\|_{L^\infty(D)} \leqslant A. \tag{3.21}$$

Now we rewrite equation (1.5) in the form

$$u_t - d_1 u_{xx} + c'(u)v_x u_x = -c(u)v_{xx} - au + bg(v)u, \tag{3.22}$$

where, by virtue of 1), (3.1), (3.10), (3.20), (3.21) the following estimates hold

$$\|c'(u)v_x\|_{L^\infty(D)} \leqslant A, \| - c(u)v_{xx} - du + bg(v)u\|_{L^p(d)} \leqslant A. \tag{3.23}$$

As in the case of problem (3.19), from (3.22) and (3.23) we conclude that

$$\|u\|_{W_p^{2,1}(D)} \leqslant A.$$

Lemma 3.3 is proved. □

Lemma 3.4. *Let a pair of functions* $(u, v) \in C^{2,1}(D)$ *be a solution to problem* (1.5)-(1.9). *Then the following inequality holds*

$$\|u, v\|_{C^{2+\alpha,1+\frac{\alpha}{2}}(D)} \leqslant A. \tag{3.24}$$

Proof. By virtue of estimate (3.17) and the results of ([13],Chapter II, Lemma 3.3 and Chapter IV, Corollary 3.9), one can assert that

$$\|u, v\|_{C^{\alpha,\frac{\alpha}{2}}(D)} \leqslant A. \tag{3.25}$$

Now, in (3.19) the equation can be considered as a linear equation with Hölder-continuous coefficients.
In this case, applying the results of ([13], Chapter IV, Theorem 2.2) and [15] to problem (3.19), we obtain

$$\|v\|_{C^{\alpha,\frac{\alpha}{2}}(D)} \leqslant A. \tag{3.26}$$

At first, internal estimates are established under the assumption that $v(t, x)$ possesses the generalized derivatives v_{xx} and v_{tx}, then, by applying the extension method through the lateral boundaries, the result is obtained in $\bar{D}$.

Now, it can be asserted that

$$\|v\|_{C^{2+\alpha,1+\frac{\alpha}{2}}(D)} \leqslant A. \tag{3.27}$$

Next, applying Schauder's parabolic estimates and the established inequalities (3.25), (3.27) from (3.22) we obtain

$$\|u\|_{C^{2+\alpha,1+\frac{\alpha}{2}}(D)} \leqslant A. \tag{3.28}$$

Lemma 3.4 is proved. □

Using the established estimates, the following theorem can be proved.

Theorem 3.1. *Under assumptions 1)–3), there exists a unique solution* $(u, v) \in C^{2+\alpha,1+\frac{\alpha}{2}(D)}$ *to problem* (1.4)-(1.8) *for any given* $T > 0$.

4. CONCLUSION

It is known that in 1970 Keller and Segel presented a famous mathematical model to describe chemotaxis. Since then, great efforts have been made to understand the classical chemotaxis model and its various variants. But there are still many open and interesting problems in understanding chemotaxis models. In particular, to the best of our knowledge, there have been no studies of chemotaxis models with periodic boundary conditions.

Therefore, we investigate the global existence of periodic solutions of the two-species Keller-Segel model with competing logistic terms. By increasing the regularity of the solution from L_1 to $L_p (p > 1)$, the existence and uniqueness of the classical global-in-time solution of this chemotaxis model are proven for any chemotactic coefficient $\chi > 0$ when the dimension of the space is equal to one.

References

[1] Keller, E.F., Segel, L.A.: *Initiation of slime mold aggregation viewed as an instability.* J. Theor. Biol. 26, 399–415 (1970).
[2] Keller, E.F., Segel, L.A.: *Model for chemotaxis.* J. Theor. Biol. 30, 225–234 (1971).
[3] Horstmann, D.: *From 1970 until present: the Keller–Segel model in chemotaxis and its consequences.* I. Jahresberichte DMV 105(3), 103–165 (2003).
[4] Maree, A.F., Hogeweg, P.: *Walter Riemannian submanifolds with concircular canonical field.* Proc. Natl. Acad. Sci. USA 98(7), 3879–3883 (2001).
[5] Mimura, M., Tsujikawa, T.: *Aggregation pattern dynamics in a chemotaxis model including growth.* Physica A 230, 499–543 (1996).
[6] Mittal, N., Budrene, E.O., Brenner, M.P., Van Oudenaarden, A.: *Motility of Escherichia coli cells in clusters formed by chemotactic aggregation.* Proc. Natl. Acad. Sci. USA 100(23), 13259–13263 (2003).
[7] Lee, J.M. et al.: *Pattern formation in prey-taxis systems.* J.Biological Dynamics. 3(6): 551–573 (2009).
[8] Tao, Y., Cui, C.: *A density-dependent chemotaxis-haptotaxis system modeling cancer invasion.* J. Math.Anal. and Appl. 367: 612–624 (2010).
[9] Li, C.: *Global existence of classical solutions to the cross-diffusion three-species model with prey-taxis.* Computers and Mathematics with Appl. 72: 1394–1401 (2016).
[10] Tao, Y.: *Global existence of classical solutions to a predator-prey model with nonlinear prey-taxis.* Nonlinear Analysis: RWA. 11: 2056–2064 (2010).
[11] Ainseba, B.E. et al.: *A reaction-diffusion system modeling predator-prey with prey-taxis.* Nonlinear Analysis: RWA. 9: 2086–2105 (2008).
[12] Benhadmane, M.: *Analysis of reaction-diffusion system modeling predator-prey with prey-taxis.* Net.Hetero.Med. 3: 863–879 (2008).
[13] Ladyzhenskaya, O.A., Solonnikov, B.A., Uralceva, N.N.: *Linear and Quasilinear Equations of Parabolic Type.* M.:Nauka. 736 p.(1967).
[14] Friedman, A.: *Partial Differential Equations of Parabolic Type.* M.:Mir. 428 p. (1968).
[15] Dzhuraev, T.D., Takhirov, J.O.:*A problem for quasilinear parabolic equation with nonlocal boundary conditions.* Georg.Math.J. 6(5): 421–428 (1999).
[16] Kruzhkov, S.N.: *Nonlinear parabolic equations with two independent variables.* Proceedings of MMS 16: 329–346 (1967).

Affiliations

Takhirov Jozil Ostonovich
Address: Institute of Mathematics, Uzbekistan Academy of Sciences, 9, University str., Tashkent 100174, Uzbekistan.
e-mail: prof.takhirov@yahoo.com
ORCID ID:

Anvarjonov bunyodbek Baxodirovich
Address: Institute of Mathematics, Uzbekistan Academy of Sciences, 9, University str., Tashkent 100174, Uzbekistan.
e-mail: bunyodbek.anvarjonov@bk.ru
ORCID ID:

Uzbekistan Journal of Mathematics and Computer Science
Volume 1 No. 1 Page 50–56 (2025)
DOI: https://doi.org/10.56143/ujmcs.v1i1.5
Research article

UZJMCS

Restoration From The External Curvature Of A Surface With A Single Vertex

Tillayev Donyorbek

Abstract

It is known that the points of a convex surface are divided into three classes: regular points, edge points, and vertices. There exists a class of surfaces that have a vertex at a single point, with all other points being regular. Such surfaces are called single-vertex surfaces, and the article provides some properties of the external curvature of such surfaces. Furthermore, the existence and uniqueness of a single-vertex surface have been proven, where the boundary consists of some closed spatial curve, and the external curvature is equal to a function defined on all Borel sets, given in advance. In this case, certain necessary conditions are imposed on the external curvature function.

In the analytical formulation, this problem proves the existence of a solution to the Dirichlet problem for a domain with a singular point.

Keywords: *surface, convex surface; point; ribbed; vertex; external curvature; tangent cone; polyhedra; support plane; tangent plane.*

AMS Subject Classification (2020): *Primary: 53A05 ; Secondary: 53C45.*

Introduction

The problem of surface recovering by a given external curvature is important in geometry "In general". This problem initially arose in the class of convex polyhedra and was generalized for regular surfaces using the well-known method of A. D. Alexandrov.

In works [4, 11], the focus is placed on identifying invariants and surfaces that are isometric on sections. This research examines the expansion properties of convex polyhedra, specifically those that maintain isometry on their sections. These studies are important for understanding the preservation of geometric properties in deformations of convex shapes.

For convex polyhedra, an invariant has been associated with the vertex of a convex polyhedral angle. By utilizing this invariant, the problem of reconstructing a convex polyhedron with specific conditional curvature values at the vertices can be addressed. This allows for the determination of a polyhedron's geometry based on curvature constraints.

In paper [12], the authors provide definitions, fundamental concepts, and formulas related to the geometric characteristics that are tied to the surface of an isotropic space. This contributes to the understanding of geometric properties in spaces that exhibit uniformity in all directions.

This article specifically tackles the problem of determining the existence of a surface defined by a given external curvature function within a convex domain, particularly when there is a singularity at a single point. The study is concerned with the conditions under which such surfaces exist and how the external curvature function influences the geometry of the surface.

Received : *5–January–2025,* ***Accepted :*** *25–march–2025*
*** Corresponding author***

This article is devoted to solving the problem of the existence of a surface defined by a given external curvature function in a convex domain with a singularity at a single point.

At the end of the article, we demonstrate the connection of the considered problem with the elliptic-type Monge-Ampère equation.

1. Basic definitions and problem statement

In the classical method of studying the internal geometry of surfaces, the points on a surface are divided into three types [1]: regular points, ribbed points, and conical points (vertices). Each of these surface types corresponds to a specific kind of tangent cone [2]. The surface has a unique tangent plane at a regular point, so in this case, the tangent cone becomes a plane. For ribbed points, the tangent cone is a dihedral angle. At conical points, the tangent cone is formed by the semi-tangents of curves on the surface that emanate from this point. Polyhedron have all three types of points.

Let F be a convex surface and $x \in F$. The plane π is a support plane of the surface at this point. A unit normal to the support plane π is associated with a point x^* on the unit sphere S, and this is called the spherical mapping of the point $x \in F$ onto the unit sphere S. This mapping is not always one-valued.

-If the spherical mapping of a point $x \in F$ is unique, then the point on the surface is called regular, and the support plane is the tangent plane.

- The spherical mapping of a point $x \in F$ can be an arc of a great circle on the unit sphere; such a point is called a ribbed point of the convex surface.

- On a convex surface, there are points whose spherical mapping is a domain on the unit sphere. Such points on the surface are called vertices of the convex surface.

The geometric nature of classified points is clearly expressed when the convex surface is a polyhedron. On a polyhedron, the internal points of the faces will be regular, the internal points of the ribs will be ribbed, and the vertices will be, accordingly, the vertices.

If a convex surface is regular, it consists of regular points.

Definition 1.1. A surface that has a finite number of vertices and consists of regular points at all other points is called a surface with vertices..

Surfaces with vertices exist. To imagine this class of surfaces, one should envision a cube made of elastic material being gradually inflated. There is a state in which the edges turn into smooth curves, but the points that are vertices remain. Additionally, by circulating an arc of the graph of the sine function around a common axis, a convex surface with two vertices is formed.

Let D be some simply connected domain in the Oxy plane in the Cartesian coordinate system $Oxyz$, and let a point A_0 be a strictly interior point of the domain D, and ∂D being the boundary of the domain D. Then, $z = f(x, y)$ is the equation of the surface F with edge L, and we will assume that the edge L is one-valued projected onto the boundary ∂D of domain D. The function $f(x, y)$ is continuous at all points of the domain D and has continuous derivatives at all points except at point A_0. The graph of such a function will describe a surface with a single vertex. Moreover, the vertex of the surface is projected along a line parallel to the Oz axis onto point $A_0 \in D$.

Definition 1.2. The external curvature of a set $M' \subset F$ is defined as the area of its spherical mapping M^* (where M^* is the spherical mapping of the set M' onto the unit sphere):

$$\omega(M') = S(M^*)$$

.

2. Properties of the External Curvature of a Convex Surface with a Vertex.

Let $M' \subset F$ be some set on a surface with a single vertex in the field D. Let us denote by $M \subset D$ the projection of the set $M' \subset F$ onto the field D, parallel to the axis Oz, and $M^* \subset S$ is the spherical mapping of the set $M' \subset F$ onto the unit sphere S. Since the projection of the surface F parallel to the axis Oz is one-valued, the external curvature $\omega(M')$ can be transferred onto $M \subset D$, and $\omega(M')$ is called the external curvature of the surface F transferred to the field D, denoted as $\omega_F(M) = S(M^*)$.

The properties of the external curvature of surfaces with vertices were studied in the work [9], where the properties of the external curvature of convex surfaces with vertices were proved.

We list the main properties of the external curvature of convex surfaces with vertices:

1. The external curvature $\omega(M)$ is a non-negative, completely additive function of Borel sets $M \subset D$.
2. If $\overline{M}$ is the closure of the set $M \subset D$ and does not contain the point A_0, then

$$\omega_F(M) = \omega_F\left(\overline{M}\right).$$

3. If $M \subset D$ does not contain the point A_0, but the closure $\overline{M}$ contains the point A_0, then

$$\omega_F\left(\overline{M}\right) = \omega_F(M).$$

4. If the point $A_0 \in M$, then

$$\omega_F(M) = \omega_F\left(\overline{M}\right) + \omega_0.$$

5. When a sequence of domains M_n, containing the point A_0 and having the properties:

$$M_1 \supset M_2 \supset \ldots \supset M_n \supset \ldots,$$

then

$$\lim_{n\to\infty} \omega_F(M_i) = \omega_0.$$

6. Furthermore, when M_i does not contain the point A_0,

$$\lim_{n\to\infty} \omega_F(M_i) = 0.$$

This means the completely additive property of the external curvature.

The problem of restoration a convex surface from its external curvature in the class of convex surfaces is formulated as follows:

if a function $\mu(M)$ is given on Borel sets $M \subset D$, and the number ω_0 is specified, is there a convex surface for which the external curvature transferred to the field D satisfies

$$\omega_F(M) = \mu(M)$$

and at point A_0

$$\omega(A_0) = \omega_0,$$

with an edge L and a single-valued projection onto the field D.

3. Solution of the restoration problem

We will prove the following theorem.

Theorem 3.1. *For a given function $\omega(M)$ of a Borel set on a convex field D to be transferred to D as the external curvature of the convex surface with an edge L, the one-valued projection onto the field D, and a vertex projecting onto the point A_0, it is necessary and sufficient that:*

1. $\mu(M)$ is a non-negative and completely additive function that having the properties of external curvature of a surface with a vertex.

2. For M, consisting of a single point, $\omega(M) < 2\pi$.

3. For the whole field, $\mu(D) = \Omega < 2\pi$, but greater than ω_0.

4. For M containing more than one point A_0,

$$\mu(M) > \omega_0.$$

Proof of the theorem.

Let us first prove the necessity of the conditions listed in the theorem. We divide the convex field D into n parts M_i in such a way that the point A_0 always coincides with the point of intersection of the curves dividing the field of some sets from M_i. In each set M_i, we mark the point A_i.

We calculate the value of the function $\mu(M)$ in the sets M_i, so that $\mu(M_i) = \omega_i$. We associate each point A_i with the number ω_i.

Thus, we have $(m+1)$ positive numbers $\omega_1, \omega_2, ..., \omega_n$. Moreover, $\sum\limits_{i=0}^{n} \omega_i < 2\pi$. This inequality follows from the conditions of the theorem.

Since the division into n-parts is chosen in such a way that the point A_0 does not belong to any of the fields M_i, this condition can be preserved as the number of divisions increases, such that the maximum diameters of the fields M_i tend to zero.

Now, we mark B_k points on the boundary ∂D of the field D and connect them with line segments $B_{k-1}B_k$, obtaining a polygon G_k inscribed in the boundary of the region. This polygon lies within the region D. From the vertices of the polygon G_k we draw rays parallel to the axis Oz and mark the points where these rays intersect the curve γ as B'_k. Connecting the points B'_k with line segments, we obtain a closed polyline L_k.At this point, the polyline L_k is one-valued projected onto the polygon G_k, with the vertices of L_k projected onto the vertices of G_k.

Thus, we have obtained all the conditions of A.D. Alexandrov's theorem on the existence of a polyhedron given its external curvature.

We will present this theorem in the form of a lemma given in the work [2].

Lemma 3.1. *Let L_k be a closed polyline in the half-space $z \geq 0$, uniquely projecting onto the plane Oxy into a convex polyline G_k, which bounds a convex polygon G_k.*

Let a polyhedron G be given with vertices A_i (for $i = 1, ..., n$), and match to each point A_i a number $\omega_i > 0$, such that

$$\sum_{i=0}^{n} \omega_i < 2\pi.$$

Then there exists a convex polyhedron with boundary L_k, uniquely projecting onto the plane Oxy, with vertices projected onto the points A_i and external curvatures at these vertices equal to $\omega_0, \omega_2, ..., \omega_n$, respectively.

The proof of this lemma is presented in the work [2].

The further transition from polyhedra to regular surfaces is carried out using A.D. Alexandrov's method [1]. However, in contrast to the well-known results, in our case there is a singularity at the point A_0. In the process of approximating the surface by polyhedra, the point of the surface projected onto the point A_0 must remain conical, and the external curvature at this point must be equal to ω_0.

Let P_0 be the polyhedron whose existence is proven by Lemma 1. The extreme vertices of the polyhedron P lie on the curve γ. To simplify the reasoning related to preserving the conical vertex, we translate the boundary of the polyhedron P onto the curve γ. To do this, it is sufficient to consider the convex hull of the polyhedron P and the curve γ. The part of this convex hull containing the polyhedron P and bounded by the curve γ is denoted by $\tilde{P}$.

Lemma 3.2. *The vertices of the polyhedron $\tilde{P}$ coincide with the vertices of the polyhedron P, and the external curvature at the vertices of $\tilde{P}$ is not greater than the external curvature at the vertices of P.*

Proof. Indeed, since the points of the curve γ, except for the points B'_k, lie outside the polyhedron P, when considering the convex hull, only a linear surface, which does not have a vertex, is added to the polyhedron. Therefore, the polyhedron P does not acquire new vertices. Since the vertices of P and $\tilde{P}$ coincide, and P is contained within $\tilde{P}$, the external curvature of P is greater than the external curvature of $\tilde{P}$. This follows from the monotonicity of external curvature. Moreover, the change can only occur at those vertices that are associated with the edge γ. Lemma 2 is proved.

It is known that when approximating surfaces by polyhedra, weak convergence of the sum of the external curvatures to the function of the set $\mu(M)$ is used. The convergence is considered as the maximum diameter of the fields M_i tends to zero. In our case, the vertex corresponding to the point A_0 does not correspond to a field on the domain D. Therefore, it does not depend on the diameter of the fields M_i.

Lemma 3.3. *When the polyhedron $\tilde{P}_n$ converges to the surface F with external curvature $\omega_F(M) = \mu(M)$, the external curvature at the point $x \in F$, which projects to the point A_0, remains equal to ω_0.*

Proof of Lemma 2: In the proof of the equality $\omega_F(M) = \mu(M)$, the integral sum of the external curvature at the points $A_i \in M_i$ is used. In this sum, ω_0 may not participate, and we consider the sum for $i = 1, 2, \ldots$. The absence of ω_0 does not affect the limite of the sum, because for the set M_i, it always holds that $\omega(M_i) = \mu\left(\overline{M}\right)$. By choosingly, the point A_0 is always located on the closure of the fields, except at this point.

Moreover, geometrically, it appears that the spherical mapping of the point A_0 is an area in the spherical mapping of the polyhedron $\tilde{P}_n$ with an area equal to ω_0, and the total area of the spherical mapping of the polyhedron $\tilde{P}_n$ is greater than ω_0. As the polyhedron $\tilde{P}_n$ converges to the surface F, the spherical mapping of $\tilde{P}_n$ increases, but it does not always restrict the spherical mapping of the point A_0. Lemma 3 is proven.

Lemma 3.4. *The boundary surface F cannot have ribs.*

Indeed, if the surface F has a rib, the spherical mapping of the rib would be a segment. This means that in the field D, there exists a set $\tilde{M}$ of points for which $\omega_F\left(\tilde{M}\right) = 0$, and therefore $\mu\left(\tilde{M}\right) = 0$, which contradicts the conditions of the theorem. Thus, the surface F cannot have ribbed points.

Therefore, the surface has a vertex at the point A_0, $\omega_F(M) = \mu(M)$, and is uniquely projected onto the field with the curve γ. The theorem is proved.

4. Connection of the Solved Problem with the Elliptic Monge-Ampère Equation

The problem we are considering is a generalization of A.D. Alexandrov's results on the existence of a surface with a given function of external curvature, which is the area of its spherical mapping. A.D. Alexandrov himself demonstrated the connection between this problem and the Monge-Ampère differential equation.

In their monographs, I.Ya. Bakelman [7] and A.V. Pogorelov [8] solved this geometric problem to prove the solvability of the Dirichlet problem for a broad class of Monge-Ampère equations. The general form of the Monge-Ampère equation is given by:

$$z_{xx}z_{yy} - z_{xy}^2 = \varphi(x, y, z, z_x, z_y)$$

When $\varphi(x, y, z, z_x, z_y) > 0$, the equation is of elliptic type.

The geometric problem solved in this article can be considered as solving the Dirichlet problem for the Monge-Ampère equation on a convex planar domain. This equation takes the form:

$$z_{xx}z_{yy} - z_{xy}^2 = \varphi(x, y)(1 + z_x^2 + z_y^2)^{\frac{3}{2}}$$

where $\varphi(x, y) > 0$ is a function in domain D.

Then, the external curvature of the surface, defined as a positive, completely additive function on the Borel set M of D, is given by the formula:

$$\mu(M) = \iint_M \varphi(x, y)\, dx\, dy.$$

If the equation of the convex surface is given by $z = f(x, y)$, $(x, y) \in D$, then the external curvature of the surface, transferred to the plane, is computed as follows:

$$\omega_F(M) = \iint_M \frac{z_{xx}z_{yy} - z_{xy}^2}{(1 + z_x^2 + z_y^2)^{\frac{3}{2}}}\, dx\, dy.$$

Therefore, the problem of reconstructing a convex surface from a given external curvature is equivalent to solving the Monge-Ampère differential equation with a given boundary condition.

It is evident that this result can be generalized to solving the Dirichlet problem for the Monge-Ampère equation in its general form using the methods developed by I.Ya. Bakelman [ ].

Unlike similar problems discussed in works [3],[6], the function under consideration is irregular at a single point in the given domain.

5. Conclusion

The problem of reconstructing a surface with a given external curvature was previously solved in the class of convex polyhedra and in the class of regular surfaces. The results of this article prove the existence of a surface based on a given external curvature for surfaces with a singularity at a single point.

This article examines the conditions for the existence of a surface defined by a given external curvature function within a convex domain, particularly in the presence of a singularity at a single point. Based on A.D. Alexandrov's method, the geometric properties of the singularity on the surface were analyzed through the study of external curvature properties for convex polyhedra and regular surfaces. The transfer properties of external curvature on Borel sets and its application methods were explained in detail.

The primary result of this research proves that for an external curvature function to define a surface, it must satisfy three fundamental conditions: the function must be non-negative and completely additive, the external curvature at the singularity point must take a specific value, and the values of external curvature must comply with the convex domain as a whole. Additionally, the geometric nature of the singularity point and the completeness property of external curvature were established through proofs involving the approximation of surfaces by polyhedra.

The findings of this article hold theoretical and practical significance in the study of geometry and the theory of convex surfaces, particularly in solving problems related to external curvature. These results provide a crucial foundation for future research in this area.

References

[1] Aleksandrov A.D. : *Intrinsic geometry of convex surfaces.*. Taylor and Francis Group. pp. 235-269 (2006).
[2] Alexandrov A.D.: *Convex Polyhedra*.Selected Works. Vol-2 Novosibirsk. Science. pp. 171-213 (2007).
[3] Artykbaev A., Sobirov J. *A development of a polyhedron in the Galilean space A development of a polyhedron in the Galilean space*, Bulletin of National University of Uzbekistan Mathematics and Natural Sciences, 2021, DOI:10.56017/2181-1318.1148
[4] Sharipov A., Topvoldiyev F. *On one invariant of polyhedra isometric on sections*, AIP Conference Proceedings, 2023, DOI:10.1063/5.0144737
[5] Artikbayev A., Tillayev D.R. *Property of external curvature of convex surfaces with a finite number of vertices.* Modern problems of Mathematics and Mechanics. 26-28 April, 2023 Baku, Azerbaijan.
[6] Artikbayev A., Ibodullayeva N. *Generalized Extrinsic Curvature of a Surface*, AIP Conf. Proc. 3004, 030007 (2024).
[7] Bakelman I. Ya., Werner A. L., Kantor B. E. *Introduction to Global Differential Geometry*.— Moscow: Nauka, 1973.(in russian)
[8] Pogorelov A. *External Geometry of Convex Surfaces*. Moscow, Nauka, 1969, pp. 496–569.(in russian)
[9] Artikbaev A., Tillaev D. *Properties of External Curvature of Surfaces with Vertices* // Reports of the Academy of Sciences of the Republic of Uzbekistan. 2023. Vol. 4, No. 1, pp. 3–6.(in russian)

Affiliations

Tilayev Donyorbek
Address: Tashkent State Transport University, Department of Higher Mathematics, Tashkent, Uzbekistan.
e-mail: drtillayev@mail.ru

Uzbekistan Journal of Mathematics and Computer Science
Volume 1 No. 1 Page 57–63 (2025)
DOI: https://doi.org/10.56143/ujmcs.v1i1.1
Research article

A Vector Field in a Semi-Riemannian Manifold

Ismoilov Sherzodbek* **and Ergashaliyev Magrurbek**

Abstract

The study of vector fields in semi-Riemannian manifolds forms a critical component in differential geometry and mathematical physics. Semi-Riemannian manifolds generalize the concept of Riemannian manifolds by allowing the metric tensor to have indefinite signature, thus encompassing both Riemannian and Lorentzian manifolds. This generalization is essential for understanding the geometry underlying General Relativity and various field theories.

Keywords: *manifold; foliation;semi-Riemannian manifold; Minkowski space; spacelike; timelike; vector field.*

AMS Subject Classification (2020): *Primary: 53A35 ; Secondary: 57R10; 57R25.*

1. Introduction

Hawking and Ellis explore the geometric and topological aspects of spacetime, which are crucial to understanding the structure of the universe within general relativity [15]. Semi-Riemannian geometry involves the study of a smooth manifold equipped with a non-degenerate metric of any given signature. [17] examines the concept of duality in semi-Riemannian geometry, offering insights into the geometric structures in general relativity. [18] this textbook introduces advanced geometric methods, including those relevant to semi-Riemannian geometry and dual transformations, with applications in physics. [20] is book provides a clear introduction to semi-Riemannian geometry and its applications in general relativity, covering essential topics like curvature and geodesics.

Ismoilov and Artikbayev studied Monge-Ampère and dual transformations in an isotropic and Galilean space, where the subspace is a semi-Riemannian submanifold [12, 13, 9, 10, 8, 7].

1.1. Preliminaries

Definition 1.1. The metric tensor g on a smooth manifold $M = (M, g)$ is said a symmetric non-degenerate tensor field on M of nonzero constant index. [25]

In other words $g \in \mathrm{T}_p(M)$ smoothly assigns to each point p of M a scalar product g_p in the tangent space $T_p(M)$, and the index of g_p is the same for all p.

Definition 1.2. A semi-Riemannian manifold is a smooth manifold M equipped with a metric tensor g.[26]

A semi-Riemannian manifold is an ordered pair (M, g): two different metric tensors on the same manifold constitute different semi-Riemannian manifolds. However, we usually denote a semi-Riemannian manifold by the name of its smooth manifold M, N, and others.

Received : *5–january–2025,* ***Accepted :*** *25–march–2025*
**** Corresponding author***

Let us consider an $n = dimM$ dimensional semi-Riemannian manifold M. The general value k of index g on M is called the index of M: $0 \leq k \leq n$. If $k = 0$, M is a Riemannian manifold; then each g is a inner product of $T_p(M)$, g be positive definite. If $k = 1$ and $n \geq 2$, M is a Lorentz manifold.

Semi-Riemannian manifolds are often called pseudo-Riemannian manifolds, or even - in the old terminology - Riemannian manifolds, but we reserve the latter term for a special positive definite case.

We use $(,\ )$ as an alternative notation for g, writing $g(u, v) = (u, v)$ for tangent vectors, and $g(V_1, V_2) = (V_1, V_2) \in F(M)$ for vector fields.

If $x_1, \ \ldots, \ x_n$ is a coordinate system on $U \subset M$ the components of the metric tensor g on U are

$$g_{ij} = (\frac{\partial}{\partial x^i}, \frac{\partial}{\partial x^j}),$$

were, $i = \overline{1.n}, \quad j = \overline{1.n}$.

Thus for vector fields $V_1 = \sum\limits_{i=1}^{n} V_{1,i} \frac{\partial}{\partial x^i}$ and $V_2 = \sum\limits_{i=1}^{n} V_{2,j} \frac{\partial}{\partial x^j}$,

$$g(V_1, V_2) = \sum_{i,j=1}^{n} g_{ij} V_{1,i} V_{2,j}$$

Denoted by matrix $\left(g^{ij}(p)\right)$ is the inverse of matrix $\left(g_{ij}(p)\right)$.

Since g is symmetric, $g_{ij} = g_{ji}$ and hence $g^{ij} = g^{ji}$ for $i = \overline{1.n}, \quad j = \overline{1.n}$. Finally on U the metric tensor can be written as

$$\boldsymbol{g} = \sum_{i,j=1}^{n} g_{ij} dx^i \otimes dx^j$$

For each $\forall p \in R_n$ there is linear isomorphism from R^n to $T_p\ (R^n)$ that, in terms of natural coordinates, sends v to $v_p = \sum\limits_{i=1}^{n} v^i \frac{\partial}{\partial x^i}$. Thus the scaly product on R^n gives rise to a metric tensor on R^n with

$$\left(v_{1,p}, v_{2,p}\right) = \sum_{i=1}^{n} v_{1,i} v_{2,i}.$$

Henceforth in any geometric context R_n will denote the resulting Riemannian manifold, called n-dimensional Euclidean space.

For an integer k with $0 \leq k \leq n$, changing the first k plus signs above to minus gives a metric tensor

$$\left(v_{1,p}, v_{2,p}\right) = -\sum_{i=1}^{k} v_{1,i} v_{2,i} + \sum_{j=k+1}^{n} v_{1,j} v_{2,j}$$

of index k. The resulting semi-Euclidean space ${}^k R_n$ reduces to R_n if $k = 0$. For $n \geq 2$,[1] R_n is called Minkowski n-space; if $n = 4$ it is the simplest example of a relativistic spacetime.

Fix the notation

$$\varepsilon_i = \begin{cases} -1 & \text{for} \quad 1 \leq i \leq v \\ +1 & \text{for} \quad v+1 \leq i \leq n \end{cases}$$

Then the metric tensor of ${}^k R_n$ can be written

$$\boldsymbol{g} = \sum_{i=1}^{n} \varepsilon_i \frac{\partial}{\partial x^i} \otimes \frac{\partial}{\partial x^i}$$

The geometric significance of the index of a semi-Riemannian manifold derives from the following trichotomy.

Definition 1.3. A tangent vector v to M is [1]

$$\begin{aligned} \text{spacelike} \ \text{if} \ (v,v) > 0 \quad &\text{or} \quad v = 0 \\ \text{null} \ \text{if} \ (v,v) = 0 \quad &\text{and} \quad v \neq 0 \\ \text{timelike} \ \text{if} \ (v,v) < 0. & \end{aligned}$$

By an orthonormal frame on a pseudo-Riemannian $n-$manifold M, we mean a set consists of n mutually orthogonal unit vector fields $e_1, \ \ldots, e_n$ on M.

The mean curvature H of a submanifold M' in a semi-Riemannian manifold (M, g) is related to the Laplace-Beltrami operator Δ acting on the embedding functions of M'. For a submanifold M' with an embedding $X : M' \to M$, the mean curvature vector H can be expressed as:

$$H = \Delta X$$

where Δ is the Laplace-Beltrami operator on M'.

Let V and W be vector fields on a semi-Riemannian manifold M. The goal of this section is to show how to define a new vector field $\nabla_V W$ on M whose value at each point p is the vector rate of change of W in the V_p direction. There is a natural way to do this on $\boldsymbol{R}^n_v$.

Definition 1.4. Let $u^1, \ldots, u^n$ be the natural coordinates on $\boldsymbol{R}^n_v$. If $V = \sum\limits_{i=1}^{n} V^i \frac{\partial}{\partial x^i}$ and $Y = \sum\limits_{i=1}^{n} Y^i \frac{\partial}{\partial x^i}$ are vector fields on $\boldsymbol{R}^n_v$, the vector field

$$\nabla_V W = \sum_{i=1}^{n} V\left(Y^i\right) \frac{\partial}{\partial x^i}$$

is called the natural covariant derivative of Y with respect to V.

The second fundamental form II is given by:

$$\mathrm{II}(X, Y) = (\nabla_X Y)^{\perp}$$

where X, Y are tangent vectors to M'. The perpendicular component of the covariant derivative is given by: $(\nabla_X Y)^{\perp} = \nabla_X Y - \langle \nabla_X Y, X \rangle X$.

The mean curvature vector h is:

$$H = \frac{1}{m} \sum_{i=1}^{m} (\nabla_{e_i} e_i)^{\perp},$$

where $\{e_i\}_{i=1}^{m}$ is an orthonormal basis of the tangent space of M and $\nabla_{e_i} e_i = e_i^j \frac{\partial e_i^k}{\partial x^j} + \Gamma_{jk}^k e_i^j e_i^k$, where $\Gamma_{jk}^i = \frac{1}{2} g^{im} \left(\frac{\partial g_{mj}}{\partial x^k} + \frac{\partial g_{mk}}{\partial x^j} - \frac{\partial g_{jk}}{\partial x^m} \right)$.

Definition 1.5. A pseudo-Riemannian submanifold N is called minimal if the mean curvature vector H vanishes identically, i.e., $H \equiv 0$. [27]

If the submanifold is given by the formula $x_{n+1} = f(x_1, \ x_2, \ \ldots, \ x_n)$ in a curvilinear coordinate system. For a function $\varphi : M \to M^*$ its Dual transform is defined to curved coordinates

$$\begin{cases} x_i^* = f'_{x_i}(x_1, x_2, ..., x_n) \quad i = \overline{1.n} \\ x_{n+1}^* = \sum\limits_{i=1}^{n} x_i \cdot f'_{x_i}(x_1, x_2, ..., x_n) - f(x_1, x_2, ..., x_n) \end{cases}.$$

Lemma 1.1. *Properties of the Dual Transform:*

1. Involutory Property: The dual transform is an involution; that is, the dual transform of f^* is f itself.

2. Duality: The transform maps the problem of finding the extremum of f to a dual problem involving f^*.

3. Smoothness: If f is smooth and strictly convex, then f^* is also smooth.[12]

2. Results

Theorem 2.1. *: If (M, g) is a semi-Riemannian manifold and $N \subset M$ is a minimal submanifold, then the dual transformation of N into $N^* \subset M$ will be conformal. That is, the dual transformation $\phi : N \to N^*$ results in metrics g and $\phi^* g$ being related as follows:*

$$\phi^* g = e^{2\lambda} g$$

where $\lambda : M \to \mathbb{R}$ is a smooth function.

Proof. To prove this theorem, we will consider the concepts of minimal submanifolds, dual transformations, and the properties of conformal changes in detail.

To understand how the metric changes under dual transformation, we first consider the pull-back of the metric via the dual transformation:

$$(\phi^* g)(X, Y) = g(d\phi(X), d\phi(Y)),$$

where X, Y are tangent vectors on M.

Conformal transformations scale the metric by a scalar factor. If $\phi : M \to M$ is a conformal transformation, then the metrics $\phi^* g$ and g are related by:

$$\phi^* g = e^{2\lambda} g,$$

where $\lambda : M \to \mathbb{R}$ is a smooth function.

This implies that the metric under dual transformation is scaled by a factor. The conformal change of the mean curvature vector is given by:

$$\mathbf{H}^* = e^{-\lambda} \mathbf{H}.$$

Since $\mathbf{H} = 0$ for a minimal submanifold:

$$\mathbf{H}^* = e^{-\lambda} \cdot 0 = 0.$$

This confirms that the dual transformation is conformal.

Theorem 2.2. *If M two dimensional is a minimal pseudo-Riemannian supmanifold in the Null submanifold, then the dual mapping will be conformal.*

Proof. A mapping is conformal if the first fundamental form is

$$g^* = \lambda(x^1, x^2) \left(\left(\frac{\partial}{\partial x^1} \right)^2 + \left(\frac{\partial}{\partial x^2} \right)^2 \right).$$

Let us determine the conditions that satisfy this equality. Calculate the first fundamental form of the dual submanifold M^* under the condition that M is the minimal submanifold:

$$g^* = \left(\frac{\partial}{\partial (x^*)^1} \right)^2 + \left(\frac{\partial}{\partial (x^*)^2} \right)^2 = \left(\frac{\partial^2 f}{\partial (x^1)^2} \frac{\partial}{\partial x^1} + \frac{\partial^2 f}{\partial x^1 \partial x^2} \frac{\partial}{\partial x^2} \right)^2 + \left(\frac{\partial^2 f}{\partial x^1 \partial x^2} \frac{\partial}{\partial x^1} + \frac{\partial^2 f}{\partial (x^2)^2} \frac{\partial}{\partial x^2} \right)^2 =$$

$$\left[\left(\frac{\partial^2 f}{\partial (x^1)^2} \right)^2 + \left(\frac{\partial^2 f}{\partial x^1 \partial x^2} \right)^2 \right] \left(\frac{\partial}{\partial x^1} \right)^2 + 2 \frac{\partial^2 f}{\partial x^1 \partial x^2} \left(\frac{\partial^2 f}{\partial (x^1)^2} + \frac{\partial^2 f}{\partial (x^2)^2} \right) \frac{\partial}{\partial x^1} \frac{\partial}{\partial x^2} +$$

$$+\left[\left(\frac{\partial^2 f}{\partial x^1 \partial x^2}\right)^2+\left(\frac{\partial^2 f}{\partial (x^2)^2}\right)^2\right]\left(\frac{\partial}{\partial x^2}\right)^2.$$

The expression $\frac{\partial^2 f}{\partial (x^1)^2}+\frac{\partial^2 f}{\partial (x^2)^2}=0$ follows from the definition of a minimal submanifold M and the mean curvature formula. Hence, if we consider the expression $\frac{\partial^2 f}{\partial (x^1)^2}=-\frac{\partial^2 f}{\partial (x^2)^2}$:

$$g^*=\left[\left(\frac{\partial^2 f}{\partial (x^1)^2}\right)^2+\left(\frac{\partial^2 f}{\partial x^1 \partial x^2}\right)^2\right]\left(\frac{\partial}{\partial x^1}\right)^2+\left[\left(\frac{\partial^2 f}{\partial x^1 \partial x^2}\right)^2+\left(\frac{\partial^2 f}{\partial (x^2)^2}\right)^2\right]\left(\frac{\partial}{\partial x^2}\right)^2=$$

$$=\left[\left(\frac{\partial^2 f}{\partial (x^1)^2}\right)^2+\left(\frac{\partial^2 f}{\partial x^1 \partial x^2}\right)^2\right]\left((\frac{\partial}{\partial x^1})^2+(\frac{\partial}{\partial x^2})^2\right)=\lambda(x^1,x^2)g.$$

We get from here that $\lambda(x^1,x^2)=(\frac{\partial^2 f}{\partial (x^1)^2})^2+(\frac{\partial^2 f}{\partial x^1 \partial x^2})^2$.

This proves that the dual mapping of the minimal submanifold is conformal.

Corollary 2.1. *If the translation submanifold satisfies the condition* $\frac{\partial^2 f}{\partial (x^1)^2}=\frac{\partial^2 f}{\partial (x^2)^2}$, *then its dual mapping will be conformal.*

To understand the mechanical meaning of the dual transformation, we need to examine the physical and geometric implications of such mathematical transformations. A dual transformation typically reflects a change in certain structures of the original submanifold, which can be crucial for studying physical mechanisms or geometric properties.

The dual transformation $\phi: N \to N^*$ generally involves mapping the new submanifold N^* such that it retains or reinterprets the specific characteristics of the original submanifold N. Mechanically, this can imply the following:

Minimal submanifolds represent minimized potential energy states in physical terms. A dual transformation re-expresses these states in a new coordinate system or geometric context, preserving energy minimization principles in a new setting.

As a result of the dual transformation, the metric changes conformally, meaning the shape is preserved while the size or scale may change:

$$\phi^* g = e^{2\lambda} g$$

This is analogous to symmetry transformations in physics, such as changes related to light propagation under heating or expansion. Conformal transformations preserve shapes and angles, but alter dimensions.

Dual transformations preserve or reinterpret geometric properties in a new geometry. For instance, minimal surfaces, elastic materials, or field theories can be re-expressed with new physical or mathematical insights through dual transformations.

In mechanical systems, dual transformations allow for the study of phenomena in the original system within a new framework. For example, studying structures through conformal transformations can be beneficial for analyzing the elastic properties of materials.

Examples.

The tension and equilibrium states of an elastic membrane can be analyzed under new conditions via dual transformation. For example, the deformation of an elastic material can be studied in a new conformal coordinate system.

The propagation of light in different media can be analyzed through dual transformations in new media. Conformal optics allows for the study of new directions and curvatures of light propagation.

Conclusion

The Dual transform is a versatile mathematical tool that offers significant advantages in the analysis of vector fields on semi-Riemannian manifolds and in the solution of the Monge-Ampère equation. By transforming the original problem into a dual formulation, we can exploit the properties of convex functions and their transforms to find solutions to complex geometric and physical equations. This approach not only simplifies the mathematical treatment but also provides deeper insights into the structure of semi-Riemannian manifolds and their applications in various fields of mathematics and physics.

Acknowledgements

We would like to extend our sincere thanks to A. Artykbaev for introducing the problem and offering invaluable guidance throughout the process of finding a solution. His thoughtful advice and constant support were crucial in helping us overcome the obstacles we encountered. We are truly grateful for his encouragement and expertise in this endeavor.

References

[1] Chen, B. Y.: Pseudo-Riemannian Geometry, δ-invariants and Applications. World Scientific Publishing, Hackensack, NJI(2011).
[2] Duggal, Krishan L., Şahin, B.: Differential geometry of lightlike submanifolds. Frontiers in Mathematics. Birkhäuser Verlag, Basel (2010).
[3] Fujioka, A., Furuhata, H., Sasaki, T.: *Projective surfaces and pre-normalized Blaschke immersions of codimension two*. Int. Electron. J. Geom. **9** (1), 100-110 (2016).
[4] Ilarslan, K.: *New results for general helix in Euclidean 3-space*. In: Proceedings of the 6th International Eurasian Conference on Mathematical Sciences and Applications (IECMSA), Aug 15-18/2017, Budapest, HUNGARY. AIP Conference Proceedings. **1926**, 1-6 (2018).
[5] O'Neill, B.: Semi-Riemannian geometry with applications to relativity. Academic Press. London (1983).
[6] Özgür, C.: *On C-Parallel Legendre Curves in Non-Sasakian Contact Metric Manifolds*. Preprint arxiv:1906.03313 (2019).
[7] Sharipov, A. S., Topvoldiyev, F. F.: *On invariant of surfaces with isometric on section*. Mathematics and Statistics, 10(3), 523–528. doi:10.13189/ms.2022.100307, (2022).
[8] Ismoilov, S. S., Sultanov, B. M.: *Invariant geometric characteristics under the dual mapping of an isotropic space*. Asia Pacific Journal of Mathematics, 10, 1–12. doi:10.28924/APJM/10-20, (2023).
[9] Ismoilov, S. S.: Geometry of the Monge - Ampere equation in an isotropic space. Uzbek Mathematical Journal, 66(2), 66–77, (2022).
[10] Artykbaev, A., Sultanov, B. M.: *Invariants of surface indicatrix in a Special linear transformation*. Mathematics and Statistics, 7(4), 106–115, (2019).
[11] Artykbaev, A., Ismoilov, S. S.: *The dual surfaces of an isotropic space* R_3^2. Bulletin of the Institute of Mathematics, 4(4), 1–8, (2021).
[12] Artikbaev, A., Ismoilov, S. S.: *Special mean and total curvature of a dual surface in isotropic spaces*. International Electronic Journal of Geometry, 15(1), 1–10, (2022).
[13] Artikbayev, A., Ismoilov, S. S.: *Surface recovering by a given total and mean curvature in isotropic space*. Palestine Journal of Mathematics, 11(3), 351–361, (2022).
[14] O'Neill, B.: Semi-Riemannian Geometry With Applications to Relativity. Academic Press, (1983).
[15] Hawking, S. W., Ellis, G. F. R.: The Large Scale Structure of Space-Time.(1973).
[16] Matsumoto, M.: *Semi-Riemannian Geometry*. Saitama Mathematical Journal, 7, 8–22, (1989).
[17] Moser, J.: *Duality in semi-Riemannian geometry*. Communications in Mathematical Physics, 32(1), 37–52, (1973).
[18] Dubrovin, B. A., Fomenko, A. T., Novikov, S. P.: Modern Geometry—Methods and Applications: Part I: The Geometry of Surfaces, Transformation Groups, and Fields. Springer, (1984).
[19] Arnold, V. I.: *Legendre Transformations in Contact Geometry*. Proceedings of the International Congress of Mathematicians, 1, 391–404,(1990).
[20] Boyer, C.: Semi-Riemannian Geometry and General Relativity. Elsevier.(2017).
[21] Kupershmidt, B. A.:*Geometry of jet bundles and the integrable systems*. Springer Science, Business Media.(2002).
[22] Esposito, G.: *Duality transformations in field theory and statistical mechanics*. International Journal of Modern Physics A, 19(01), 135–146,(2004).
[23] Carroll, S. M.: Spacetime and Geometry: An Introduction to General Relativity,(2004).
[24] García-Río, E., Kupeli, D. N.: *Semi-Riemannian Manifolds. In Semi-Riemannian Maps and Their Applications*. Dordrecht: Springer Netherlands,pp. 19–57,(1999).
[25] Gao, T., Lim, L.-H., Ye, K.: *Semi-Riemannian Manifold Optimization*. Journal of Geometry, 35(2). doi:10.1007/s00022-020-00500-1, (2018).
[26] Shahi, F.: *Semi-Riemannian Structures on Manifolds*. Journal of Differential Geometry, 112(2), 345–367, (2024).
[27] Smith, John.: *Minimal Pseudo-Riemannian Submanifolds*. Journal of Geometry, vol. 35, no. 2, Springer, pp. 123–145, (2020), https://doi.org/10.1007/s00022-020-00500-1.

Affiliations

Ismoilov Sherezodbek
Address: Tashkent State Transport University, Department of Higher Mathematics, 100060, Tashkent, Uzbekistan.
e-mail: sh.ismoilov@nuu.uz
ORCID ID:0000-0002-4338-3852

Ergashaliyev Magrurbek
Address: Tashkent State Transport University, Department of Higher Mathematics, 100060, Tashkent, Uzbekistan.
e-mail: magrurbekergashaliyev@gmail.com
ORCID ID:0009-0007-4372-4657

Uzbekistan Journal of Mathematics and Computer Science
Volume 1 No. 1 Page 64–70 (2025)
DOI: https://doi.org/10.56143/10.56143/ujmcs.v1i1.10
Research article

UZJMCS

Technical diagnostics of diesel locomotive units and assemblies using mathematical modeling

Kasimov Sh. A.* Kendjayev R.Kh. and Kudratov Sh.I.

Abstract

The operational efficiency of diesel locomotives is largely determined by their reliability. The problem of ensuring the reliable operation of diesel locomotives has always been considered as one of the priority tasks for railway transport.

Reliability management of diesel locomotives consists in establishing, ensuring and maintaining its level standardized by technical conditions at all stages of creating diesel locomotives and using them for their intended purpose.

The effective use of diesel locomotives provides, in particular, their high reliability in operation, minimum maintenance and repair costs, maximum use of resource and energy potential. In this regard, a special role is given to the technical diagnosis of components and assemblies of a diesel locomotive.

The current reliability of a diesel locomotive at each given moment of its use depends on a number of factors acting in the period of time preceding this moment. For example, the reliability of a newly built locomotive depends on the level of research and development, the quality of the manufacture of components and parts, as well as their assembly and adjustment.

Keywords: *Crankshaft, thermal index, reliability, performance, diesel locomotives, thermal strength, design.*

AMS Subject Classification (2020): *Primary: 34A25 ; Secondary: 34C07;*

1. Introduction

The reliability of a locomotive in operation is determined by the conditions in which it operates (climate, dust content of air, track plan and profile, mass of trains, etc.), as well as the organization of its maintenance and repair (method of servicing the locomotive by crews, qualification of locomotive crews, frequency of inspections and repairs, scope of repair work performed during these inspections and repairs, quality of repair work, etc.).

Thus, the reliability of locomotives, their assembly units and parts depends on a large number of different factors, which can be divided into three main groups:

- design and engineering;
- production and process;
- operational and repair.

Received : *05–January–2025,* ***Accepted :*** *27–march–2025*
**** Corresponding author***

To assess the level of reliability of a technical object, a system of special numerical characteristics – reliability indicators is used. Depending on the properties of the object characterized by these indicators, single and complex indicators are distinguished [1-2].

One of the main single indicators of reliability is the failure flow parameter ω, which is the average number of failures of the repaired product per unit of time and characterizes the reliability of the locomotive. Complex indicators quantitatively characterize at least two properties that make up reliability. An example of a complex indicator is the availability factor, which simultaneously characterizes two different reliability properties of diesel locomotives - reliability and maintainability. Normalization and reliable assessment of the reliability level should be carried out using complex indicators. The use of single indicators for these purposes (the most popular among specialists is the failure flow parameter) can distort the true picture of the state of reliability of diesel locomotives.

2. Problem statement.

Technical dagnostics in order to ensure the required level of reliability and strength of such a complex object as a diesel locomotive is associated with comprehensive analytical and numerical studies on mathematical modeling of its components and parts. At the same time, an integrated approach involves solving the problems of assessing the stress-strain state, as well as studying the operating modes of the crankshaft systems of a diesel locomotive.

One of the main diesel engine systems for which the solution of such tasks is necessary is the most important and responsible system of an internal combustion engine - a crank mechanism, since it is with the help of the units of this mechanism that the thermal energy of the working gases is converted into mechanical energy of rotation of the crankshaft. The reliability of the crank mechanism directly determines the reliability and durability of the entire diesel engine of the diesel locomotive as a whole, which imposes strict requirements on the design, manufacture, installation, operation, maintenance and repair of the mechanism components, as well as on the quality of materials used in the manufacture of these components, which should ultimately ensure the required engine life.

In a diesel locomotive, steady-state torsional vibrations are forced. Under conditions of resonance of angular displacements of sections, a malfunction occurs in the area of ? ? the crankshaft. The shaft revolutions at which these resonant phenomena occur are called *critical*. The occurrence of critical crankshaft conditions leads to destruction. The task of the thermal monitoring diagnostic complex is to timely determine the malfunction of the facility:

- diagnostics during operation of critical speeds;
- determination of resonance amplitudes;
- calculation of high dynamic stresses occurring on the diesel engine crankshaft of a diesel locomotive [3 - 4].

In this work, mathematical modeling of torsional vibrations of crankshafts of diesel locomotives was carried out, taking into account the impact of operational loads. A mathematical model has been developed, an algorithm and a program have been drawn up, numerical studies have been performed in the MATHCAD 15 programming environment.

3. Method of solution

This paragraph presents a mathematical model for numerical studies of the torsional vibrations of the crankshafts of diesel locomotives, taking into account the impact of operational loads, based on the Gauss method and the iteration method.

The mathematical model for dynamic modeling is based on the assumption of calculating the crankshaft of a diesel locomotive as an eight mass discrete system consisting of a shaft of main journals with torsional stiffnesses $K_{12} - K_{78}$, as well as connecting rods mounted on it with mass moments of inertia $J_1 - J_8$.

At that, rear output part of crankshaft is connected to flywheel (flywheel flange FW), and through it - to transmission, and front part of crankshaft (FR), to which sprocket is attached, is connected to pulley of gas distributing mechanism drive and auxiliary systems.

The design diagram for this eight mass discrete system is shown in Figure 1.

Figure 1 shows the following symbols:

$1 - 9$ — numbers of main journals (shaft segments located on its axis of rotation) (see Figure 1);

$I - VIII$ — numbers of crankpins (shaft segments offset from its axis of rotation and main crankpins), at $i = 1, 2, \ldots, 8$;

$K_{12} - K_{78}$ — torsional stiffnesses of the main journals (stiffness of the adjacent section of the shaft between masses) in $(n \cdot m)/rad$;

$J_1 - J_8$ — mass moments of inertia CR (crank pins) relative to axis OX in $kg \cdot m^2$.

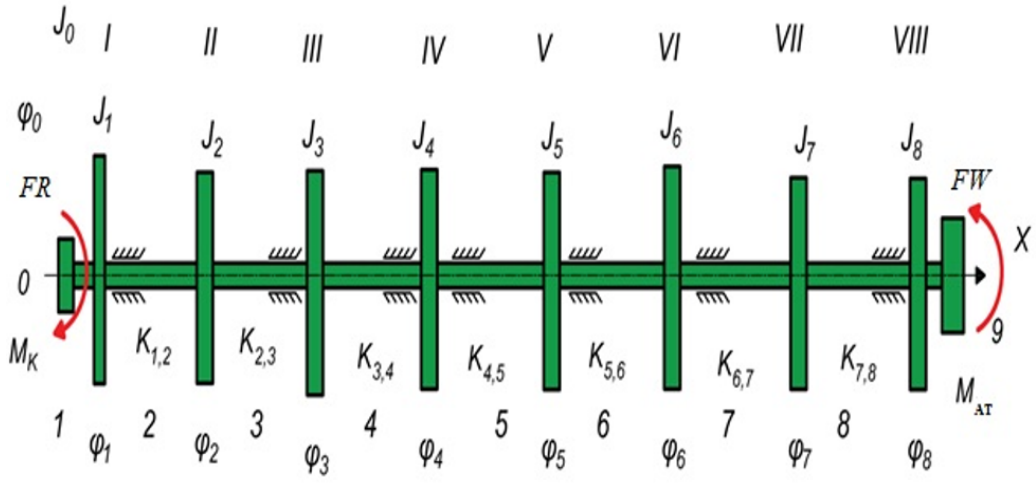

Fig. 1. Design scheme for analysis of torsional vibrations of diesel engine crankshaft in the form of eight-weight discrete system

FW — flywheel flange (shaft end) – the rear output part of the crankshaft, connected to the flywheel, and through it – to the transmission.

FR — the front part of the crankshaft (nose), to which the sprocket is attached, the drive pulley of the gas distribution mechanism and auxiliary systems.

The crankshaft of a diesel locomotive is modeled in the form of a rod with a piecewise continuous distribution of mass along the length, taking into account eight mass systems.

The calculation of the torsional oscillations of the crankshaft of a diesel locomotive with a piecewise continuous distribution of mass along the length can be represented in matrix form and "transition matrices" for sections of the rod.

We will justify the model of torsional vibrations of the masses of the crankshaft of a diesel locomotive in the form of a discrete system in the following sequence:

1. Secured crank pins rotate on crankshaft axle OX . Note here that their number for diesel generator 1A – 9 DG diesel locomotive UzTE16M [4] equals eight, i.e. $i = 1,\ 2,\ \ldots\ ,\ 8$.

2. From front part of crankshaft – LE flap (FR), to which sprocket is attached, pulley of gas distributing mechanism drive and auxiliary systems, power from fuel combustion is transmitted to crankshaft and then rear output part of crankshaft, which is connected to flywheel (FW), and through it – to transmission, transmits mechanical power required for diesel locomotive movement.

3. Design scheme for analysis of torsional vibrations of diesel locomotive crankshaft in the form of eight-weight discrete system, on which the following are highlighted:

- $\varphi_j(t)$ – angles of rotation of main journals together with connecting rods on crankshaft ($j = 0,\ 1,\ \ldots\ ,\ 8$) in radians, which take into account functions of rotary (kinematic) movement of each of nine masses;
- rotational moment of inertia of i-th weight of connecting rod journal J_i relative to axis OX in $kg \cdot m^2$;
- driving moment M_K at a point O, wherein the angle of rotation of the journal $\varphi_0(t)$, and the mass moment of inertia is J_0;
- antitorque moment M_{AT} is applied to the flywheel flange FW.

4. To derive the equations of oscillations of mass moments of inertia, the Lagrange method and functions were used:

4.1. kinematic energy:

$$T = \frac{1}{2}\left\{J_0\left(\varphi_0\right)^2 + \left(J_0 + J_1\right)\left(\varphi_0 + \varphi_1\right)^2 + \ldots + \left(J_0 + J_j\right)\left(\varphi_0 + \varphi_1 + \ldots + \varphi_j\right)^2\right\}, \tag{3.1}$$

4.2. potential energy:

$$P = \frac{1}{2}\left\{K_{12}\left(\varphi_1 - \varphi_2\right) + K_{23}\left(\varphi_2 - \varphi_3\right) + \ldots + K_{(j-1)j}\left(\varphi_{j-1} - \varphi_j\right)\right\}, \tag{3.2}$$

4.3. operation of external forces (torque and resistance moment in the system):

$$dA = M_K\delta\varphi_0 - M_{AT}\left(\delta\varphi_0 + \delta\varphi_1 + \delta\varphi_2 + \ldots + \delta\varphi_j\right), \tag{3.3}$$

4.4. The Lagrange equation for each j-th coordinate φ_j ($j = 0,\ 1,\ \ldots\ ,\ 8$) to describe the rotation of each i-th mass ($i = 1,\ 2,\ \ldots\ ,\ 8$) of a given discrete eight mass system for the crankshaft of a diesel locomotive can be written as:

$$\frac{\partial}{\partial t}\left[\frac{\partial T}{\partial \varphi_j}\right] + \frac{\partial P}{\partial \varphi_j} = \frac{\partial A}{\partial \varphi_j}, \tag{3.4}$$

for φ_0:

$$\varphi_0\left(J_0 + J_1 + J_2 + \ldots + J_j\right) + \varphi_1\left(J_0 + J_1\right) + \ldots + \varphi_j\left(J_0 + J_j\right) = M_K - M_{AT}, \tag{3.5}$$

for φ_1:

$$\varphi_0\left(J_0 + J_1\right) + \varphi_1\left(J_0 + J_1\right) + K_{12}\left(\varphi_1 - \varphi_2\right) = -M_1, \tag{3.6}$$

for φ_2:

$$\varphi_0\left(J_0 + J_2\right) + \varphi_2\left(J_0 + J_2\right) + K_{23}\left(\varphi_2 - \varphi_3\right) = -M_2, \tag{3.7}$$

for φ_i ($i = 1,\ 2,\ \ldots\ ,\ 8$):

$$\varphi_0\left(J_0 + J_i\right) + \varphi_J\left(J_0 + J_i\right) + K_{(i-1)i}\left(\varphi_{i-1} - \varphi_i\right) = -M_i. \tag{3.8}$$

5. The resulting system of differential equations:

- at $M_i = 0$ and $\ddot{\varphi}_0(t) = 0$ is a system of homogeneous equations;
- at $\ddot{\varphi}_0(t) \neq 0$ shows variable rotation;
- at $M_i \neq 0$ shows the action of variable loads.

6. Solving the system of differential equations (3.5) - (3.8) for the first case. The condition in this case refers to the uneven rotation of the crankshaft of the diesel locomotive:

$$\varphi_0(t) = \varphi_0 \cos(\omega t), \tag{3.9}$$

where φ_0 is the amplitude of the circular frequency.

6.1. For system solutions,

$$\varphi_1(t) = \varphi_1 \cos(\omega t), \varphi_2(t) = \varphi_2 \cos(\omega t), \varphi_j(t) = \varphi_j \cos(\omega t), \tag{3.10}$$

where φ_j – amplitudes of model mass fluctuations as per Figure 1.

6.2. After calculating the time derivatives from (3.10) in the system of differential equations (3.5) - (3.8), a system of algebraic equations is obtained to determine the amplitudes φ_j:

$$-\varphi_1\omega^2(J_0+J_1) - \varphi_2\omega^2(J_0+J_2) - \ldots - \varphi_j\omega^2\left(J_0+J_j\right) = \frac{M_K - M_{AT}}{\varphi_0\omega^2\left(J_0+J_1+\ldots+J_j\right)} = B_0 \tag{3.11}$$

$$-\varphi_1\omega^2(J_0+J_1) + K_{12}(\varphi_1-\varphi_2) = \frac{-M_1}{\varphi_0\omega^2(J_0+J_1)} = B_1, \tag{3.12}$$

$$-\varphi_2\omega^2(J_0+J_2) + K_{23}(\varphi_2-\varphi_3) = \frac{-M_2}{\varphi_0\omega^2(J_0+J_2)} = B_2, \tag{3.13}$$

$$-\varphi_i\omega^2(J_0+J_i) + K_{(i-1)i}(\varphi_{i-1}-\varphi_i) = \frac{-M_j}{\varphi_0\omega^2(J_0+J_i)} = B_i(i = 1,\ 2,\ \ldots,\ 8). \tag{3.14}$$

6.3. We introduce the designations of the coefficients A_{ij} and B_j for φ_j in the system of algebraic equations (3.11) - (3.14):

$$A_{11}\varphi_1 + A_{12}\varphi_2 + A_{13}\varphi_3 + \ldots + A_{1j}\varphi_j = B_1, \tag{3.15}$$

$$A_{21}\varphi_1 + A_{22}\varphi_2 + A_{23}\varphi_3 + \ldots + A_{2j}\varphi_j = B_2, \tag{3.16}$$

$$A_{31}\varphi_1 + A_{32}\varphi_2 + A_{33}\varphi_3 + \ldots + A_{3j}\varphi_j = B_3, \tag{3.17}$$

$$A_{i1}\varphi_1 + A_{i2}\varphi_2 + A_{i3}\varphi_3 + \ldots + A_{ij}\varphi_i = B_i(i = 1,\ 2,\ \ldots,\ 8). \tag{3.18}$$

4. Discussion of results.

The resulting system of equations can be solved by the numerical Gauss method [5-8] in the MATHCAD 15 programming environment. To do this, at the beginning, a determinant is obtained from the coefficients at φ_j

$$\Delta = \begin{vmatrix} A_{11} & A_{12} & A_{13} & A_{14}\ldots & A_{18} \\ A_{21} & A_{22} & A_{23} & A_{24}\ldots & A_{28} \\ A_{31} & A_{32} & A_{33} & A_{34}\ldots & A_{38} \\ A_{41} & A_{42} & A_{43} & A_{44}\ldots & A_{48} \\ A_{51} & A_{52} & A_{53} & A_{54}\ldots & A_{58} \\ A_{61} & A_{62} & A_{63} & A_{64}\ldots & A_{68} \\ A_{71} & A_{72} & A_{73} & A_{74}\ldots & A_{78} \\ A_{81} & A_{82} & A_{83} & A_{84}\ldots & A_{88} \end{vmatrix}, \tag{4.1}$$

After that, according to Cramer's rule, the formulas for φ_j

$$\varphi_1 = \frac{1}{\Delta}\begin{vmatrix} B_1 & A_{12} & A_{13} & A_{14}\ldots & A_{18} \\ B_2 & A_{22} & A_{23} & A_{24}\ldots & A_{28} \\ B_3 & A_{32} & A_{33} & A_{34}\ldots & A_{38} \\ B_4 & A_{42} & A_{43} & A_{44}\ldots & A_{48} \\ B_5 & A_{52} & A_{53} & A_{54}\ldots & A_{58} \\ B_6 & A_{62} & A_{63} & A_{64}\ldots & A_{68} \\ B_7 & A_{72} & A_{73} & A_{74}\ldots & A_{78} \\ B_8 & A_{82} & A_{83} & A_{84}\ldots & A_{88} \end{vmatrix}, \tag{4.2}$$

$$\varphi_2 = \frac{1}{\Delta}\begin{vmatrix} A_{11} & B_1 & A_{13} & A_{14}\ldots & A_{18} \\ A_{21} & B_2 & A_{23} & A_{24}\ldots & A_{28} \\ A_{31} & B_3 & A_{33} & A_{34}\ldots & A_{38} \\ A_{41} & B_4 & A_{43} & A_{44}\ldots & A_{48} \\ A_{51} & B_5 & A_{53} & A_{54}\ldots & A_{58} \\ A_{61} & B_6 & A_{63} & A_{64}\ldots & A_{68} \\ A_{71} & B_7 & A_{73} & A_{74}\ldots & A_{78} \\ A_{81} & B_8 & A_{83} & A_{84}\ldots & A_{88} \end{vmatrix}, \tag{4.3}$$

And so on . . .

$$\varphi_8 = \frac{1}{\Delta}\begin{vmatrix} A_{11} & A_{12} & A_{13} & A_{14}\ldots & B_1 \\ A_{21} & A_{22} & A_{23} & A_{24}\ldots & B_2 \\ A_{31} & A_{32} & A_{33} & A_{34}\ldots & B_3 \\ A_{41} & A_{42} & A_{43} & A_{44}\ldots & B_4 \\ A_{51} & A_{52} & A_{53} & A_{54}\ldots & B_5 \\ A_{61} & A_{62} & A_{63} & A_{64}\ldots & B_6 \\ A_{71} & A_{72} & A_{73} & A_{74}\ldots & B_7 \\ A_{81} & A_{82} & A_{83} & A_{84}\ldots & B_8 \end{vmatrix}, \tag{4.4}$$

The system of equations (3.15) - (3.18) for calculating torsional oscillations of the crankshaft of a diesel locomotive with piecewise continuous distribution of mass along the length is presented in matrix form using concentrated mass matrices and «transition matrices» for sections of the rod according to the Gauss method and the Kramer rule. An algorithm was developed and a program was compiled based on the Gauss method and the iteration method. Numerical studies are performed in the MATHCAD 15 programming environment.

Author's contributions

All authors contributed equally to the writing of this paper. All authors read and approved the final manuscript.

References

[1] Chesnokov A.L. Heat engineering and heat exchange in internal combustion engines. - M.: 2002.

[2] Kamenev V.M. Numerical Methods of Heat Transfer Modelling. - Moscow state technical university, 2009.

[3] Nazarenko A.S., Nazarenko, O.S. Mathematical Modelling of Heat Transfer in Technical Systems. - M.: Mashinostroenie, 2011.

[4] Chetvergov V.A. Reliability of the locomotives / V.A. Chetvergov, V.D. Puzankov. - Moscow: Marshrut, 2003. – 415 p.

[5] Krivorudchenko, V.F. Modern methods of the technical diagnostics and non-destructive control of the parts and units of the rolling stock of the railway transport: Textbook for the universities of the railway transport / R.A. Akhmedjanov, V.F. Krivorudchenko. - Moscow: Marshrut, 2005. - 436 p.

[6] Kasimov Sh.A., Sulliev A. and Eshkabilov A.A. Tashkent State Transport University, Tashkent, Uzbekistan. Optimizing Pulse Combustion Systems for Enhanced Efficiency and Sustainability in Thermal Power Engineering. E3S Web of Conferences 449, 06006 (2023). pp. 5 -16, November 2023.

[7] Khamidov O., Yusufov A., Kudratov Sh., Yusupov A. (2023). Evaluation of the technical condition of locomotives using modern methods and tools. In E3S Web of Conferences (Vol. 365, p. 05004). EDP Sciences.
[8] Kasimov Sh.A., Kendjayev R.Kh. , Islomov Yo.A. Mathematical simulation of flow of gas liquid flow in improved devices in pump compressor tubing to increase oil production. AIP Conference Proceedings, Volume 3045, Issue 1, 050032 (2024), 11 March 2024. https://doi.org/10.1063/5.0197374, pp.7. Melville, New York, 2024.

Affiliations

Kasimov Shuhrat.
Address: Tashkent State Transport University, Dept. of Higher mathematics, Tashkent-Uzbekistan.
e-mail: shuxrat1812@mail.ru
ORCID ID: 0000-0003-2390-980X

Kendjayev Ravshan
Address: Tashkent State Transport University, Dept. of Higher mathematics, Tashkent-Uzbekistan.
e-mail: lovsan63@mail.ru
ORCID ID: 0000-0003-2390-980X

Kudratov Shohijakhon
Address: Tashkent State Transport University, Tashkent-Uzbekistan.
e-mail: lovsan63@mail.ru
ORCID ID: 0000-0003-2390-980X

Uzbekistan Journal of Mathematics and Computer Science
Volume 1 No. 1 Page 71–80 (2025)
DOI: https://doi.org/10.56143/ujmcs.v1i1.6
Research article

UZJMCS

The singular value function, associated with a Maharam trace

Zakirov B.S.*

Abstract

Let M be a finite von Neumann algebra, let $S(M)$ be the $*$-algebra of measurable operators affiliated with M. Maharam traces Φ on a von Neumann algebra M with values in complex Dedekind complete vector lattices are considered. The singular value function of operators from $S(M)$, associated with such a trace Φ are determined. The main properties of these singular value functions, similar to classical singular value functions of measurable operators, are studied.

Keywords: *von Neumann algebra, algebra of measurable operators, vector-valued trace, Dedekind complete vector lattice, singular value function, Maharam trace.*

AMS Subject Classification (2020): *Primary: 28B15; Secondary: 46L52.*

Introduction

The modern theory of noncommutative measure and integration finds its roots in the seminal papers of I.E.Segal [1] and J.Dixmier [2]. The introduced by I.E.Segal noncommutative L^1-space associated with an exact normal semiinfinite trace is the main object of many investigations both in the theory of noncommutative integration and in its multiple applications (for example,[3], [4], [5], [6]). Detailed information on the current state of this theory is presented in [7], [8], [9], [10] and [11].

The existence of the center-valued traces in finite von Neumann algebras makes it natural to construct the theory of integration for traces with values in the complex Dedekind complete vector lattice $F_{\mathbb{C}} = F \oplus iF$. If the von Neumann algebra is commutative, then construction of $F_{\mathbb{C}}$-valued integration for it is the component part for the investigation of the properties of order continuous maps of vector lattices. The theory of such mappings is described rather thoroughly in the monograph [12]. An import role among these mappings is played by operators with the Maharam property. L^p-spaces associated with such operators are profound examples of Banach-Kantorovich lattices.

In [13], [14] and [15] a theory of non-commutative integration for traces Φ with values in the complex Dedekind complete vector lattice $F_{\mathbb{C}}$ was constructed. In particular, for Maharam traces Φ, with the help of the locally measure topology in the algebra $S(M)$ of all measurable operators affiliated with the von Neumann algebra M, the Banach-Kantorovich space $L^p(M,\Phi) \subset S(M), 1 \leq p < \infty$ was constructed and properties of such spaces are considered.

Received : *5–January–2025,* ***Accepted :*** *27–march–2025*
*** Corresponding author***

This article is devoted to a study of singular value function of operators from $S(M)$, associated with a Maharam trace Φ. Also dominated properties of these singular value functions, similar to classical singular value functions of measurable operators, are proved.

In studying the $*$-algebra $S(M,\tau)$ of all τ-measurable operators, the notion of singular value functions plays an important role. There is an intimate relationship between the properties of τ-measurable operators and the properties of the singular value function (see for example ([11], Chapter 3)). For $x \in S(M,\tau)$, the singular value function $\mu(x)$ is defined by

$$\mu(t;x) := \inf\{s \geq 0 : \ \tau(E_{(s,\infty)}(x)) \leq t\}, \ t \geq 0,$$

where $E_{(s,\infty)}(x)$ is the spectral projection of the operator x corresponding to the interval (s,∞). The following expression is classical:

$$\mu(t;x) := \inf\{\|xp\|_M : \ p \in P(M), \ \tau(\mathbf{1}-p) \leq t\}, \ x \in S(M,\tau), \ t \geq 0,$$

where $P(M)$ is the set of all projectors in von Neumann algebra M.

In the present article, we will study the corresponding notion for traces $\Phi : M \to F_{\mathbb{C}}$. More precisely, let M be a finite von Neumann algebra, with center $Z(M)$, on the Hilbert space H. Let $\mathcal{B}$ be a commutative von Neumann algebra, $*$-isomorphic to a von Neumann subalgebra $\mathcal{A}$ in $Z(M)$, and let Φ be a $S(\mathcal{B})$-valued Maharam trace on M. Denote by $\mathcal{P}(\mathcal{B})$ the set of all $f \in S_h(\mathcal{B})$, for which the support $s(f) = \mathbf{1}_{\mathcal{B}}$.

For $x \in S(M)$, the singular value function, associated with a Maharam trace Φ is the map $\Phi(x) : (0,\infty) \to S_h(\mathcal{B})$ defined by the equality

$$\Phi(t;x) := \inf\{g \in \mathcal{P}(\mathcal{B}) : \ \Phi(E_g(x)) \leq t \cdot \mathbf{1}\}, \ t > 0,$$

where $E_g(x) \in P(M)$ is the projector in M, which is a projection onto a closed subspace $\overline{\{\xi \in H : x(\xi) > g(\xi)\}}$.

For all $t > 0$, the singular value function $\Phi(x)$ admits the characterization

$$\Phi(t;x) = \inf\{\|xe\|_{\mathcal{A}} : \ e \in P(M), \ xe \in E(M,\mathcal{A}), \ \Phi(\mathbf{1}-e) \leq t \cdot \mathbf{1}\},$$

where

$$E(M,\mathcal{A}) = \left\{x \in S(M) : |x| \leq a \ \text{ for some } \ a \in S_+(\mathcal{A})\right\}$$

is a Banach-Kantorovich space with $S_h(\mathcal{A})$-valued norm

$$\|x\|_{\mathcal{A}} = \inf\{a \in S_+(\mathcal{A}) : |x| \leq a\}.$$

We use the terminology and results of the theory of von Neumann algebras [8], [9], the theory of measurable operators [1], [10], [11] and of the theory of Dedekind complete vector lattices and Banach-Kantorovich spaces theory [12].

1. Preliminaries

Let H be a Hilbert space over the field $\mathbb{C}$ of complex numbers, let $B(H)$ be the $*$-algebra of all bounded linear operators on H, and $\mathbf{1}$ be the identity operator on H. Let M be a von Neumann algebra acting on H, let $Z(M)$ be the center of M and $P(M) = \{p \in M : p^2 = p = p^*\}$ be the lattice of all projectors in M. We denote by $P_{fin}(M)$ the set of all finite projectors in M.

A densely-defined closed linear operator x (possibly unbounded) affiliated with M is said to be *measurable* if there exists a sequence $\{p_n\}_{n=1}^{\infty} \subset P(M)$ such that $p_n \uparrow \mathbf{1}$, $p_n(H) \subset \mathfrak{D}(x)$ and $p_n^{\perp} = \mathbf{1} - p_n \in P_{fin}(M)$ for every $n = 1, 2, \ldots$ (here $\mathfrak{D}(x)$ is the domain of x).

The set $S(M)$ of all measurable with respect to M operators is a complex $*$-algebra with unit element $\mathbf{1}$, with respect to the operations of strong sum, strong product and the $*$-operation of taking adjoints (see [1]). The von Neumann algebra M is a $*$-subalgebra of $S(M)$. The set of all self-adjoint elements in $S(M)$ is denoted by $S_h(M)$, which is a real linear subspace of $S(M)$.

Let $x \in S(M)$ and $x = u|x|$ be the polar decomposition, where $|x| = (x^*x)^{\frac{1}{2}}$, u is a partial isometry in $B(H)$. Then $u \in M$ and $|x| \in S(M)$. If $x \in S_h(M)$ and $\{E_\lambda(x)\}$ are the spectral projections of x, then $\{E_\lambda(x)\} \subset P(M)$.

Let M be a commutative von Neumann algebra. Then M admits a faithful semi-finite normal trace τ, and M is $*$-isomorphic to the $*$-algebra $L^\infty(\Omega, \Sigma, \mu)$ of all bounded complex measurable functions with the identification almost everywhere, where (Ω, Σ, μ) is a measurable space. In addition, $\mu(A) = \tau(\chi_A),\ A \in \Sigma$. Moreover, $S(M) \cong L^0(\Omega, \Sigma, \mu)$, where $L^0(\Omega, \Sigma, \mu)$ is the $*$-algebra of all complex measurable functions with the identification almost everywhere [1].

Let M be an von Neumann algebra, let F be an Dedekind complete vector lattice, and let $F_{\mathbb{C}} = F \oplus iF$ be a complexification of F. If $z = \alpha + i\beta \in F_{\mathbb{C}},\ \alpha, \beta \in F$, then $\overline{z} := \alpha - i\beta$, and $|z| := \sup\{Re(e^{i\theta}z) : 0 \le \theta < 2\pi\}$ (see[12], 1.3.13).

An *$F_{\mathbb{C}}$-valued trace* on the von Neumann algebra M is a linear mapping $\Phi : M \to F_{\mathbb{C}}$ given $\Phi(x^*x) = \Phi(xx^*) \ge 0$ for all $x \in M$. It is clear that $\Phi(M_h) \subset F,\ \Phi(M_+) \subset F_+ = \{a \in F : a \ge 0\}$. A trace Φ is said to be *faithful* if the equality $\Phi(x^*x) = 0$ implies $x = 0$, *normal* if $\Phi(x_\alpha) \uparrow \Phi(x)$ for every $x_\alpha, x \in M_h,\ x_\alpha \uparrow x$.

If M is a finite von Neumann algebra, then its center-valued trace $\Phi_M : M \to Z(M)$ is an example of a $Z(M)$-valued faithful normal trace.

Let Δ be a separating family of finite normal numerical traces on the von Neumann algebra M, $\mathbb{C}^\Delta = \prod_{\tau \in \Delta} \mathbb{C}_\tau$, where $\mathbb{C}_\tau = \mathbb{C}$ for all $\tau \in \Delta$. Then $\Phi(x) = \{\tau(x)\}_{\tau \in \Delta}$ is also an example of an faithful normal $\mathbb{C}^\Delta$-valued trace on M.

Let us list some properties of the trace $\Phi : M \to F_{\mathbb{C}}$.

Proposition 1.1. *([13]) (i) Let $x, y, a, b \in M$. Then*
$\Phi(x^*) = \overline{\Phi(x)},\ \Phi(xy) = \Phi(yx), \Phi(|x^*|) = \Phi(|x|)$,
$|\Phi(axb)| \le \|a\|_M \|b\|_M \Phi(|x|)$;
(ii) If Φ is a faithful trace, then M is finite;
(iii) If M is a finite von Neumann algebra, then $\Phi(\Phi_M(x)) = \Phi(x)$ for all $x \in M$;
(iv) $\Phi(|x + y|) \le \Phi(|x|) + \Phi(|y|)$ for all $x, y \in M$.

The trace $\Phi : M \to F_{\mathbb{C}}$ possesses *the Maharam property* if for any $x \in M_+,\ 0 \le f \le \Phi(x),\ f \in F$, there exists a positive $y \le x$ such that $\Phi(y) = f$. A faithful normal $F_{\mathbb{C}}$-valued trace Φ with the Maharam property is called *a Maharam trace* (compare with [12], III, 3.4.1). Obviously, any faithful finite numerical trace on M is a $\mathbb{C}$-valued Maharam trace.

Let us give another examples of Maharam traces. Let M be a finite von Neumann algebra, let $\mathcal{A}$ be a von Neumann subalgebra in $Z(M)$, and let $T : Z(M) \to \mathcal{A}$ be an injective linear positive normal operator. If $f \in S(\mathcal{A})$ is a reversible positive element, then $\Phi(T, f)(x) = fT(\Phi_M(x))$ is an $S(\mathcal{A})$-valued faithful normal trace on M. In addition, if $T(ab) = aT(b)$ for all $a \in \mathcal{A}, b \in Z(M)$, then $\Phi(T, f)$ is a Maharam trace on M.

Note that if τ is a faithful normal finite numerical trace on M and $\dim(Z(M)) > 1$, then $\Phi(x) = \tau(x)\mathbf{1}$ is a $Z(M)$-valued faithful normal trace. In addition, Φ does not possess the Maharam property (see [13]).

Let F have an order unit $\mathbf{1}_F$. Denote by $B(F)$ the complete Boolean algebra of unitary elements with respect to $\mathbf{1}_F$, and let Q be the Stone representation space of the Boolean algebra $B(F)$. Let $C_\infty(Q)$ be the order complete vector lattice of all continuous functions $a : Q \to [-\infty, +\infty]$ such that $a^{-1}(\{\pm\infty\})$ is a nowhere dense subset of Q. We identify F with the order-dense ideal in $C_\infty(Q)$ containing algebra $C(Q)$ of all continuous real functions on Q. In addition, $\mathbf{1}_F$ is identified with the function equal to 1 identically on Q ([12], 1.4.4).

The next theorem gives the description of Maharam traces on von Neumann algebras.

Theorem 1.1. *([13]) Let Φ be an $F_{\mathbb{C}}$-valued Maharam trace on a von Neumann algebra M. Then there exists a von Neumann subalgebra $\mathcal{A}$ in $Z(M)$, a $*$-isomorphism ψ from $\mathcal{A}$ onto the $*$-algebra $C(Q)_{\mathbb{C}}$, an injective positive linear normal operator $\mathcal{E}$ from $Z(M)$ onto $\mathcal{A}$ with $\mathcal{E}(\mathbf{1}) = \mathbf{1}$, $\mathcal{E}^2 = \mathcal{E}$, such that*

1) $\Phi(x) = \Phi(\mathbf{1})\psi(\mathcal{E}(\Phi_M(x)))$ *for all* $x \in M$;
2) $\Phi(zy) = \Phi(z\mathcal{E}(y))$ *for all* $z, y \in Z(M)$;
3) $\Phi(zy) = \psi(z)\Phi(y)$ *for all* $z \in \mathcal{A}$, $y \in M$.

Due to Theorem 1.1, the $*$-algebra $\mathcal{B} = C(Q)_{\mathbb{C}}$ is $*$-isomorphic to a von Neumann subalgebra in $Z(M)$. Therefore $\mathcal{B}$ is a commutative von Neumann algebra, and $*$-algebra $C_\infty(Q)_{\mathbb{C}}$ is identified with $*$-algebra $S(\mathcal{B})$. It is clear that the $*$-isomorphism ψ from $\mathcal{A}$ onto $\mathcal{B}$ can be extended to a $*$-isomorphism from $S(\mathcal{A})$ onto $S(\mathcal{B})$. We denote this mapping also by ψ.

Let Φ be an $S(\mathcal{B})$-valued Maharam trace on a von Neumann algebra M. Next we will need the concept of a central extension of a von Neumann algebra from [16].

A set $\{z_j\}_{j\in J}$ of pairwise orthogonal nonzero central projections from M will be called a partition of unity $\mathbf{1}$, if $\sup_{j\in J} z_j = \mathbf{1}$. Following [16], denote by $E(M, \mathcal{A})$ the set of all those operators $x \in S(M)$ for which there exists a partition of unity $\{z_j\}_{j\in J} \subset P(\mathcal{A})$ and a set $\{x_j\}_{j\in J} \subset M$ such that $xz_j = x_jz_j$ for all $j \in J$. It is clear that $M \subset E(M, \mathcal{A})$, $S(\mathcal{A}) \subset E(M, \mathcal{A})$ and $E(M, \mathcal{A})$ is an $*$-subalgebra of $S(M)$ with respect to the natural operations in $S(M)$. $E(M, \mathcal{A})$ is called the central extension of the algebra M with respect to the subalgebra $\mathcal{A} \subset Z(M)$.

Proposition 1.2. *([17], Proposition 3.4) For the operator $x \in S(M)$ the following conditions are equivalent:*

(i) $x \in E(M, \mathcal{A})$;

(ii) there exists $a \in S_+(\mathcal{A})$ such that $|x| \le a$.

According to proposition 1.2, for each $x \in E(M, \mathcal{A})$, an element $\|x\|_{\mathcal{A}} = \inf\{a \in S_+(\mathcal{A}) : |x| \le a\}$ from $S_+(\mathcal{A})$ is defined. The following theorem follows from the results of [17].

Theorem 1.2. *$(E(M, \mathcal{A}), \|\cdot\|_{\mathcal{A}})$ is a Banach-Kantorovich space over $S_h(\mathcal{A})$.*

It follows directly from Theorem 1.2 that the mapping $\|x\|_{\mathcal{B}} = \Psi(\|x\|_{\mathcal{A}})$ defines an $S_h(\mathcal{B})$-valued norm on $E(M, \mathcal{A})$, with respect to which $E(M, \mathcal{A})$ becomes a Banach-Kantorovich space over $S_h(\mathcal{B})$.

2. Spectral distribution functions and singular value functions, associated with a Maharam trace

Let $\mathcal{B}$ be a commutative von Neumann algebra $*$-isomorphic to the von Neumann subalgebra $\mathcal{A}$ in the center $Z(M)$ of M and $\Phi : M \to S(\mathcal{B})$ be the Maharam trace on M (see Theorem 1.1). We suppose that $\Phi(\mathbf{1}) = \mathbf{1}_{\mathcal{B}}$.

For each $f \in S_h(\mathcal{B})$, we denote by $s(f)$ the support of f, i.e. $s(f) = \mathbf{1}_{\mathcal{B}} - \sup\{e \in P(\mathcal{B}) : fe = 0\}$. It is clear that $s(\Phi(\mathbf{1})) = \mathbf{1}_{\mathcal{B}}$. Let $\mathcal{P}(\mathcal{B})$ denote the set of all $f \in S_+(\mathcal{B})$ for which the support $s(f) = \mathbf{1}_{\mathcal{B}}$. It is clear that each element $f \in \mathcal{P}(\mathcal{B})$ is invertible in the algebra $S_h(\mathcal{B})$, i.e. there exists an element $g \in S_h(\mathcal{B})$ such that $f \cdot g = \mathbf{1}_{\mathcal{B}}$, and $g \in \mathcal{P}(\mathcal{B})$.

Definition 2.1. Let $0 \le x \in S(M)$ and $g \in \mathcal{P}(\mathcal{B})$. The $S(\mathcal{B})$-valued spectral distribution function $d(.; x) : \mathcal{P}(\mathcal{B}) \to S_h(\mathcal{B})$ is defined by

$$d(g; x) := \Phi(E_g(x)),$$

where $E_g(x) \in P(M)$ is the projector in M, which is a projection onto a closed subspace $\overline{\{\xi \in H : x(\xi) > g(\xi)\}}$.

Evidently, the mapping $d(.;x)$ is decreasing. If $g, g_n \in \mathcal{P}(\mathcal{B})$, $n = 1, 2, ...,$ and $g_n \downarrow g$, then $E_g(x) = \sup\limits_{n\geq 1} E_{g_n}(x)$ in M_+, and so, $\Phi(E_g(x)) = \sup\limits_{n\geq 1} \Phi(E_{g_n}(x))$. Hence, $d(.;x)$ is right-continuous on $\mathcal{P}(\mathcal{B})$.

Definition 2.2. For $x \in S(M)$, the singular value function, associated with a Maharam trace Φ is the map $\Phi(.;x) : (0,\infty) \to S_h(\mathcal{B})$ defined by the equality

$$\Phi(t;x) := \inf\{g \in \mathcal{P}(\mathcal{B}) : \ d(g;|x|) \leq t \cdot \mathbf{1}\}, \ t > 0. \tag{2.1}$$

It is clear that $\Phi(t;x) \leq \Phi(s;x)$ at $s < t$. In addition, the map $\Phi(t;x)$ has the following useful continuity property.

Proposition 2.1. *If* $t_n, t > 0, n = 1, 2, ...,$ *and* $t_n \downarrow t$, *then* $\Phi(t;x) = \sup\limits_{n\geq 1} \Phi(t_n;x)$.

Proof. Let $t_n, t > 0, n = 1, 2, ...,$ and $t_n \downarrow t$. Then

$$\Phi(t;x) = \inf\{g \in \mathcal{P}(\mathcal{B}) : d(g;|x|) \leq \inf_{n\geq 1}(t_n \cdot \mathbf{1})\}$$

$$= \inf\left\{g \in \mathcal{P}(\mathcal{B}) : d(g;|x|) \leq t_n \cdot \mathbf{1} \ \text{ for all } \ n \geq 1\right\}$$

$$= \sup_{n\geq 1}\left\{\inf\{g \in \mathcal{P}(\mathcal{B}) : d(g;|x|) \leq t_n \cdot \mathbf{1}\}\right\} = \sup_{n\geq 1} \Phi(t_n;x),$$

i.e. $\Phi(t;x) = \sup\limits_{n\geq 1} \Phi(t_n;x)$. $\triangleright$

Example 2.1. Let $x = p \in P(M)$ and $g \in \mathcal{P}(\mathcal{B})$. Then $d(g;p) = \Phi(E_g(p)) = \Phi(p)$, if $g < \mathbf{1}$, and $d(g;p) = \mathbf{0}$, if $g \geq \mathbf{1}$. Hence by (1) $\Phi(t;p) = \mathbf{1}$, if $\mathbf{0} < t \cdot \mathbf{1} \leq \Phi(p)$, and $\Phi(t;p) = \mathbf{0}$, if $t \cdot \mathbf{1} > \Phi(p)$.

Example 2.2. Let M be a finite von Neumann algebra and suppose that $x = \sum\limits_{j=1}^{m} \alpha_j p_j$, where $p_1, \ldots, p_m \in P(M)$ with $p_j p_k = 0$ whenever $j \neq k$, and $\alpha_1, \ldots, \alpha_m \in \mathbb{R}^+$ are such that $\alpha_j \neq \alpha_k$ whenever $j \neq k$. For the computation of $\Phi(x)$, it may be assumed that $\alpha_1 > \alpha_2 > \ldots > \alpha_m > 0$. If $g \in \mathcal{P}(\mathcal{B})$ and $g \geq \alpha_1 \cdot \mathbf{1}$, then clearly $d(g;x) = 0$. However, if $\alpha_2 \cdot \mathbf{1} \leq g < \alpha_1 \cdot \mathbf{1}$, then $E_g(x) = p_1$, and so $d(g;x) = \Phi((p_1))$. Similarly, if $\alpha_3 \cdot \mathbf{1} \leq g < \alpha_2 \cdot \mathbf{1}$, then $E_g(x) = p_1 + p_2$, and so $d(g;x) = \Phi(p_1 + p_2) = \Phi(p_1) + \Phi(p_2)$. In general, we have

$$d(g;x) = \sum_{i=1}^{j} \Phi(p_i), \quad \text{if } \ \alpha_{j+1} \cdot \mathbf{1} \leq g < \alpha_j \cdot \mathbf{1} \ (g \in \mathcal{P}(\mathcal{B})),$$

where $j = 1, 2, \ldots, m,$ and $\alpha_{m+1} = 0$.

Define $\rho_k = \sum\limits_{i=1}^{j} \Phi(p_i)$ for $j = 1, 2, \ldots, m$. Referring to (2.1), we see that $\Phi(t;x) = \mathbf{0}$ if $t \cdot \mathbf{1} \geq \rho_m$. Also, if $\rho_m > t \cdot \mathbf{1} \geq \rho_{m-1}$, then $\Phi(t;x) = \alpha_m \cdot \mathbf{1}$, and if $\rho_{m-1} > t \cdot \mathbf{1} \geq \rho_{m-2}$, then $\Phi(t;x) = \alpha_{m-1} \cdot \mathbf{1}$, and so on. Hence,

$$\Phi(t;x) = \begin{cases} \alpha_1 \cdot \mathbf{1}, & \mathbf{0} < t \cdot \mathbf{1} \leq \rho_1; \\ \alpha_j \cdot \mathbf{1}, & \rho_j > t \cdot \mathbf{1} \geq \lambda_{j-1}, \ 2 \leq j \leq m-1; \\ \mathbf{0}, & t \cdot \mathbf{1} > \rho_m. \end{cases}$$

Theorem 2.1. *Let* $x \in S(M)$. *For all* $t > 0$, *the singular value function* $\Phi(.,x)$ *admits the characterization*

$$\Phi(t;x) = \inf\{\|xe\|_{\mathcal{B}} : \ e \in P(M), \ xe \in E(M,\mathcal{A}), \ \Phi(\mathbf{1} - e) \leq t \cdot \mathbf{1}\}. \tag{2.2}$$

Proof. We fix $t > 0$ and put

$$G(x) = \{g \in \mathcal{P}(\mathcal{B}) : \ d(g; |x|) \leq t \cdot \mathbf{1}\}.$$

If $g_1, g_2 \in G(x)$, $e = s((g_2 - g_1)_+)$, then $g = g_1 \wedge g_2 = g_1 \cdot e + g_2 \cdot (\mathbf{1} - e) \in \mathcal{P}(\mathcal{B})$, at the same time

$$d(g; |x|) = \Phi(E_g(x)) = \Phi(E_{g_1}(x)) \cdot e + \Phi(E_{g_2}(x)) \cdot (\mathbf{1} - e)$$

$$\leq t \cdot e + t \cdot (\mathbf{1} - e) = t \cdot \mathbf{1},$$

i.e. $g_1 \wedge g_2 \in G(x)$. Using mathematical induction, we obtain that for any finite set $\{g_i\}_{i=1}^n \subset G(x)$ the inclusion holds true $\bigwedge_{i=1}^{n} g_i \in G(x)$. Since the Boolean algebra $P(\mathcal{B})$ has a countable type, there exists a sequence $\{g_k\}_{k=1}^{\infty} \subset G(x)$ for which $g_k \downarrow f$, where

$$f = \Phi(t; x) := \inf\{g \in \mathcal{P}(\mathcal{B}) : \ d(g; |x|) \leq t \cdot \mathbf{1}\} \in S_h(\mathcal{B}).$$

Since $g_k \downarrow f$ and for all $k \in \mathbb{N}$ the inequality $d(g_k; |x|) \leq t \cdot \mathbf{1}$ is true, then

$$t \cdot \mathbf{1} \geq d(g_k; |x|) \uparrow d(f; |x|).$$

In particular, the inequality is true

$$\Phi(E_f(x)) = d(f; |x|) \leq t \cdot \mathbf{1} \ \text{ i.e. } \ \Phi(\mathbf{1} - e) \leq t \cdot \mathbf{1},$$

where $e = \mathbf{1} - E_f(x) \in P(M)$. Since $|x|e \leq f \in S_h(\mathcal{B})$, then $xe \in E(M, \mathcal{A})$. Moreover, using the polar decomposition $x = u|x|$ of the operator x, we obtain $\|xe\|_{\mathcal{B}} = \|u|x|e\|_{\mathcal{B}} \leq \||x|e\|_{\mathcal{B}} \leq f$. Therefore,

$$\Psi(t; x) = \inf\{\|xe\|_{\mathcal{B}} : \ e \in P(M), \ xe \in E(M, \mathcal{A}), \ \Phi(\mathbf{1} - e) \leq t \cdot \mathbf{1}\} \leq f = \Phi(t; x).$$

To prove the reverse inequality, we set

$$\Lambda(x) = \{e \in P(M) : xe \in E(M, \mathcal{A}), \ \Phi(\mathbf{1} - e) \leq t \cdot \mathbf{1}\}.$$

Then, we have $\Psi(t; x) = \inf\{\|xe\|_{\mathcal{B}} : e \in \Lambda(x)\}$. Suppose that the inequality $\Phi(t; x) = f \leq \Psi(t; x)$ is not satisfied. Therefore, there exists an $e \in \Lambda(x)$ for which the inequality $f \leq \|xe\|_{\mathcal{B}}$ does not hold. In particular, this means that there exist $0 \neq q \in P(M)$, $\varepsilon > 0$, for which the inequalities

$$|xeq| \leq \|xeq\|_{\mathcal{B}} = \|xe\|_{\mathcal{B}} \cdot q \leq qf + \varepsilon q.$$

are true. Therefore, there exists an $e \in \Lambda(x)$ for which the inequality $f \leq \|xe\|_{\mathcal{B}}$ does not hold. In particular, this means that there exist $0 \neq q \in P(M)$, $\varepsilon > 0$, for which the inequalities

$$|xeq| \leq \|xeq\|_{\mathcal{B}} = \|xe\|_{\mathcal{B}} \cdot q \leq qf + \varepsilon q$$

are true. Let $q_1 = qg + 2\varepsilon \cdot q$. Consider the element $r = s((|xe| - q_1)_+)$ from $P(M)$. From the relations

$$|xe|rq \geq (qg + 2\varepsilon \cdot q)q = qg + 2\varepsilon \cdot q > qg + \varepsilon \cdot q \geq |xeq| = |xe|q$$

it follows that $|xe|rq > |xe|q$, which is impossible.

Thus, the inequality $\Phi(t; x) \leq \Psi(t; x)$ is satisfied. Consequently, the equality $\Phi(t; x) = \Psi(t; x)$ is true. ▷

Recall that for each $x \in S(M)$, the support projection of x is denoted by $s(x)$, that is, $s(x) = \mathbf{1} - n(x)$, where $n(x)$ is the projection onto $Ker(x)$. For $t > 0$, define

$$R_t = \{x \in S(M) : \Phi(s(x)) \leq t \cdot \mathbf{1}\}.$$

The following proposition presents a geometric interpretation of the singular value function in terms of what might be called generalized approximation numbers.

Proposition 2.2. *If $x \in S(M)$, then*

$$\Phi(t;x) = \inf\{\|x-y\|_{\mathcal{B}} : y \in R_t,\ (x-y) \in E(M,\mathcal{A})\}$$

for all $t > 0$.

Proof. Let $t > 0$ and $x \in S(M)$ be fixed. Let $x = u|x|$ is the polar decomposition of x, $\Phi(t;x) = f$ and $p = E_f(|x|) \in P(M)$. Defining $y = xp$, $e = \mathbf{1} - p$, it follows that $x - y = x(\mathbf{1} - p) = xe$, and so, $x - y \in E(M,\mathcal{A})$ with

$$\|x-y\|_{\mathcal{B}} = \|ue|x|e\|_{\mathcal{B}} = \||e|x|\|_{\mathcal{B}} \le \Phi(t;x).$$

Moreover, $s(y) \le p$, which implies that

$$\Phi(s(y)) \le \Phi(p) = \Phi(E_f(|x|)) = d(f;|x|) \le t \cdot \mathbf{1}.$$

Consequently,

$$\inf\{\|x-y\|_{\mathcal{B}} : y \in R_t,\ (x-y) \in E(M,\mathcal{A})\} \le \Phi(t;x).$$

To obtain the reverse inequality, suppose that $y \in R_t$ is such that $x - y \in E(M,\mathcal{A})$. Since $xn(y) = (x-y)n(y)$, it is clear that $\|xn(y)\|_{\mathcal{B}} \le \|x-y\|_{\mathcal{B}}$. Furthermore, $\Phi(\mathbf{1} - n(y)) = \Phi(s(y) \le t \cdot \mathbf{1}$, and so, by Theorem 2.1 implies that

$$\Phi(t;x) = \inf\{\|xe\|_{\mathcal{B}} :\ e \in P(M),\ xe \in E(M,\mathcal{A}),\ \Phi(\mathbf{1}-e) \le t \cdot \mathbf{1}\} \le \|x-y\|_{\mathcal{B}}.$$

This shows that

$$\Phi(t;x) \le \inf\{\|x-y\|_{\mathcal{B}} : y \in R_t,\ (x-y) \in E(M,\mathcal{A})\},$$

which concludes that proof of the proposition. ▷

In the next theorem, some basic properties of singular value functions are collected.

Theorem 2.2. *Let $t > 0$. For all $x, y \in S(M)$, the following hold:*

(i). $\Phi(t;x) = \Phi(t;|x|) = \Phi(t;x^*)$ *and* $\Phi(t;\alpha x) = |\alpha|\Phi(t;x)$ *for all* $\alpha \in \mathbb{C}$.
(ii). $\Phi(t;xe) = \mathbf{0}$ *whenever* $\Phi(e) \le t \cdot \mathbf{1}$ *for all* $e \in P(M)$. *In particular,* $\Phi(t;x) = \mathbf{0}$ *for all* $t \cdot \mathbf{1} \ge \Phi(s(x))$.
(iii). *If* $|x| \le |y|$, *then* $\Phi(t;x) \le \Phi(t;y)$.
(iv). $\Phi(t_1 + t_2; x + y) \le \Phi(t_1;x) + \Phi(t_2;y)$ *for all* $t_1, t_2 > 0$.
(v). *If* $x \in E(M,\mathcal{A})$, $t_n > 0$, $n = 1,2,\ldots$, *and* $t_n \downarrow 0$, *then*

$$\|x\|_{\mathcal{B}} = \sup_{n \ge 1} \Phi(t_n;x).$$

Proof. *(i).* The equality $\Phi(t;x) = \Phi(t;|x|)$ follows directly from the definition of the mapping $\Phi(t;x)$.

Let $x = u|x|$ be the polar decomposition of the operator x. Then $|x^*| = u|x|u^*$. Therefore, for $g \in \mathcal{P}(\mathcal{B})$ we have

$$d(g;x^*) = \Phi(E_g(x^*)) = \Phi(uE_g(x)u^*) = \Phi(E_g(x) = d(g;x).$$

Consequently, $\Phi(t;x) = \Phi(t;x^*)$.

Finally, for any $\alpha \in \mathbb{C}$, $t > 0$ we have that

$$\Phi(t;\alpha x) = \inf\{\|\alpha xe\|_{\mathcal{B}} :\ e \in P(M),\ \alpha xe \in E(M,\mathcal{A}),\ \Phi(\mathbf{1}-e) \le t \cdot \mathbf{1}\}$$

$$= |\alpha| \inf\{\|xe\|_{\mathcal{B}} :\ e \in P(M),\ xe \in E(M,\mathcal{A}),\ \Phi(\mathbf{1}-e) \le t \cdot \mathbf{1}\} = |\alpha|\Phi(t;x).$$

(ii). If $\Phi(e) \le t \cdot \mathbf{1}$, then, trivially, $xe(\mathbf{1}-e) = 0$ and $\Phi(\mathbf{1} - (\mathbf{1}-e)) \le t \cdot \mathbf{1}$; hence, $\Phi(t;xe) = \mathbf{0}$ follows immediately from (2.2).

(iii). If $|x| \le |y|$, then $d(g;|x|) \le d(g;|y|)$ for all $g \in \mathcal{P}(\mathcal{B})$. Hence $\Phi(t;x) \le \Phi(t;y)$.

(iv). For all $g_1, g_2 \in \mathcal{P}(\mathcal{B})$ the following inequality holds

$$E_{g_1+g_2}(|x+y|) \le E_{g_1}(|x|) \vee E_{g_2}(|y|).$$

It follows that

$$\Phi(E_{g_1+g_2}(|x+y|)) \le \Phi(E_{g_1}(|x|)) + \Phi(E_{g_2}(|y|)).$$

We fix $\varepsilon > 0$ and set $g_1 = \Phi(t_1;x)$, $g_2 = \Phi(t_2;y) + \varepsilon \cdot \mathbf{1}$. Using the inequality $\Phi(E_{g_2}(|y|) \le \Phi(E_{\Phi(t_2;y)}(|y|)$ we have

$$\Phi(E_{\Phi(t_1;x)+\Phi(t_2;y)+\varepsilon\cdot\mathbf{1}} \le \Phi(E_{\Phi(t_1;x)}(|x|)) + \Phi(E_{\Phi(t_2;y)+\varepsilon\cdot\mathbf{1}}(|y|))$$
$$\le t_1 \cdot \mathbf{1} + \Phi(E_{\Phi(t_2;y)}(|y|)) \le (t_1+t_2)\cdot\mathbf{1},$$

i.e. $\Phi(E_{\Phi(t_1;x)+\Phi(t_2;y)+\varepsilon\cdot\mathbf{1}} \le (t_1+t_2)\cdot\mathbf{1}$.

Since $\Phi(t_1;x) + \Phi(t_2;y) + \varepsilon \cdot \mathbf{1} \in \mathcal{P}(\mathcal{B})$, then from the definition of the mapping $\Phi(t;x)$ the following inequality follows

$$\Phi((t_1+t_2);x+y) \le \Phi(t_1;x) + \Phi(t_2;y) + \varepsilon \cdot \mathbf{1}.$$

From here, at $\varepsilon \downarrow 0$, we obtain the required inequality

$$\Phi((t_1+t_2);x+y) \le \Phi(t_1;x) + \Phi(t_2;y).$$

(vi). First we show that for all $q \in P(\mathcal{B})$, $x \in E(M,\mathcal{A})$, $t > 0$ the equality $\Phi(t;qx) = q\Phi(t;x)$ is true. Because

$$\Phi(t;qx) = \inf\{\|qxe\|_{\mathcal{B}} : e \in P(M),\ qxe \in E(M,\mathcal{A}),\ \Phi(\mathbf{1}-e) \le t\cdot\mathbf{1}\}$$
$$= \inf\{q\|qxe\|_{\mathcal{B}} : e \in P(M), qxe \in E(M,\mathcal{A}),\ \Phi(\mathbf{1}-e) \le t\cdot\mathbf{1}\} = q\Phi(t;qx),$$

then from the inequality $|qx| \le |x|$ follows the inequality $q\Phi(t;qx) \le q\Phi(t;x)$ (see the property (iii) proved above).

On the other hand, if $e \in P(M)$, $qxe \in E(M,\mathcal{A})$ and $\Phi(\mathbf{1}-e) \le t\cdot\mathbf{1}$, then

$$\Phi(t;x) = q\Phi(t;x) + (\mathbf{1}-q)\Phi(t;x) \le q\|qxe\|_{\mathcal{B}} + (\mathbf{1}-q)\Phi(t;x).$$

Therefore,

$$q\Phi(t;x) \le q\|qxe\|_{\mathcal{B}} \le \|qxe\|_{\mathcal{B}},$$

and hence $q\Phi(t;x) \le \Phi(t;qx)$. Thus, the equality is true $\Phi(t;qx) = q\Phi(t;x)$.

If $x \in E(M,\mathcal{A})$, then $x\cdot\mathbf{1} \in E(M,\mathcal{A})$, and it follows directly from Proposition 2.1 that $\Phi(t;x) \le \|x\|_{\mathcal{B}}$ for all $t > 0$. In addition, the inequality $\Phi(t_1;x) \le \Phi(t_2;x)$ is true for $0 < t_2 < t_1$.

Thus, $\Phi(t_n;x) \uparrow z \le \|x\|_{\mathcal{B}}$ as $t_n \downarrow 0$ for some $0 \le z \in S_h(\mathcal{B})$.

If $z \ne \|x\|_{\mathcal{B}}$, then for any $\varepsilon > 0$ there is $q_\varepsilon \in P(\mathcal{B})$, such that

$$\Phi(t_n;xq_\varepsilon) = \Phi(t_n;x)q_\varepsilon \le zq_\varepsilon < q_\varepsilon \cdot \|x\|_{\mathcal{B}}$$

for all $t_n \in (0,\varepsilon)$. From here, by virtue of proposition 2.1, we obtain that

$$\Phi(t_n;xq_\varepsilon) \le zq_\varepsilon \text{ for all } t_n \in (0,\varepsilon).$$

Again using proposition 2.1, we have,

$$\Phi(\{|xq_\varepsilon| > zq_\varepsilon\}) \le \Phi(\{|xq_\varepsilon| > \Phi(t_n, xq_\varepsilon)\}) \le t_n \cdot \mathbf{1}$$

for all $t_n \in (0, \varepsilon)$. Hence, $\Phi(\{|xq_\varepsilon| > zq_\varepsilon\}) = 0$. This means that $|xq_\varepsilon| \le zq_\varepsilon$, in particular, $\|xq_\varepsilon\|_{\mathcal{B}} \le zq_\varepsilon$, which is not the case. Thus,

$$\|x\|_{\mathcal{B}} = \sup_{n\ge 1} \Phi(t_n; x).$$

▷

Corollary 2.1. *For any $x, y \in E(M, \mathcal{A})$, $t > 0$ the inequality holds*

$$|\Phi(t; x) - \Phi(t; y)| \le \|x - y\|_{\mathcal{B}}.$$

Proof. By Theorem 2.2 (iv) we have that

$$\Phi(t_1 + t_2; x) = \Phi(t_1 + t_2; y + (x - y)) \le \Phi(t_1; y) + \Phi(t_2; x - y) \le \Phi(t_1; y) + \|x - y\|_{\mathcal{B}}.$$

Similarly,

$$\Phi(t_1 + t_2; y) = \Phi(t_1 + t_2; x + (y - x)) \le \Phi(t_2; x) + \Phi(t_1; y - x) \le \Phi(t_2; x) + \|x - y\|_{\mathcal{B}}.$$

Assuming in these inequalities $t_1 = t$, $t_2 = 0$, we obtain

$$\Phi(t; x) \le \Phi(t; y) + \|x - y\|_{\mathcal{B}} \text{ and } \Phi(t; y) \le \Phi(t; x) + \|x - y\|_{\mathcal{B}},$$

from which it follows that $|\Phi(t; x) - \Phi(t; y)| \le \|x - y\|_{\mathcal{B}}$. ▷

The following proposition establishes the relation between ordinal convergence in $S(M)$ and ordinal convergence of singular values functions.

Proposition 2.3. *If $x_n, x \in S(M)$, $n \in \mathbb{N}$ and $0 \le x_n \uparrow x$, then $\Phi(t, x_n) \uparrow \Phi(t, x)$ for all $t > 0$.*

Proof. Let $x_n, x \in S(M)$ and $0 \le x_n \uparrow x$. First, let us show that

$$d(g, x_n) \uparrow d(g, x), g \in \mathcal{P}(\mathcal{B}) \tag{2.3}$$

We fix $g \in \mathcal{P}(\mathcal{B})$ and put $G_g(x) = \{\xi \in H : x(\xi) > g(\xi)\}$, $G_g(x_n) = \{\xi \in H : x_n(\xi) > h(\xi)\}$, $(n = 1, 2, ...)$. Since $x_n \le x_{n+1}$, then $G_g(x_n) \subset G_g(x_{n+1})$. Furthermore, the condition $x_n \uparrow x$ imply that $G_g(x) = \bigcup\limits_{n=1}^{\infty} G_g(x_n)$ and $E_g(x_n) \uparrow E_g(x)$. Hence, by normality of trace Φ,

$$d(h; x_n) = \Phi(E_g(x_n)) \uparrow \Phi(E_g(x)) = d(h; x).$$

Since

$$\Phi(t, x_n) \le \Phi(t, x_{n+1}) \le \Phi(t, x)$$

for all $n = 1, 2, \ldots$ and $t > 0$, it is clear that $\Phi(t, x_n) \uparrow_n$ and that

$$\sup_{n\ge 1} \Phi(t, x_n) \le \Phi(t, x)$$

for all $t > 0$. For the proof of the reverse inequality, it may be assumed that $t > 0$ is such that $\Phi(t, x_n) < g$, for all n and some $g \in \mathcal{P}(\mathcal{B})$. Hence $d(g, x_n) \le t \cdot \mathbf{1}$ for all n. Then by (2.3), it follows that $d(g, x) \le t \cdot \mathbf{1}$. Consequently, $\Phi(t, x) < g$. This suffices to show that $\Phi(t, x) \le \sup_{n\ge 1} \Phi(t, x_n)$. The proof is complete. ▷

Conclusion

In this paper, the Maharam trace Φ on a von Neumann algebra M with values in complex Dedekind complete vector lattice is considered. For an operator x from the $*$-algebra $S(M)$ of measurable operators affiliated with M, the singular value function of x, associated with such a trace Φ are determined. The main properties of these singular value functions, similar to classical singular value functions of measurable operators with respect numerical trace, are studied.

References

[1] Segal I.E. *A non-commutative extension of abstract integration*, Ann. Math. – 1953. – 57. – P. 401–457.
[2] Dixmier J. *Formes lineares sur un anneau d'operators*. Bull. de la Soc. Math. de France 1953, V. 81, 9–39.
[3] Nelson E. *Notes on non commutative integration* J. Funct. Anal. 1974. No 15. p. 103–116.
[4] Yeadon F.J. *Convergence of measurable operators* Proc. Camb. Phil. Soc. – 1973. – V. 74. – P. 257–268.
[5] Yeadon F.J. *Non-commutative L^p-spaces* Math. Proc. Camb. Phil. Soc. – 1975. – V. 77. – P. 91–102.
[6] Fack T., Kosaki H. *Generalised s-numbers of τ-measurable operators* Pacif. J. Math. 123 (1986), 269–300.
[7] Dixmier J. *Les algebras d'operateurs dans l'espace Hilbertien (Algebres de von Neunann)*. Paris: Gauthier-Villars, 1969. –367 p.
[8] Stratila S., Zsido L. *Lectures on von Neumann algebras*. – England Abacus Press, 1975. –477 p.
[9] Takesaki M. *Theory of operator algebras I.* – New York: Springer, 1979. –415 p.
[10] Muratov M.A., Chilin V.I. *Algebras of measurable and locally measurable operators*. Kyiv, Pratsi In-ty matematiki NAN Ukraini. 2007. V. 69. 390 p. (Russian).
[11] Dodds P.G., Ben de Pagter, Sukochev F.A. *Noncommutative integration and operator theory*. Progress in Nathematics 349, Birkhauser, 2023, 577 p.
[12] Kusraev A.G., *Dominanted Operators, Mathematics and its Applications,* 519, Kluwer Academic Publishers, Dordrecht, 2000. 446 p.
[13] Chilin V., Zakirov B. *Maharam traces on von Neumann algebras* Methods of Functional Analysis and Topology Vol. 16 (2010), 2. pp. 101–111.
[14] Zakirov B.S., Chilin V.I. *Noncommutative integration for traces with values in Kantorovich-Pinsker spaces* Russian Math. (Iz. VUZ), 2010, 54(10), 15-26.
[15] Chilin V., Zakirov B. *Non-commutative L^p-spaces associated with Maharam trace* J. Operator theory, 2012, 68(1), 67–83.
[16] Muratov M.A., Chilin V.I. *Central extensions of $*$-algebras of measurable operators* Dokl. NAN Ukraini, Kyiv, 2009. 7. –P. 24–28. (Russian).
[17] Zakirov B.S., Chilin V.I. *Duality for non-commutative L^1-spaces, associated with Maharam trace* Research in Mathematical Analysis. Series Mathematical Forum. V.3. VSC RAS, Vladikavkaz, 2009, 67–91.

Affiliations

Zakirov B.S.
Address: Tashkent State Transport University, Tashkent, Uzbekistan
e-mail: botirzakirov@list.ru
ORCID ID: https://orcid.org/0000-0001-8381-8518

Uzbekistan Journal of Mathematics and Computer Science
Volume 1 No. 1 Page 81–86 (2025)
DOI: https://doi.org/10.56143//ujmcs.v1i1.11
Research article

The effect of air flow generated by the movement of a high-speed train on the boundary layer

Isanov R.Sh.* Azimov J.B. and Sharipova L.D.

Abstract

In this paper, we investigate the flow around a high-speed train, both below and above it. Our aim is to ensure the safety of people and objects near high-speed trains by studying the air flow around them. Specifically, we aim to solve the problem of determining the velocity and pressure distributions in air around a moving train in a horizontal plane. We assume that the flow is two-dimensional, potential, and stationary, and use the Zhukovsky's conformal mapping method, the Christopher – Schwartz integral, and Chaplygin's source and sink methods to obtain the velocity field. Based on this velocity field, we calculate pressures and the distance of the air flow from the train's surface. We also determine the force of the air flow on solid particles on a horizontal surface to assess the possibility of their separation from the surface.

Keywords: *Flat Problem, High-Speed Train, Air Flow, Boundary Layer.*

1. Introduction

In railway transport, determining aerodynamic drag and the force of dynamic impact on the train's body are among the most significant problems. In [1, 2, 3, 4, 5, 6, 7, 8, 9, 10, 11], the problem of airflow around the composition in a plane parallel to the horizon is considered. We will explore this problem in a plane perpendicular to the horizon. Let's consider a plane problem in the horizontal plane. The airflow is flat, potential and stationary.

In Figure 1, the boundaries of the flow domain are represented by $ABFDA$. The solid boundaries are AB and DC, while FD represents the frontal section. FD and DC define the composition of a high-speed train. The free surface FD has an atmospheric pressure. According to the Bernoulli integral (because the air has no weight), the velocity along the surface DA is constant and equal to V_0.

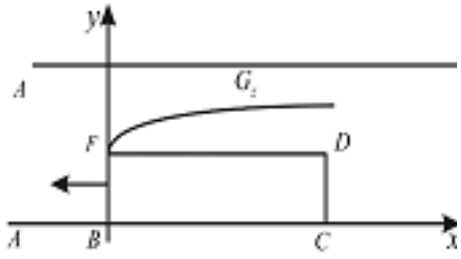

Fig. 1. Semi-infinite body in Cartesian coordinate system. Source: [Compiled by the authors]

Received : *5–January–2025,* ***Accepted :*** *28–march–2025*
**** Corresponding author***

With a comfortable mapping, using the Zhukovsky function, we obtain the coordinates indicated in Fig. 2.

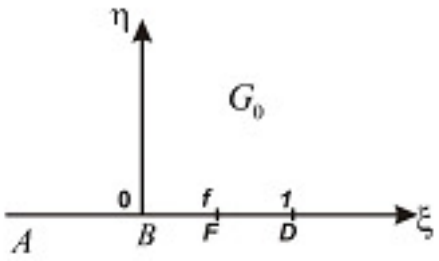

Fig. 2. Semi-infinite body under conformal mapping. Source: [Compiled by the authors]

The pressure in the airflow domain is determined by the following equation:

$$p = p_0 + \rho \frac{V_n^2 - V^2}{2}, \tag{1.1}$$

where V_n is the train speed, $\vec{V}$ is the velocity vector of air particles, $\vec{V} = u\vec{i} + v\vec{j}$, $V = \sqrt{u^2 + v^2}$, u and v denote longitudinal and transverse velocities, respectively.

2. Materials and Methods

Using the Zhukovsky function by a conformal mapping, we study the problem. We use the Christopher – Schwartz integral and Chaplygin's source and sink method to obtain the velocity field function.

In [8] and [9], a method is developed for solving plane and axisymmetric problems related to the potential flow of an ideal, compressible fluid at subsonic velocities.

Introduce the Zhukovsky function

$$\omega(\zeta) = \ln \frac{V_0}{\bar{V}(\zeta)} = \ln \frac{V_0}{V(\zeta)} + i\theta \tag{2.1}$$

where θ is the inclination angle of the velocity vector, V_0, V are the velocity modules on the free surface in the flow domain.

We have the following boundary conditions for the Zhukovsky function in the domain G_0 :

$$\left.\begin{array}{l} \text{Along } AB: \ \eta = 0, \ -\infty < \xi < 0, \ Im\omega = \theta(\xi) = 0; \\ \text{along } BF: \ \eta = 0, \ 0 < \xi < f, \ Im\omega = \theta(\xi) = \frac{\pi}{2}; \\ \text{along } FD: \ \eta = 0, \ f < \xi < 1, \ Re\omega = \theta(\xi) = 0; \\ \text{along } DA: \ \eta = 0, \ 1 < \xi < \infty, \ Im\omega = 0. \end{array}\right\} \tag{2.2}$$

3. Analysis and Results

Introduce the function $\omega_1(\zeta) = \frac{\omega(\zeta)}{\sqrt{\zeta - f}\sqrt{\zeta - 1}}$. $\omega_1(\zeta)$ has the form

$$\omega_1(\zeta) = \frac{1}{2}\int_0^f \frac{dt}{(t-1)\sqrt{(1-t)(t-\zeta)}}.$$

Integrating the last equality, we obtain

$$\omega_1(\zeta) = \frac{1}{2\sqrt{\zeta - f}\sqrt{\zeta - 1}} \ln \sqrt{\frac{\zeta}{\zeta - f}}. \tag{3.1}$$

From here, we obtain the Zhukovsky function in the domain G_0.

For the Zhukovsky function, we have

$$\omega(\zeta) = \ln\sqrt{\frac{\zeta}{\zeta - f}}. \tag{3.2}$$

Then the conjugate complex velocity will be

$$\vec{V} = V_0\sqrt{\frac{\zeta}{\zeta - f}}. \tag{3.3}$$

From the last relation, we obtain the velocity field for air in the domain G_z.

Taking into account that the sources of both inflow and sink are located at points $\xi = 0,\ \eta = 0,\ \xi = 1$, using the Chaplygin source and sink method, we obtain expressions for determining the complex potential in the domain G_0 :

$$\frac{dw}{d\zeta} = \frac{q}{\pi}\frac{1}{1-\zeta}. \tag{3.4}$$

Then we obtain an expression for determining the mapping function $Z(\zeta)$:

$$Z(\zeta) = \frac{q}{\pi\Phi_0}\int_0^{\zeta}\sqrt{\frac{t}{t-f}}\frac{dt}{(1-t)}. \tag{3.5}$$

The velocity V_0 on the free surface DA will be determined from the condition $\lim\limits_{\xi\to\infty,\ \text{at}\ \eta=0}\left[\vec{V}(\xi,\eta)\right] = V_n$ and obtained taking into account equality (3.3).

To integrate equation (3.5), we introduce a variable τ instead ζ in the form: $\tau = \sqrt{\frac{\zeta}{\zeta-f}}$, whence we obtain $\zeta = \frac{\tau^2 f}{\tau^2-1} = f + \frac{f}{\tau^2-1}$, $d\zeta = \frac{-2\tau f}{(\tau^2-1)^2}$.

Integrating differential equation (3.5) with respect to ζ, we get $Z(\zeta) = h_n\int_0^{\zeta}\sqrt{\frac{\zeta}{\zeta-f}}\frac{d\zeta}{1-\zeta}$ where h_n is the wagon width.

The expression for the integrand has the form:

$$I = \int\sqrt{\frac{\zeta}{\zeta-f}}\frac{d\zeta}{1-\zeta} = \int\frac{-2\tau^2 f}{(\tau^2-1)^2}\frac{d\tau}{\left(1-\frac{\tau^2 f}{(\tau^2-1)}\right)} = \int\frac{-2\tau^2 f}{(\tau^2-1)}\frac{d\tau}{\left[\tau^2(1-f)-1\right]}. \tag{3.6}$$

Expanding the integrand into rational fractions, we have:

$$I = \int\frac{d\tau}{\tau-1} - \int\frac{d\tau}{\tau+1} - \int\frac{d\tau}{\tau\sqrt{1-f}-1} + \int\frac{d\tau}{\tau\sqrt{1-f}+1} =$$

$$= \ln|\tau-1| - \ln|\tau+1| - \frac{1}{\sqrt{1-f}}\int\frac{d\tau}{\tau-\frac{1}{\sqrt{1-f}}} + \frac{1}{\sqrt{1-f}}\int\frac{d\tau}{\tau+\frac{1}{\sqrt{1-f}}} =$$

$$= \ln\left|\frac{\tau-1}{\tau+1}\right| + \frac{1}{\sqrt{1-f}}\ln\left|\frac{\tau+\frac{1}{\sqrt{1-f}}}{\tau-\frac{\tau}{\sqrt{1-f}}}\right| = \ln\left|\frac{\sqrt{\frac{t}{t-f}}-1}{\sqrt{\frac{t}{t-f}}+1}\right| + \frac{1}{\sqrt{1-f}}\ln\left|\frac{\sqrt{\frac{t}{t-f}}\sqrt{1-f}+1}{\sqrt{\frac{t}{t-f}}\sqrt{1-f}-1}\right| =$$

$$= \ln\left|\frac{\sqrt{t}-\sqrt{t-f}}{\sqrt{t}+\sqrt{t-f}}\right| + \frac{1}{\sqrt{1-f}}\ln\left|\frac{\sqrt{t}\sqrt{1-f}+\sqrt{t-f}}{\sqrt{t}\sqrt{1-f}-\sqrt{t-f}}\right|\Bigg|\begin{matrix}\xi\\0\end{matrix}.$$

Integrating this equation, we have

$$I_0 = I \left| \begin{matrix} \xi \\ 0 \end{matrix} \right. = \ln \left| \frac{\sqrt{t} - \sqrt{t-f}}{\sqrt{t} + \sqrt{t-f}} \right| + \frac{1}{\sqrt{1-f}} \ln \left| \frac{\sqrt{t}\sqrt{1-f} + \sqrt{t-f}}{\sqrt{t}\sqrt{1-f} - \sqrt{t-f}} \right| \left| \begin{matrix} \xi \\ 0 \end{matrix} \right. .$$

We obtain from here the expression for the mapping function $Z(\zeta)$:

$$\omega_1(\zeta) = \frac{1}{2\sqrt{\zeta - f}\sqrt{\zeta - 1}} \ln \sqrt{\frac{\zeta}{\zeta - f}}.$$

$$\begin{aligned} Z(\xi) = \hat{Z} = \hat{x} + i\hat{y} = \\ = \hat{h}_n \cdot \left(\ln \left| \frac{\sqrt{t} - \sqrt{t-f}}{\sqrt{t} + \sqrt{t-f}} \right| + \frac{1}{\sqrt{1-f}} \ln \left| \frac{\sqrt{t}\sqrt{1-f} + \sqrt{t-f}}{\sqrt{t}\sqrt{1-f} - \sqrt{t-f}} \right| \left| \begin{matrix} \xi \\ 0 \end{matrix} \right. \right). \end{aligned} \tag{3.7}$$

This is to define the mapping function $Z(\tau)$ of the domain G_0 onto the domain G_z, where $\tau = \sqrt{\frac{\zeta}{\zeta - f}}$.

Consider the velocity distributions on the side surface FD of the wagon where $h = 0,\ f \le \xi \le 1$. Velocity distribution $u(\xi)$, taking into account equalities (3.1) for the velocity distribution along the side surface of a wagon of a high-speed train

$$V(\xi) = V_n \sqrt{\frac{\xi}{\xi - f}},\ f < \xi < 1, \tag{3.8}$$

where V_n is the train speed.

Equalities (3.3) and (3.4), when taken into account along with equalities (3.7) and (3.8), provide the velocity field on the surface FD of the wagon (refer to Fig. 1).

Let's perform a numerical calculation for $h = 0,\ f + \varepsilon < \xi < 1$. At the acute corner of the car, at the point f, a very high speed occurs. Therefore, in practice, we will conduct an approximate study at points where the angles between the polygonal boundaries are greater than π.

$$f = 0,28; \quad 1 - f = 0,72 \quad \sqrt{1-f} = 0,84853.$$

$$\tau_0 = \sqrt{\frac{\xi}{\xi - f}} = \sqrt{\frac{\xi}{\xi - 0,28}}$$

$$\frac{Z}{H}\pi = I, \left(\hat{Z} - i\hat{h}_n \right) \pi.$$

Dividing into real and imaginary parts, we have

$$\left(\hat{Z} - i\hat{h}_n \right) \pi = \frac{(1-\tau)}{(1+\tau)} \frac{(1+f)}{(1-f)} \left(\frac{f + \sqrt{1-f}}{f - \sqrt{1-f}} \right)^{\sqrt{1-f}};$$

$$\left(\hat{Z} - i\hat{h}_n \right) \pi = \ln \left(\frac{(1-\tau)}{(1+\tau)} \frac{(1+f)}{(1-f)} \right) + \ln \left[\left(\frac{\tau + \sqrt{1-f}}{f + \sqrt{1-f}} \frac{f - \sqrt{1-f}}{\tau - \sqrt{1-f}} \right)^{\sqrt{1-f}} \right]$$

or, simplifying, we have

$$\begin{aligned} \left(\hat{Z} - i\hat{h}_n \right) \pi = \hat{x} + i\hat{y} - i\hat{h}_n\pi = \ln \left(\frac{(1-\tau)}{(1+\tau)} \left(\frac{\tau + \sqrt{1-f}}{\tau - \sqrt{1-f}} \right)^{\sqrt{1-f}} \right) - \\ - \ln \left[\left(\frac{1+f}{1-f} \right) \left(\frac{f - \sqrt{1-f}}{f + \sqrt{1-f}} \right)^{\sqrt{1-f}} \right] \end{aligned} \tag{3.9}$$

$$\exp\left[\left(\hat{Z}-i\hat{h}_n\right)\pi\right]=\frac{(1+\tau)}{(1-\tau)}\frac{(1-f)}{(1+f)},$$

$$\exp\left[\left(\hat{Z}-i\hat{h}_n\right)\pi\right]=\left[\frac{(1+\tau)}{(1-\tau)}\left(\frac{\tau+\sqrt{1-f}}{\tau-\sqrt{1-f}}\right)^{\sqrt{1-f}}\right]\cdot C_0 \tag{3.10}$$

where $C_0=\left(\frac{1+f}{1-f}\right)\left(\frac{\sqrt{1-f}-f}{\sqrt{1-f}+f}\right)^{\sqrt{1-f}}$.

If $f=0,28$, then $C_0\cong 0,596$.

The resulting velocity field makes it possible to determine the pressure along DA at the distance $H_0=\frac{H}{1,178}=\frac{4}{1,178}=3,3955$ determined by the formula $p=p_0-\rho\frac{V^2}{2}$, where H_0 is the distance from the cars.

Using the Delfi program, we obtained the graph shown in Figure 3.

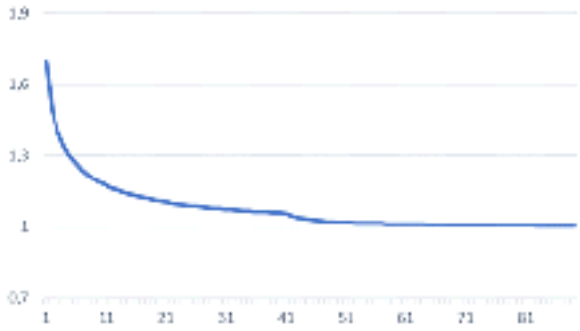

Fig. 3. Air flow velocity during the movement of a high-speed train. Source: [Compiled by the authors]

4. Discussion

Earlier, using the Zhukovsky function, similar to methods, the problem of optics of an aircraft wing with an air flow was solved. In the article of the author entitled «The problem of the flow around the movement of a high-speed train for a flat case» at the international conference «Resource-saving technologies in railway transport» (Tashkent, 2016), this study was discussed.

For the results obtained in this article, the methods considered in the works [1,2,4] were used. In this article, we consider the simplest plane problem in the horizontal plane to de-termine the velocity vector and pressure in the vicinity of a high-speed train.

5. Conclusion

Formulas were derived for calculating the air flow velocity during the movement of a high-speed train using the Zhukovsky method using the Christophel – Schwartz integrals, as well as the distribution of velocities on the side surface of the high-speed train (see Fig. 3). Based on the velocity field obtained, pressures were determined, as well as the distance of the air flow impact formed by the movement of a high-speed train from the side surface of the train.

This study aims to investigate the safety of high-speed trains. We used the results to solve the problem of particles being entrained from the ground by the air flow generated by a high-speed train and also determined the velocity fields for uniform acceleration and deceleration of a high-speed train.

Author's contributions

All authors contributed equally to the writing of this paper. All authors read and approved the final manuscript.

References

[1] Hamidov A.A., Isanov R.Sh., Ruzmatov, M.I. (2008) The problem of the flow around a car by a flow of an ideal compressible fluid. Materials of the conference «On the prob-lems of land transport systems», Tashiit, 211-213.

[2] Isanov R.Sh. (2013) Two-Layer air flow in the flow of high-speed trains. In: «Science and progress of transport». Dnepropetrovsk, VDNUZT, Ukraine. 127-132.

[3] Kravets V.V., Kravets E.V. (2005) High-speed rolling stock and aerodynamics. Prob-lems and prospects of railway transport development: Abstr. 65-th Intern. Scient. Pract. Conf. (19.05–20.05.2005) / DOIT. Dnepropetrovsk, 31-32.

[4] Khamidov A.A., Balabin V.N., Isanov R.Sh., Yaronova N.V. (2013) Plane problem of a jet flow of high-speed trains. Problems of mechanics, No. 1-2. Tashkent.

[5] Ruize Hu, Caglar Oskay (2017) Nonlocal Homogenization Model for Wave Dispersion and Attenuation in Elastic and Viscoelastic Periodic Layered Media. Journal of Applied Mechanics, Vol. 84, No.3, 53-63.

[6] Pshenichnikov S. G. (2016) Dynamic problems of linear viscoelasticity for piecewise homogeneous bodies. Proceedings of the Russian Academy of Sciences, No. 1, 79-89.

[7] Willis J.R. (2009) Exact Effective Relations for Dynamics of a Laminated Body. Mech. Mater., 41(4), 385-393.

[8] Willis J.R. (2011) Effective Constitutive Relations for Waves in Composites and Met-amaterials. Proc. R. Soc. London, Ser. A, 467 (2131), 1865-1879.

[9] Willis J.R. (2012) The Construction of Effective Relations for Waves in a Composite. C. R. Mec., 340 (4-5), 181-192.

[10] Kim J. (2004) On Generalized Self-Consistent Model for Elastic Wave Propagation in Composites Materials. International Journal of Solids and Structures, Volume 41, 4349-4360.

[11] Verbis J.T., Kattis S.E., Tsinopoulos S. V., Polyzos D. (2001) Wave Dispersion and At-tenuation in Fiber Composites. Comput. Mech., 27 (3), 244-252.

Affiliations

Isanov Rovshanbek
Address: Tashkent State Transport University, Dept. of Higher mathematics, Tashkent-Uzbekistan.
e-mail: diyora.isanova.97@bk.ru
ORCID ID: 0000-0001-8490-9489

Azimov Jakhongir
Address: Tashkent State Transport University, Dept. of Higher mathematics, Tashkent-Uzbekistan.
e-mail: azimovjb@gmail.com
ORCID ID: 0000-0002-0859-3184

Sharipova Lola
Address: Tashkent State Transport University, Dept. of Higher mathematics, Tashkent-Uzbekistan.
e-mail: lolaxon@gmail.com
ORCID ID: 0000-0002-6628-2990

Uzbekistan Journal of Mathematics and Computer Science
Volume 1 No. 1 Page 87–95 (2025)
DOI: https://doi.org/10.56143/ujmcs.v1i1.12
Research article

UZJMCS

Classification of Character of Rest Points of the Lotka-Volterra Operator Acting in S^4

U.R. Muminov, D.B. Eshmamatova* R.N. Ganikhodzhaev, D.A. Xakimova and S.S. Turdiev

Abstract

In the paper, we consider the problem of studying the trajectories of points under the action of the Lotka-Volterra operator. In short, the goal is to study the dynamics of trajectories of interior points by finding fixed points and studying the Jacobian spectrum at these points of the operator in question. It turned out that in a number of applied problems, there are Lotka-Volterra mappings of exactly this type, and the points of the simplex in this case are considered as the states of the system under study. In this case, the simplex-preserving mapping defines the discrete law of evolution of the given system. Starting from a certain starting point, we can consider the sequence that determines the evolution of this point. The work explicitly shows sets of limit points for positive and negative trajectories, which in turn describe in applied problems the beginning and the end of the evolutionary process, respectively.

Keywords: *skew-symmetric matrix; boundary point; interior point; fixed point; partially oriented graph; eigenvalue; saddle point; attractor; repeller.*

AMS Subject Classification (2020): *Primary: 37B25; Secondary: 37C25; 37C27.*

1. Introduction

It is known that nonlinear dynamics has been formed relatively over the last 30 – 35 years, using systems of nonlinear mathematical models [1-4]. In this it is necessary to note differential equations and discrete mappings, among which an important role is played by discrete Lotka-Volterra mappings.

It is known [5],[6] that discrete Lotka-Volterra mappings are uniquely determined by specifying the skew-symmetric matrix $A = (a_{ij})$, $a_{ij} = -a_{ji}$, $i, j = \overline{1, m}$ and act on the simplex

$$S^{m-1} = \left\{ x \in R^m : \sum_{i=1}^{m} x_i = 1,\ x_i \geq 0 \right\}$$

according to the formulas

$$V : x'_k = x_k \left(1 + \sum_{i=1}^{m} a_{ki} x_i \right), k = 1, ..., m \tag{1.1}$$

on condition $|a_{ki}| \leq 1$. We define it as $V : S^{m-1} \to S^{m-1}$ [5-7]. By specifying the mapping in the form (1.1), it is not difficult to notice that it is uniquely determined by the skew-symmetric matrix of $A = (a_{ki})$. In [5-7] the concepts of a skew-symmetric matrix of general position are introduced.

Received : *05–Yanuary–2025,* ***Accepted :*** *25–April–2025*
**** Corresponding author***

Definition 1.1. A skew-symmetric matrix $A = (a_{ki})$ is called in general position if the major minors of an even order are nonzero.

If the definition condition is not met, then such a skew-symmetric matrix is called degenerate.

Also, from the works [5-7] we know that if a skew-symmetric matrix is in general position, then in this case a complete oriented graph corresponds to this matrix, i.e. a tournament. In this paper, we consider the degenerate case of Lotka-Volterra mappings. Mappings of this type are defined by a degenerate skew-symmetric matrix. This type of mapping, acting in two-dimensional and three-dimensional simplexes, began to be considered in [8],[9] and they show that partially oriented graphs correspond to matrices of this type.

Interest in the study of degenerate Lotka-Volterra mappings arises from the fact that they can be used in modeling epidemiological situations, up to recurrent ([8],[10]) and non-recurrent diseases [9], as well as in modeling environmental problems ([11]). Consequently, the work is devoted to the continuation of the study of mappings of this type.

Partially oriented graphs in the cases of $m = 3, 4$ are given in the monograph [12]. This work is devoted to finding rest points and investigating their character of the degenerate Lotka-Volterra mapping operating in a four-dimensional simplex, i.e. S^4. This study gives us a picture of the flow of trajectories of the internal points of the simplex.

Now let us introduce the basic definitions that we will refer to throughout our work.

Definition 1.2. [1] Let $x \in S^{m-1}$. If condition $Vx = x$ is satisfied, then point x is called fixed.

The Jacobi matrix for some $f_k\ (x_1,\ x_2, ..., x_m)$ has the following form:

$$J(x) = \begin{pmatrix} \frac{\partial f_1}{\partial x_1} & \frac{\partial f_1}{\partial x_2} & \cdots & \frac{\partial f_1}{\partial x_m} \\ \frac{\partial f_2}{\partial x_1} & \frac{\partial f_2}{\partial x_2} & \cdots & \frac{\partial f_2}{\partial x_m} \\ \cdots & \cdots & \cdots & \cdots \\ \frac{\partial f_m}{\partial x_1} & \frac{\partial f_m}{\partial x_2} & \cdots & \frac{\partial f_m}{\partial x_m} \end{pmatrix} \tag{1.2}$$

Let $x^* = (x_1,\ x_2, ..., x_m) \in S^{m-1}$ be a fixed point of a system of type (1.1). If

$$|J\ (x^*) - \lambda E| = 0, \tag{1.3}$$

then the numbers $\lambda_i,\ i = \overline{1, m}$, which are solutions to the equation (1.3), are called the eigenvalues of the fixed point x^* [9].

Definition 1.3. If at a fixed point $x^* = (x_1,\ x_2, ..., x_m) \in S^{m-1}$ all eigenvalues $\lambda_i,\ i = \overline{1, m}$ are less than 1 in absolute value, then this point is called attracting.

Definition 1.4. If all eigenvalues $\lambda_i,\ i = \overline{1, m}$ at a fixed point $x^* = (x_1,\ x_2, ..., x_m) \in S^{m-1}$ are greater than 1, then this fixed point is called repulsive.

In all other cases, the fixed point is called a saddle point.

2. Results

Let the degenerate skew-symmetric matrix A have the form

$$A = \begin{pmatrix} 0 & 0 & -a & b & 0 \\ 0 & 0 & c & -e & 0 \\ a & -c & 0 & 0 & -d \\ -b & e & 0 & 0 & f \\ 0 & 0 & d & -f & 0 \end{pmatrix}, and\ 0 < a,\ b,\ c,\ d,\ e,\ f \leq 1.$$

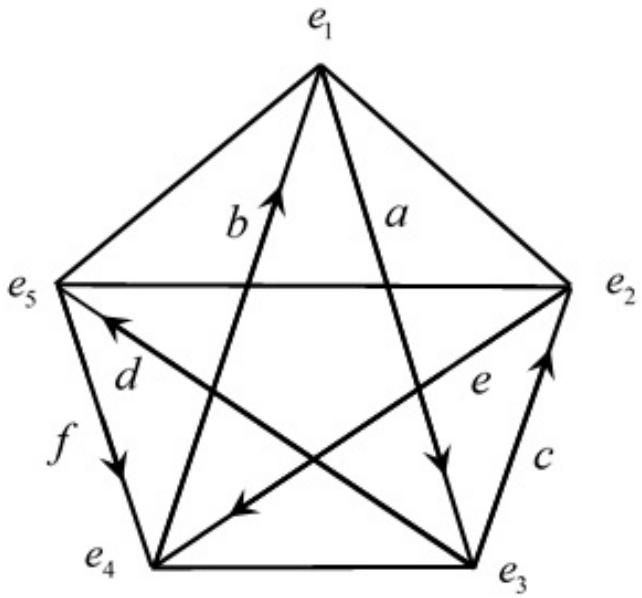

Figure 1. Partially directed graph corresponding to matrix A.

Then the matrix A defines a partially directed graph (see Figure 1).

In this case, operator $V : S^4 \to S^4$, defined by matrix A, will have the following form:

$$V : \begin{cases} x_1' = x_1(1 - ax_3 + bx_4), \\ x_2' = x_2(1 + cx_3 - ex_4), \\ x_3' = x_3(1 + ax_1 - cx_2 - dx_5), \\ x_4' = x_4(1 - bx_1 + ex_2 + fx_5), \\ x_5' = x_5(1 + dx_3 - fx_4). \end{cases} \tag{2.1}$$

We are faced with the task of studying the dynamics of the interior points of operator (2.1). To do this, we find fixed points and study their characters.

First, we introduce the following notation:

Let $I = \{1, 2, ..., m\}$, points $e_i = (\delta_{i1}, ..., \delta_{im})$ be the vertices of the simplex, where δ_{ij} is the Kronecker symbol, $(i, j \in I)$. $\Gamma_\alpha-$ convex hull of vertices $\{e_i\}_{i\in\alpha}$ for $\alpha \subset I$. The interior of the face is $\Gamma_\alpha - ri\Gamma_\alpha$ and the relative boundary is $\partial\Gamma_\alpha$. Let $|\alpha|$ be the number of elements of $\alpha \subset I$. First, let us find the fixed points of operator (2.1). To do this, we solve the system of equations $Vx = x$. As a result, they belong to S^4, i.e. that is, the edges and faces of the simplex

$$\Gamma_{34} = \left\{(0,\, 0,\, \gamma,\, 1-\gamma,\, 0) \in S^4,\, 0 \le \gamma \le 1\right\},$$

$$\Gamma_{125} = \left\{(\alpha,\, \beta\,,\, 0,\, 0,\, 1-\alpha-\beta) \in S^4,\, 0 \le \alpha,\, \beta \le 1,\ \alpha+\beta \le 1\right\}.$$

Let us be given the Lotka-Volterra operator of the form (2.1). First, we write down the general Jacobian matrix for $Vx = \left(x_1',\ x_2',\ x_3',\ x_4',\ x_5'\right) \in S^4$. To do this, we use formula (1.2) for operator (2.1):

$$J(Vx) = \begin{pmatrix} 1 - ax_3 + bx_4 & 0 & -ax_1 & bx_1 & 0 \\ 0 & 1 + cx_3 - ex_4 & cx_2 & -ex_2 & 0 \\ ax_3 & -cx_3 & 1 + ax_1 - cx_2 - dx_5 & 0 & -dx_3 \\ -bx_4 & ex_4 & 0 & 1 - bx_1 + ex_2 + fx_5 & -fx_4 \\ 0 & 0 & dx_5 & -fx_5 & 1 + dx_3 - fx_4 \end{pmatrix}.$$

Theorem 2.1. *All vertices of simplex S^4 are fixed saddle points.*

Proof. We know that the vertices of the simplex S^4 lie at points
$e_1 = (1, 0, 0, 0, 0),\ e_2 = (0, 1, 0, 0, 0), e_3 = (0, 0, 1, 0, 0),\ e_4 = (0, 0, 0, 1, 0),\ e_5 = (0, 0, 0, 0, 1)$.
All these points satisfy the condition $Vx = x$.

1) Find the eigenvalues using the Jacobian matrix for point $e_1 = (1, 0, 0, 0, 0)$ and formula (1.3), i.e. solve an equation of the form

$$(1-\lambda)^3 (1+a-\lambda)(1-b-\lambda) = 0.$$

Its solutions have the form $\lambda_1 = \lambda_2 = \lambda_3 = 1,\ \ \lambda_4 = 1+a,\ \lambda_5 = 1-b$. This means that $|\lambda_4| > 1,\ |\lambda_5| < 1$. Vertex e_1 is a saddle point.

2) For vertex $e_2 = (0, 1, 0, 0, 0)$ we obtain equation

$$(1-\lambda)^3 (1+e-\lambda)(1-c-\lambda) = 0.$$

Its solutions $\lambda_1 = \lambda_2 = \lambda_3 = 1,\ \ \lambda_4 = 1+e,\ \lambda_5 = 1-c$, i.e. $|\lambda_4| > 1,\ |\lambda_5| < 1$. Vertex e_2 is also a saddle. Carrying out the same actions for $e_3,\ e_4$ and e_5, we establish that among their eigenvalues there are modulo greater than 1 and less than 1. This means that the vertices $e_3,\ e_4,\ e_5$ are also saddles. The theorem has been proven.

Now let us turn our attention to other fixed points of the simplex. All points of edge $\Gamma_{34} \subset S^4$ satisfy condition $Vx = x$. We solve equations $-ax_3 + bx_4 = 0,\ \ cx_3 - ex_4 = 0,\ dx_3 - fx_4 = 0$ taking into account $x_3 + x_4 = 1$.

The solutions to these equations consist of neutral fixed points. Defining them as

$$E_1 = \left(0,\ 0,\ \frac{b}{a+b},\ \frac{a}{a+b},\ 0\right),\ E_2 = \left(0,\ 0,\ \frac{e}{c+e},\ \frac{c}{c+e},\ 0\right),\ E_3 = \left(0,\ 0,\ \frac{f}{d+f},\ \frac{d}{d+f},\ 0\right),$$

respectively.

Theorem 2.2. *If condition $de > cf$ is satisfied, then all fixed points belonging to the interval $[E_1,\ E_2] \subset \Gamma_{34}$ are repellers, if condition $de > cf$ is satisfied, then $[E_1,\ E_3] \subset \Gamma_{34}$ the interval also consists entirely of repellers.*

Proof. Consider the set consisting of these fixed points of the edge Γ_{34}. According to (1.3), we find the eigenvalues:

$$(1-\lambda)^2 (1-a\gamma+b(1-\gamma)-\lambda)(1+c\gamma-e(1-\gamma)-\lambda)(1+d\gamma-f(1-\gamma)-\lambda) = 0.$$

Its solutions have the form $\lambda_1 = \lambda_2 = 1,\ \lambda_3 = 1+(-a\gamma+b(1-\gamma)),\ \lambda_4 = 1+c\gamma-e(1-\gamma)$,$\lambda_5 = 1+d\gamma-f(1-\gamma)$. In simplex S^4 we consider the system of inequalities

$$\begin{cases} -a\gamma + b(1-\gamma) > 0, \\ c\gamma - e(1-\gamma) > 0, \\ d\gamma - f(1-\gamma) > 0. \end{cases} \tag{2.2}$$

And according to the results found λ, we divide the set of points Γ_{34} into classes. If condition $de > cf$ is satisfied, then the solutions to the system of inequalities (2.2) consist of interval $[E_1,\ E_2] \subset \Gamma_{34}$ (see Figure 2). The eigenvalues of fixed points belonging to both sets $[E_1,\ E_2]$ and $[E_1,\ E_3]$ have the form
$\lambda_1 = \lambda_2 = 1, \lambda_3, \lambda_4, \lambda_5 > 1$,. This means that the intervals consist entirely of repellers.

Under condition $de < cf$, the solutions to the system of inequalities (2.2) consist of interval $[E_1,\ E_3] \subset \Gamma_{34}$ (see Figure 3).

Theorem 2.3. *When condition $de > cf$ is satisfied, points belonging to interval $[E_3, E_1] \subset \Gamma_{34}$, and when condition $de < cf$ is satisfied, points belonging to interval $[E_2, E_1] \subset \Gamma_{34}$ are attractors.*

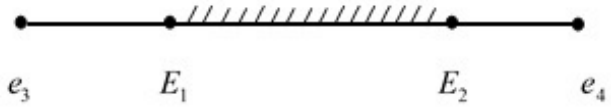

Figure 2. $[E_1, E_2]$ is part of the edge Γ_{34}.

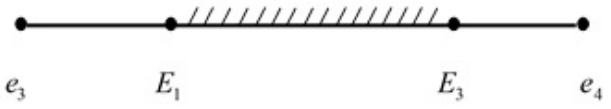

Figure 3. $[E_1, E_3]$ is part of the edge Γ_{34}.

Proof. In the proof of the above theorem, we will find the eigenvalues for the fixed points belonging to Γ_{34}. Consider the system of inequalities

$$\begin{cases} -a\gamma + b\,(1-\gamma) < 0, \\ c\gamma - e\,(1-\gamma) < 0, \\ d\gamma - f\,(1-\gamma) < 0 \end{cases} \tag{2.3}$$

in simplex S^4 . If $de > cf$ is true for the system of inequalities, then the solution to the system of inequalities (2.3) consists of the interval $[E_3, E_1] \subset \Gamma_{34}$. If $de < cf$ holds, then the solution to the system of inequalities (2.3) consists of $[E_2, E_1] \subset \Gamma_{34}$ the interval. The coordinates of points, E_1, E_2 and E_3 are indicated above. The eigenvalues of fixed points belonging to sets $[E_2, E_1]$, $[E_3, E_1]$, consisting of solutions to the system of inequalities (2.3), have the form $\lambda_1 = \lambda_2 = 1$, $|\lambda_3|$, $|\lambda_4|$, $|\lambda_5| < 1$. This means that they are attractors.The theorem has been proven.

Theorem 2.4. *If* $-a\gamma + b\,(1-\gamma)$, $c\gamma - e\,(1-\gamma)$, $d\gamma - f\,(1-\gamma)$ *have different signs, then the fixed points belonging to* Γ_{34} *consist of saddle points.*

Proof. We are interested in cases when these polynomials have different signs. Cases with the same symptoms were considered as follows. The table below shows cases when the signs of these polynomials are different.

	$-a\gamma + b\,(1-\gamma)$	$c\gamma - e\,(1-\gamma)$	$d\gamma - f\,(1-\gamma)$
1	−	+	+
2	−	−	+
3	−	+	+
4	+	−	−
5	+	−	+
6	+	+	−

Table 1. Combinations of signs of polynomials

If you create a system of inequalities using the signs of polynomials from the table, then it will consist of six inequalities. Each solution to this system of inequalities consists of an interval belonging to edge Γ_{34}. Analyzing the eigenvalues for points belonging to these intervals, we come to the conclusion that they are saddle points. The theorem has been proven.

All points belonging to face $\Gamma_{125} \subset S^4$ satisfy condition $Vx = x$. Let us study the relative boundary $\partial\Gamma_{125} \subset \Gamma_{125}$ and the relative interior $ri\Gamma_{125} \subset \Gamma_{125}$ separately. We know there is equality

$$\partial\Gamma_{125} = \partial\Gamma_{12} \cup \partial\Gamma_{25} \cup \partial\Gamma_{15}.$$

Theorem 2.5. *The set of fixed points belonging to the edge Γ_{25} consists of saddle points.*

Proof. Let $\alpha = 0$, then $\Gamma_{25} = \{(0,\ \beta,\ 0,\ 0,\ 1-\beta) \in S^4,\ 0 \le \beta \le 1\}$. We find the eigenvalues for the points from Γ_{25}. From formula (1.3) we obtain

$$(1-\lambda)^3 (1 - c\beta - d(1-\beta) - \lambda)(1 + e\beta + f(1-\beta) - \lambda) = 0.$$

Its solutions have the form $\lambda_1 = \lambda_2 = \lambda_3 = 1,\quad \lambda_4 = 1 - c\beta - d(1-\beta)$, $\lambda_5 = 1 + e\beta + f(1-\beta)$ and $|\lambda_4| < 1,\ |\lambda_5| > 1$. So, the set of fixed points of the edge Γ_{25} consists of saddle points. The theorem has been proven. Consider the equations $ax_1 - cx_2 - dx_5 = 0, -bx_1 + ex_2 + fx_5 = 0$. The solutions to these equations on section Γ_{15} consist of neutral fixed points. Let us denote them as $G_1\left(\frac{d}{a+d},\ 0,\ 0,\ 0,\ \frac{a}{a+d}\right)$, $G_2\left(\frac{f}{b+f},\ 0,\ 0,\ 0,\ \frac{b}{b+f}\right)$, respectively.

Theorem 2.6. *If condition $bd < af$ is satisfied, then the points belonging to the interval $[e_5, G_1] \cup [G_2,\ e_1] \subset \Gamma_{15}$ are saddles, and the points belonging to the interval $[G_1,\ G_2] \subset \Gamma_{15}$ are repellers.*

Proof. We know that if $\beta = 0$ then $\Gamma_{15} = \{(\alpha,\ 0\ ,\ 0,\ 0,\ 1-\alpha) \in S^4,\ 0 \le \alpha \le 1\}$. We find the eigenvalues of points belonging to edge Γ_{25}. From formula (1.3) we obtain

$$(1-\lambda)^3 (1 + a\alpha - d(1-\alpha) - \lambda)(1 - b\alpha + f(1-\alpha) - \lambda) = 0.$$

Solutions to this equation:

$$\lambda_1 = \lambda_2 = \lambda_3 = 1,\ \lambda_4 = 1 + (a+d)\alpha - d, \lambda_5 = 1 + f - (b+f)\alpha.$$

Then, if $\alpha < \frac{d}{a+d}$, then we have $(a+d)\alpha - d < 0$, hence $|\lambda_4| < 1$. But if $bd < af$, then $f - (b+f)\alpha > 0$. Means $|\lambda_5| > 1$. So, the points of interval $[e_5, G_1] \subset \Gamma_{15}$ are saddle points. Similarly, if $bd < af$ and $\alpha > \frac{f}{b+f}$ are satisfied, then we have $|\lambda_4| > 1$ and $|\lambda_5| < 1$. Then all points of interval $[G_2,\ e_1] \subset \Gamma_{15}$ are saddle points. Values α belonging to the range $\frac{d}{a+d} < \alpha < \frac{f}{b+f}$ have $(a+d)\alpha - d > 0$ and $f - (b+f)\alpha > 0$. Then $|\lambda_4| > 1,\ |\lambda_5| > 1$. Consequently, the set of all points in interval $[G_1, G_2] \subset \Gamma_{15}$ are repulsive.The theorem has been proven.

Let us move on to considering the solution of equations $ax_1 - cx_2 - dx_5 = 0, -bx_1 + ex_2 + fx_5 = 0$ for points belonging to edge Γ_{12}. The solutions to these equations consist of neutral points in Γ_{12}, having the form $F_1\left(\frac{c}{a+c},\ \frac{a}{a+c},\ 0,\ 0,\ 0\right), F_2\left(\frac{e}{e+b},\ \frac{b}{e+b},\ 0,\ 0,\ 0\right)$.

Theorem 2.7. *If condition $bc < ae$ is satisfied, then the points belonging to the interval $[e_2, F_1] \cup [F_2,\ e_1] \subset \Gamma_{15}$ are saddle, and the points belonging to the interval $[F_1,\ F_2] \subset \Gamma_{15}$ are repulsive.*

Proof. The theorem is proved similarly to Theorem 2.6.

Above we studied the dynamics of points belonging to the boundary part of the face Γ_{125}. Now consider the set of internal points of the face

$$ri\Gamma_{125} = \{(\alpha,\ \beta\ ,\ 0,\ 0,\ 1-\alpha-\beta) \in S^4,\ 0 < \alpha,\ \beta < 1,\ \alpha + \beta < 1\}\ .$$

We find the eigenvalues for these points using the Jacobi matrix and formula (1.3):

$$(1-\lambda)^3 (1 + a\alpha - c\beta - d(1-\alpha-\beta) - \lambda)(1 - b\alpha + c\beta + f(1-\alpha-\beta) - \lambda) = 0.$$

As a result, we get $\lambda_1 = \lambda_2 = \lambda_3 = 1$, $\lambda_4 = 1 + a\alpha - c\beta - d\,(1 - \alpha - \beta)$, $\lambda_5 = 1 - b\alpha + c\beta + f\,(1 - \alpha - \beta)$. Let us denote the set of solutions to the system of inequalities by T,

$$\begin{cases} a\alpha - c\beta - d\,(1 - \alpha - \beta) < 0, \\ -b\alpha + c\beta + f\,(1 - \alpha - \beta) < 0, \end{cases}$$

and the set of solutions to the system of inequalities through I ,

$$\begin{cases} a\alpha - c\beta - d\,(1 - \alpha - \beta) > 0, \\ -b\alpha + c\beta + f\,(1 - \alpha - \beta) > 0. \end{cases}$$

And the set of solutions to the system of inequalities

$$\begin{cases} a\alpha - c\beta - d\,(1 - \alpha - \beta) > 0, \\ -b\alpha + c\beta + f\,(1 - \alpha - \beta) < 0, \end{cases} \qquad \begin{cases} a\alpha - c\beta - d\,(1 - \alpha - \beta) < 0, \\ -b\alpha + c\beta + f\,(1 - \alpha - \beta) > 0. \end{cases}$$

denote by E . Based on the above mentioned, we get the following Proposition.

Proposition 1. When conditions $af < bd$, $ae < bc$ are met, the following confirmations are appropriate:

1. $T \subset \Gamma_{125}$ – all points belonging to the set are attractors;
2. All points belonging to the set $I \subset \Gamma_{125}$ are repellers;
3. All points belonging to the set $E \subset \Gamma_{125}$ are saddle points (see Figure 4).

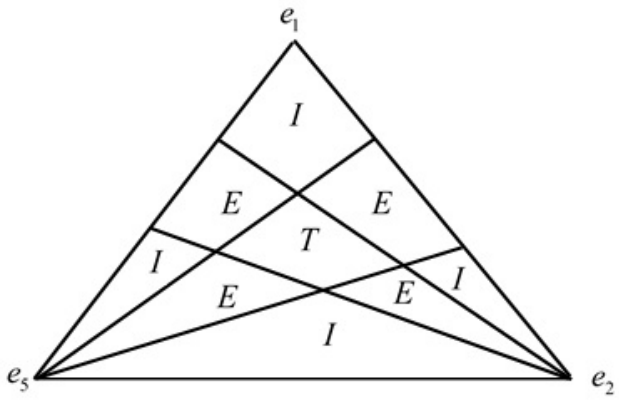

Figure 4. Classification of points belonging to the set in $ri\Gamma_{125}$.

The dynamics of internal points is studied similarly to the dynamics of boundary points discussed above.

3. Conclusion

The works devoted to discrete Lotka-Volterra mappings with non-degenerate skew-symmetric matrices are quite well known [5-7], [10]. From these works it is known that mappings of this type can be associated with elements of graph theory, in particular with the theory of tournaments. But, as it turned out, in the case when the skew-symmetric matrix is singular, then a mapping of this type can be associated with a partially directed graph. The study of this type of Lotka-Volterra mappings is relevant, since they can be considered as discrete models of epidemiology, ecology, and population genetics [8], [10]. In this regard, the work is devoted to the study of the dynamics of internal points of the degenerate Lotka-Volterra mapping acting in a four-dimensional simplex. Fixed points have been found for the operator under consideration; it turns out that

there are infinitely many of them. The characters of fixed points on which the flow of trajectories of internal points of a given operator depends are studied. The following work will be devoted to finding the Fatou and Julia sets for mappings of this kind [1].

Acknowledgements

The authors express their gratitude to the Tashkent State University of Transport, the Institute of Mathematics of the Academy of Sciences of the Republic of Uzbekistan, the National University of Uzbekistan, as well as Ferghana State University.

References

[1] Devaney R.L.: *A First Course in Chaotic Dynamical Systems. Theory and Experiment. Second edition*. Taylor and Francis Group, 2020. - 329 p.
[2] Holmgren R.A. : *A first Course in Discrete Dynamical Systems*. Springer Verlag, 1994. - 225 p.
[3] Brin M., Stuck G. : *Introduction to Dynamical Systems*. Cambridge University Press, 2004. - 254 p.
[4] Subathra G. and Jayalalitha G. : *Fixed Points-Julia sets*. Advances in Mathematics: Scientific Journal, 2020. - 9. – P. 6759–6763.
[5] Eshmamatova D.B., Tadzhieva M.A., Ganikhodzhaev R.N.: *Criteria for internal fixed points existence of discrete dynamic Lotka-Volterra systems with homogeneous tournaments*. Izvestiya Vysshikh Uchebnykh Zavedeniy. Prikladnaya Dinamika. 2023. – 30. – No. 6. – P. 702-716. https://doi.org/10.18500/0869-6632-003012
[6] Eshmamatova D. B., Tadzhieva M.A., Ganikhodzhaev R.N.: *Criteria for the Existence of Internal Fixed Points of Lotka-Volterra Quadratic Stochastic Mappings with Homogeneous Tournaments Acting in an (m-1)-Dimensional Simplex*. Journal of Applied Nonlinear Dynamics. 2023. – 12 – No. 4. – P. 679-688. https://doi.org/10.5890/JAND.2023.12.004
[7] Tadzhieva M.A., Eshmamatova D. B., Ganikhodzhaev R.N.: *Volterra-Type Quadratic Stochastic Operators with a Homogeneous Tournament*. Journal of Mathematical Sciences. 2024. – 278. No. 3. – P. 546-556. DOI: 10.1007/s10958-024-06937-0
[8] Eshmamatova D. B., Tadzhieva M.A., Ganikhodzhaev R.N.: *Degenerate cases in Lotka-Volterra systems*. AIP Conference Proceedings. 2023. – 2781. – P. 020034-1-8. DOI: 10.1063/5.0144887
[9] Eshmamatova D. B.: *Discrete Analogue of the SIR Model*. AIP Conference Proceedings. 2023. – 2781. – P. 020024-1-8. DOI: 10.1063/5.0144884
[10] Eshmamatova D.B., Seytov Sh. J., Narziev N. B.: *Basins of Fixed Points for the Composition of the Lotka-Volterra Mappings and Their Classification*. Lobachevskii Journal of Mathematics. 2023. – 44. No. 2. – P. 558-569. DOI: 10.1134/S1995080223020142
[11] Eshmamatova D. B., Seytov Sh. J.: *Discrete Dynamical Systems of Lotka Volterra and Their Applications on the Modeling of the Biogen Cycle in Ecosystem*. Lobachevskii Journal of Mathematics. 2023. – 44. No. 4. – P. 1462-1476. DOI: 10.1134/S1995080223040248
[12] Harari F., Palmer E.: *Perechisleniye grafov [Enumeration of graphs] (monograph)*. M.: Mir. – 324 p. [in Russian].

Affiliations

Muminov, U.R.
Address: PhD student of Ferghana State University, Ferghana, Uzbekistan.
e-mail: ulugbek.muminov.2020@mail.ru
ORCID ID: 0000-0001-9232-3365

Eshmamatova, D.B.
Address: Professor, department of higher mathematics, Tashkent State Transport University, Institute of Mathematics named after V.I. Romanovsky Academy of Sciences of the Republic of Uzbekistan, Senior Researcher. Tashkent, Uzbekistan.
e-mail: 24dil@mail.ru
ORCID ID: 0000-0002-1096-2751

Ganikhodzhaev, R.N.
Address: Professor of the Department of Algebra and Functional Analysis, National University of Uzbekistan,

Tashkent, Uzbekistan.
E-MAIL: rasulganikhodzhaev@gmail.com
ORCID ID: 0000-0001-6551-5257

XAKIMOVA, D.A.
ADDRESS: PhD student of Tashkent State Transport University, Tashkent, Uzbekistan.
E-MAIL: xakimovadildora47@gmail.com
ORCID ID: 0000-0001-5181-7182

TURDIEV, S.S.
ADDRESS: Assistant of the department of higher mathematics, Tashkent State Transport University, Tashkent, Uzbekistan.
E-MAIL: s.turdiev@alumni.nsu.ru
ORCID ID: 0000-0003-3599-1716

Uzbekistan Journal of Mathematics and Computer Science
Volume 1 No. 1 Page 96–104 (2025)
DOI: https://doi.org/10.56143/ujmcs.v1i1.13
Research article

UZJMCS

Dynamics of Compositions of Lotka-Volterra Operators Corresponding to Some Partially Oriented Graphs in a Three-Dimensional Simplex

F.Yusupov*, D.Akhmedova and U.Shamsiyeva

Abstract

The paper is devoted to the study of the dynamics of the trajectories of the inner points of the composition of two quadratic Lotka-Volterra dynamical systems operating in a three-dimensional simplex. Four compositional operators are investigated in this work. Fixed points are found for them and their characters are investigated by analyzing the Jacobian spectrum. The compositions of two discrete dynamic Lotka-Volterra systems are interesting because they can be applied in epidemiology problems.

Keywords: *Lotka–Volterra mapping, oriented graph, fixed point, repeller, attractor.*

AMS Subject Classification (2020): *Primary: 37B25; Secondary: 37C25, 37C27.*

1. Introduction

It is known that many applied problems today are solved using non-linear dynamics. In [1], the dynamics of the composition of some Lotka-Volterra operators operating in a two-dimensional simplex is investigated. Later work [2] was devoted to the classification of fixed points, according to the theory introduced in [3] for the composition of some Lotka-Volterra operators operating in two- and three-dimensional simplexes. In [4], the composition of two Lotka-Volterra operators corresponding to strong oppositely directed tournaments is proposed as a discrete model of sexually transmitted viruses. In this paper, these studies continue; that is, the dynamics of the composition of Lotka-Volterra operators operating in a three-dimensional simplex corresponding to partially oriented graphs is investigated. Here, for the first time, according to the works [6]-[8], the correspondence of partially oriented graphs for the operators under consideration is shown. In [9], compositions of operators of this type were also studied using the one-dimensional dynamics apparatus of A.N. Sharkovsky. In this paper, fixed points are found for the compositional operators considered and their characters are investigated. Composite operators of this type are relevant for research because they act as discrete models to study the dynamics of the spread of computer viruses in two operating systems.

Received : *02–march–2025,* ***Accepted :*** *02–april–2025*
*** Corresponding author***

2. Preliminary information.

Let be us quadratic Lotka—Volterra operator

$$V_1 : x'_k = x_k \left(1 + \sum_{i=1}^{m} a_{ki} x_i\right), \ and \ \ V_2 : x'_k = x_k \left(1 + \sum_{i=1}^{m} b_{ki} x_i\right), \ k = \overline{1, m} \tag{2.1}$$

on the simplex

$$S^3 = \left\{ x = (x_1, x_2, x_3, x_4) : x_i \geq 0, \sum_{i=1}^{4} x_i = 1 \right\} \subset R^4$$

Definition 2.1. [1]. A complex operator satisfying the equalities

$$(V_1 \circ V_2)(x) = V_1(V_2(x)) \ or \ (V_2 \circ V_1)(x) = V_2(V_1(x))$$

is called a composition of operators V_1 and V_2.

Confirmation. According to [1], the composition of operators and can be expressed in the form

$$W = V_1 \circ V_2 : x'_k = x_k \left(1 + f_k(x_1, x_2, ..., x_{k-1}, x_{k+1}, ..., x_m)\right), \ k = \overline{1, m} \tag{2.2}$$

Before proceeding to the main results, we recall the information from [2]-[5] related to fixed points and their characters.

Definition 2.2. [2] A point x satisfying the equality $W(x) = x$ is called a fixed point of the operator W and is denoted as $Fix(W) = \left\{ x \in S^{m-1} : \ W(x) = x \right\}$.

Definition 2.3. [3], [4]. Suppose x_0 is a fixed point for W. Then x_0 is an attracting fixed point if $|W(x_0)| < 1$.

Definition 2.4. [3], [4]. The point x_0 is a repelling fixed point if $|W(x_0)| > 1$.

Definition 2.5. [5]. Matrix of partial derivatives of operator Lotka – Volterra type is called Jacobi matrix and denoted as

$$J(W) = \begin{pmatrix} \frac{\partial x'_1}{\partial x_1} & \frac{\partial x'_1}{\partial x_2} & \cdots & \frac{\partial x'_1}{\partial x_n} \\ \frac{\partial x'_2}{\partial x_1} & \frac{\partial x'_2}{\partial x_2} & \cdots & \frac{\partial x'_2}{\partial x_n} \\ ..... & ..... & ..... & ..... \\ \frac{\partial x'_n}{\partial x_1} & \frac{\partial x'_n}{\partial x_n} & \cdots & \frac{\partial x'_n}{\partial x_n} \end{pmatrix} \tag{2.3}$$

Undirected, partially directed graphs and tournaments in S^3 are shown in Figure 1. ([6] -[8]).

3. Main results.

Let us assume that the Lotka–Volterra quadratic operators corresponding to partially oriented graphs (see Figure 1) and the compositions of their compositions

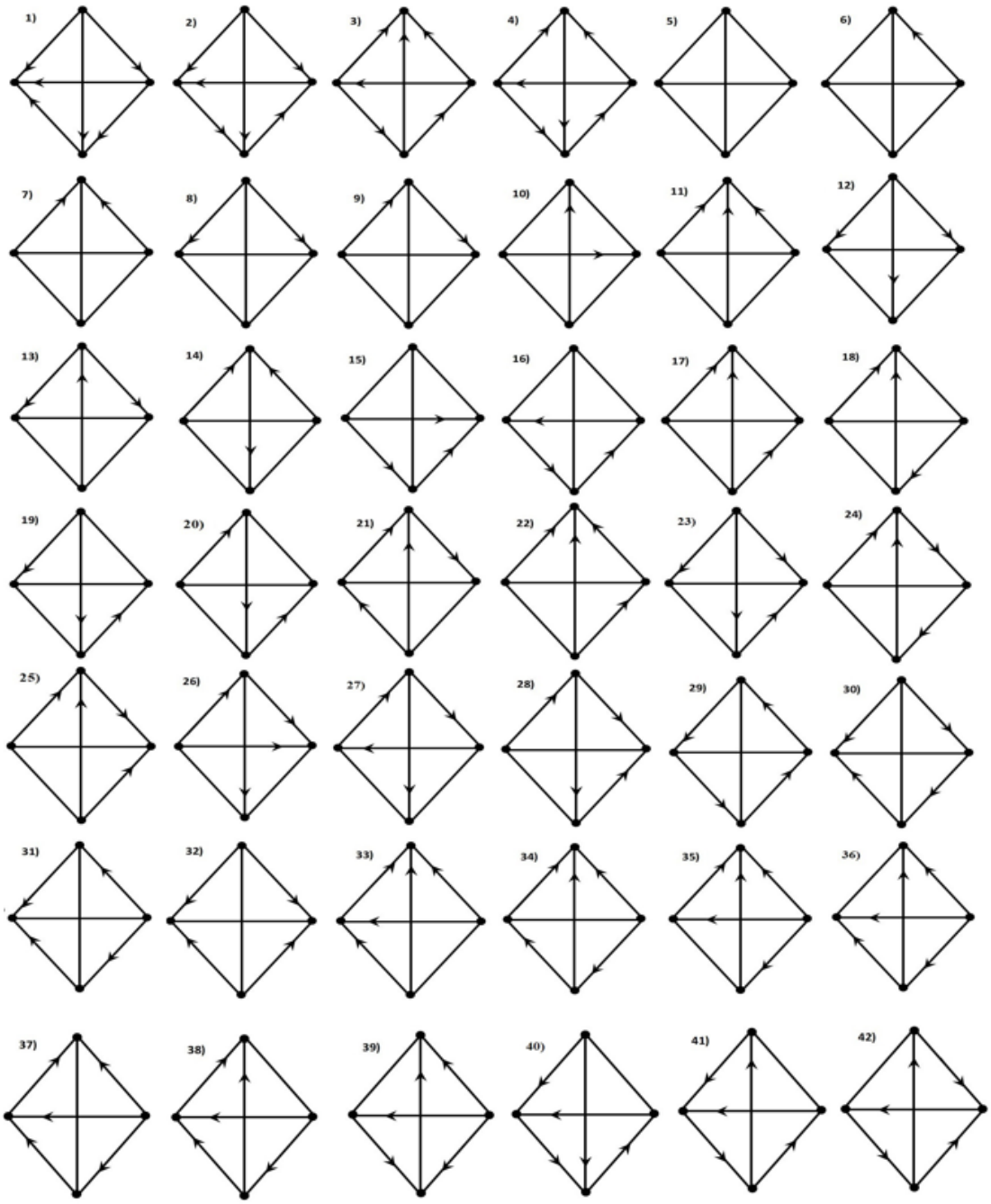

Figure 1. Tournaments defined in three-dimensional simplex.

$$V_1 : \begin{cases} x'_1 = x_1\,(1 + a_{12}x_2 + a_{13}x_3 + a_{14}x_4)\,; \\ x'_2 = x_2\,(1 - a_{12}x_1)\,; \\ x'_3 = x_3\,(1 - a_{13}x_1)\,; \\ x'_4 = x_4\,(1 - a_{14}x_1)\,; \end{cases} \qquad V_2 : \begin{cases} x'_1 = x_1\,(1 - b_{12}x_2 - b_{13}x_3 - b_{14}x_4)\,; \\ x'_2 = x_2\,(1 + b_{12}x_1)\,; \\ x'_3 = x_3\,(1 + b_{13}x_1)\,; \\ x'_4 = x_4\,(1 + b_{14}x_1)\,. \end{cases} \tag{3.1}$$

Partially oriented graphs corresponding to these operators are imaged in Figure 2.

The composition of these operators is

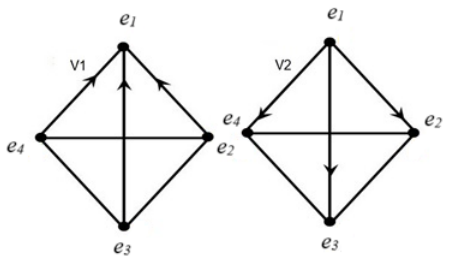

Figure 2. Partially oriented graphs corresponding to operators V_1 and V_2

$$V_1 \circ V_2 : \begin{cases} x'_1 = x_1 (1 - b_{12}x_2 - b_{13}x_3 - b_{14}x_4)(1 + a_{12}x_2 (1 + b_{12}x_1) + \\ +a_{13}x_3 (1 + b_{13}x_1) + a_{14}x_4 (1 + b_{14}x_1)); \\ x'_2 = x_2 (1 + b_{12}x_1)(1 - a_{12}x_1 (1 - b_{12}x_2 - b_{13}x_3 - b_{14}x_4)); \\ x'_3 = x_3 (1 + b_{13}x_1)(1 - a_{13}x_1 (1 - b_{12}x_2 - b_{13}x_3 - b_{14}x_4)); \\ x'_4 = x_4 (1 + b_{14}x_1)(1 - a_{14}x_1 (1 - b_{12}x_2 - b_{13}x_3 - b_{14}x_4)); \end{cases} \tag{3.2}$$

Lemma 3.1. *The following confirmations are satisfying for operator $V_1 \circ V_2$:*
i. Vertices of simplex I, P, H, and D i, points on the edges Γ_{IP}, Γ_{IH}, Γ_{ID} and side Γ_{PHD} are fixed points of composition operator;
ii. All vertices of operator $V_1 \circ V_2$ are attractor;
iii. Fixed points on the edges operator $V_1 \circ V_2$ are saddle point.

Proof. According to the definition of a fixed point, the solutions of the equation $Vx = x$ define the fixed points of the operator.

$$\begin{cases} x_1 = x_1 (1 - b_{12}x_2 - b_{13}x_3 - b_{14}x_4)(1 + a_{12}x_2 (1 + b_{12}x_1) + \\ +a_{13}x_3 (1 + b_{13}x_1) + a_{14}x_4 (1 + b_{14}x_1)); \\ x_2 = x_2 (1 + b_{12}x_1)(1 - a_{12}x_1 (1 - b_{12}x_2 - b_{13}x_3 - b_{14}x_4)); \\ x_3 = x_3 (1 + b_{13}x_1)(1 - a_{13}x_1 (1 - b_{12}x_2 - b_{13}x_3 - b_{14}x_4)); \\ x_4 = x_4 (1 + b_{14}x_1)(1 - a_{14}x_1 (1 - b_{12}x_2 - b_{13}x_3 - b_{14}x_4)); \\ x_1 + x_2 + x_3 + x_4 = 1. \end{cases} \tag{3.3}$$

The solution of the system of equations define the fixed points of the given operator. The solutions of equation (2.3) are vertices of simplex $I\,(1;0;0;0)$, $P\,(0;1;0;0)$, $H\,(0;0;1;0)$, $D\,(0;0;0;1)$ and points

$$O_1\left(\frac{(b_{12}-2)\sqrt{a_{12}} + \sqrt{a_{12}b_{12}^2 + 4b_{12}}}{2b_{12}\sqrt{a_{12}}}; \frac{(b_{12}+2)\sqrt{a_{12}} - \sqrt{a_{12}b_{12}^2 + 4b_{12}}}{2b_{12}\sqrt{a_{12}}}; 0; 0\right),$$

$$O_2\left(\frac{(b_{13}-2)\sqrt{a_{13}} + \sqrt{a_{13}b_{13}^2 + 4b_{13}}}{2b_{13}\sqrt{a_{13}}}; 0; \frac{(b_{13}+2)\sqrt{a_{13}} - \sqrt{a_{13}b_{13}^2 + 4b_{13}}}{2b_{13}\sqrt{a_{13}}}; 0\right),$$

$$O_3\left(\frac{(b_{14}-2)\sqrt{a_{14}} + \sqrt{a_{14}b_{14}^2 + 4b_{14}}}{2b_{14}\sqrt{a_{14}}}; 0; 0; \frac{(b_{14}+2)\sqrt{a_{14}} - \sqrt{a_{14}b_{14}^2 + 4b_{14}}}{2b_{14}\sqrt{a_{14}}}\right),$$

$$O_4\,(0; x_2; x_3; 1 - x_2 - x_3),$$

they represent the points belongs to edges Γ_{IP}, Γ_{IH}, Γ_{ID} and sides Γ_{PHD} of the simplex. The elements of the Jacobi matrix of this operator are:

$\frac{\partial x'_1}{\partial x_1} = (1 - b_{12}x_2 - b_{13}x_3 - b_{14}x_4)\,(1 + a_{12}x_2\,(1 + b_{12}x_1) + a_{13}x_3\,(1 + b_{13}x_1) + a_{14}x_4\,(1 + b_{14}x_1)) +$
$+x_1\,(1 - b_{12}x_2 - b_{13}x_3 - b_{14}x_4)\,(a_{12}b_{12}x_2 + a_{13}b_{13}x_3 + a_{14}b_{14}x_4)\,;$

$\frac{\partial x'_1}{\partial x_2} = -\,b_{12}x_1\,(1 + a_{12}x_2\,(1 + b_{12}x_1) + a_{13}x_3\,(1 + b_{13}x_1) + a_{14}x_4\,(1 + b_{14}x_1)) +$
$+a_{12}x_1\,(1 - b_{12}x_2 - b_{13}x_3 - b_{14}x_4)\,(1 + b_{12}x_1)\,;$

$\frac{\partial x'_2}{\partial x_1} = b_{12}x_2\,(1 - a_{12}x_1\,(1 - b_{12}x_2 - b_{13}x_3 - b_{14}x_4)) - a_{12}x_2\,(1 + b_{12}x_1)\,(1 - b_{12}x_2 - b_{13}x_3 - b_{14}x_4)\,;$

$\frac{\partial x'_2}{\partial x_2} = (1 + b_{12}x_1)\,(1 - a_{12}x_1\,(1 - b_{12}x_2 - b_{13}x_3 - b_{14}x_4)) + a_{12}b_{12}x_1x_2\,(1 + b_{12}x_1)\,;$

$\frac{\partial x'_2}{\partial x_3} = a_{12}b_{13}x_1x_2\,(1 + b_{12}x_1)\,;$

$\frac{\partial x'_2}{\partial x_4} = a_{12}b_{14}x_1x_2\,(1 + b_{12}x_1)\,;$

$\frac{\partial x'_3}{\partial x_1} = b_{13}x_3\,(1 - a_{13}x_1\,(1 - b_{12}x_2 - b_{13}x_3 - b_{14}x_4)) - a_{13}x_3\,(1 + b_{13}x_1)\,(1 - b_{12}x_2 - b_{13}x_3 - b_{14}x_4)\,;$

$\frac{\partial x'_3}{\partial x_2} = a_{13}b_{12}x_1x_3\,(1 + b_{13}x_1)\,;$

$\frac{\partial x'_3}{\partial x_3} = (1 + b_{13}x_1)\,(1 - a_{13}x_1\,(1 - b_{12}x_2 - b_{13}x_3 - b_{14}x_4)) + a_{13}b_{13}x_1x_3\,(1 + b_{13}x_1)\,;$

$\frac{\partial x'_3}{\partial x_4} = a_{13}b_{14}x_1x_3\,(1 + b_{13}x_1)\,;$

$\frac{\partial x'_4}{\partial x_1} = b_{14}x_4\,(1 - a_{14}x_1\,(1 - b_{12}x_2 - b_{13}x_3 - b_{14}x_4)) - a_{14}x_4\,(1 + b_{14}x_1)\,(1 - b_{12}x_2 - b_{13}x_3 - b_{14}x_4)\,;$

$\frac{\partial x'_4}{\partial x_2} = a_{14}b_{12}x_1x_4\,(1 + b_{14}x_1)\,;$

$\frac{\partial x'_4}{\partial x_3} = a_{14}b_{13}x_1x_4\,(1 + b_{14}x_1)\,;$

$\frac{\partial x'_4}{\partial x_4} = (1 + b_{14}x_1)\,(1 - a_{14}x_1\,(1 - b_{12}x_2 - b_{13}x_3 - b_{14}x_4)) + a_{14}b_{14}x_1x_4\,(1 + b_{14}x_1)\,.$

The elements of Jacobi matrix for simplex vertices are listed in Table 1.

Table 1.

	e_1	e_2	e_3	e_4
$\frac{\partial x'_1}{\partial x_1}$	1	$(1 - b_{12})\,(1 + a_{12})$	$(1 - b_{13})\,(1 + a_{13})$	$(1 - b_{14})\,(1 + a_{14})$
$\frac{\partial x'_1}{\partial x_2}$	$-b_{12} + a_{12}\,(1 + b_{12})$	0	0	0
$\frac{\partial x'_1}{\partial x_3}$	$-b_{13} + a_{13}\,(1 + b_{13})$	0	0	0
$\frac{\partial x'_1}{\partial x_4}$	$-b_{14} + a_{14}\,(1 + b_{14})$	0	0	0
$\frac{\partial x'_2}{\partial x_1}$	0	$b_{12} - a_{12}\,(1 - b_{12})$	0	0
$\frac{\partial x'_2}{\partial x_2}$	$(1 + b_{12})\,(1 - a_{12})$	1	1	1
$\frac{\partial x'_2}{\partial x_3}$	0	0	0	0
$\frac{\partial x'_2}{\partial x_4}$	0	0	0	0
$\frac{\partial x'_3}{\partial x_1}$	0	0	$b_{13} - a_{13}\,(1 - b_{13})$	0
$\frac{\partial x'_3}{\partial x_2}$	0	0	0	0
$\frac{\partial x'_3}{\partial x_3}$	$(1 + b_{13})\,(1 - a_{13})$	1	1	1
$\frac{\partial x'_3}{\partial x_4}$	0	0	0	0
$\frac{\partial x'_4}{\partial x_1}$	0	0	0	$b_{14} - a_{14}\,(1 - b_{14})$
$\frac{\partial x'_4}{\partial x_2}$	0	0	0	0
$\frac{\partial x'_4}{\partial x_3}$	0	0	0	0
$\frac{\partial x'_4}{\partial x_4}$	$(1 + b_{14})\,(1 - a_{14})$	1	1	1

Table 2 below lists the eigenvalues of fixed points I, P, H and D of the composition operator $V_1 \circ V_2$.

Table 2.

	e_1	e_2	e_3	e_4
λ_1	1	1	1	1
λ_2	$1-a_{12}b_{12}-a_{12}+b_{12}$	1	1	1
λ_3	$1-a_{13}b_{13}-a_{13}+b_{13}$	1	1	1
λ_4	$1-a_{14}b_{14}-a_{14}+b_{14}$	$1-a_{12}b_{12}+a_{12}-b_{12}$	$1-a_{13}b_{13}+a_{13}-b_{13}$	$1-a_{14}b_{14}+a_{14}-b_{14}$

According to Table 2, the absolute value of eigenvalues of fixed points I, P, H and D of the composition operator $V_1 \circ V_2$ is $|\lambda_i| < 1$, $i = \overline{1,4}$. Then, I, P, H and D points are attractor. The eigenvalues of point O_1 are:

$\lambda_1 = 1$;

$\lambda_2 = 1 - \frac{1}{4b_{13}\sqrt{a_{13}}}\left(b_{13}\sqrt{a_{13}} - \sqrt{b_{13}\left(a_{13}b_{13}+4\right)}\right)\left(-2b_{13}+a_{13}b_{13}+3\sqrt{a_{13}b_{13}\left(a_{13}b_{13}+4\right)}-2a_{13}\right)$

$\lambda_3 = 1 - \frac{1}{4b_{14}^2\sqrt{a_{14}^3}}\left((b_{14}-2)\sqrt{a_{14}} + \sqrt{b_{14}\left(a_{14}b_{14}+4\right)}\right)\cdot$

$\cdot\left(\sqrt{b_{14}\left(a_{14}b_{14}+4\right)}\sqrt{a_{14}}\left(a_{14}b_{12}-a_{12}b_{14}+a_{12}b_{14}\right)+a_{14}^2b_{12}b_{14}+a_{12}a_{14}b_{14}^2-a_{12}a_{14}b_{12}b_{14}-2a_{12}b_{12}b_{14}\right)$;

$\lambda_4 = 2 + \frac{1}{4b_{14}^2\sqrt{a_{14}^3}}\left((b_{14}-2)\sqrt{a_{14}} + \sqrt{b_{14}\left(a_{14}b_{14}+4\right)}\right)$.

The eigenvalues of point O_2:

$\lambda_1 = 1$;

$\lambda_2 = 1 - \frac{1}{4b_{13}\sqrt{a_{13}}}\left(b_{13}\sqrt{a_{13}} - \sqrt{b_{13}\left(a_{13}b_{13}+4\right)}\right)\left(-2b_{13}+a_{13}b_{13}+3\sqrt{a_{13}b_{13}\left(a_{13}b_{13}+4\right)}-2a_{13}\right)$;

$\lambda_3 = 1 - \frac{1}{4b_{13}^2\sqrt{a_{13}^3}}\left((b_{13}-2)\sqrt{a_{13}} + \sqrt{b_{13}\left(a_{13}b_{13}+4\right)}\right)\cdot$

$\cdot\left(\sqrt{b_{13}\left(a_{13}b_{13}+4\right)}\sqrt{a_{13}}\left(a_{13}b_{12}-a_{12}b_{13}+a_{12}b_{12}\right)+a_{13}^2b_{12}b_{13}+a_{12}a_{13}b_{13}^2-a_{12}a_{13}b_{12}b_{13}-2a_{12}b_{12}b_{13}\right)$;

$\lambda_4 = 2 + \frac{\left(b_{13}\sqrt{a_{13}}-2\sqrt{a_{13}}+\sqrt{b_{13}(a_{13}b_{13}+4)}\right)\left(a_{13}b_{13}-2b_{13}+\sqrt{a_{13}b_{13}(a_{13}b_{13}+4)}\right)}{4\sqrt{a_{13}}b_{13}}$;

The eigenvalues of point O_3:

$\lambda_1 = 1$;

$\lambda_2 = 1 - \frac{1}{4b_{14}\sqrt{a_{14}}}\left(b_{14}\sqrt{a_{14}} - \sqrt{b_{14}\left(a_{14}b_{14}+4\right)}\right)\left(-2b_{14}+a_{14}b_{14}+3\sqrt{a_{14}b_{14}\left(a_{14}b_{14}+4\right)}-2a_{14}\right)$;

$\lambda_3 = 1 - \frac{1}{4b_{14}^2\sqrt{a_{14}^3}}\left((b_{14}-2)\sqrt{a_{14}} + \sqrt{b_{14}\left(a_{14}b_{14}+4\right)}\right)\cdot$

$\cdot\left(\sqrt{b_{14}\left(a_{14}b_{14}+4\right)}\sqrt{a_{14}}\left(a_{14}b_{12}-a_{12}b_{14}+a_{12}b_{14}\right)+a_{14}^2b_{12}b_{14}+a_{12}a_{14}b_{14}^2-a_{12}a_{14}b_{12}b_{14}-2a_{12}b_{12}b_{14}\right)$;

$\lambda_4 = 2 + \frac{1}{4b_{14}^2\sqrt{a_{14}^3}}\left((b_{14}-2)\sqrt{a_{14}} + \sqrt{b_{14}\left(a_{14}b_{14}+4\right)}\right)\cdot$

$\cdot\left(\sqrt{b_{14}\left(a_{14}b_{14}+4\right)}\sqrt{a_{14}}\left(a_{14}b_{12}-a_{12}b_{14}+a_{12}b_{14}\right)+a_{14}^2b_{12}b_{14}+a_{12}a_{14}b_{14}^2-a_{12}a_{14}b_{12}b_{14}-2a_{12}b_{12}b_{14}\right)$.

Lemma is proved.

Since the proof of the results derived from this lemma can be applied to the dynamics of compositions of Lotka-Volterra type quadratic operators corresponding to partially oriented graphs and fully oriented tournaments given in Fig. 1, we present the rest of the lemmas without proof. Let us first consider the composition of Lotka–Volterra type quadratic operators corresponding to fully oriented and unoriented graphs. Suppose the following operators are given:

I)

$$1): \begin{cases} x'_1 = x_1\left(1-a_{12}x_2-a_{13}x_3-a_{14}x_4\right); \\ x'_2 = x_2\left(1+a_{12}x_1-a_{23}x_3-a_{24}x_4\right); \\ x'_3 = x_3\left(1+a_{13}x_1+a_{23}x_2-a_{34}x_4\right); \\ x'_4 = x_4\left(1+a_{14}x_1+a_{24}x_2+a_{34}x_3\right); \end{cases} \qquad 5): \begin{cases} x'_1 = x_1; \\ x'_2 = x_2; \\ x'_3 = x_3; \\ x'_4 = x_4. \end{cases} \tag{3.4}$$

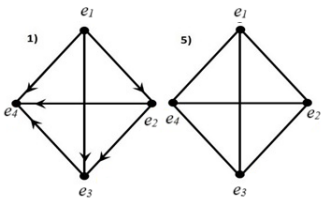

Figure 3. Complete oriented tournament and unoriented graph.

The form of Composition of these operators is

$$1) \circ 5) : \begin{cases} x'_1 = x_1 (1 - a_{12}x_2 - a_{13}x_3 - a_{14}x_4) ; \\ x'_2 = x_2 (1 + a_{12}x_1 - a_{23}x_3 - a_{24}x_4) ; \\ x'_3 = x_3 (1 + a_{13}x_1 + a_{23}x_2 - a_{34}x_4) ; \\ x'_4 = x_4 (1 + a_{14}x_1 + a_{24}x_2 + a_{34}x_3) ; \end{cases} \tag{3.5}$$

Lemma 3.2. *The subsequent confirmations are pleasing to the operator* $1) \circ 5)$*:*
i. There are no fixed points other than simplex vertices I, P, H, and D;
ii.Vertice I of operator $1) \circ 5)$ *is repeller, Vertices P and H are saddle point and vertice D is attractor;*

II)

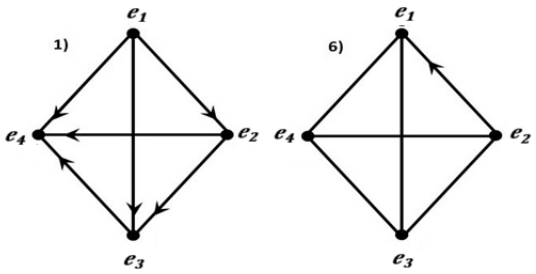

Figure 4. Complete oriented tournament and graph which one edge is oriented.

$$1) : \begin{cases} x'_1 = x_1 (1 - a_{12}x_2 - a_{13}x_3 - a_{14}x_4) ; \\ x'_2 = x_2 (1 + a_{12}x_1 - a_{23}x_3 - a_{24}x_4) ; \\ x'_3 = x_3 (1 + a_{13}x_1 + a_{23}x_2 - a_{34}x_4) ; \\ x'_4 = x_4 (1 + a_{14}x_1 + a_{24}x_2 + a_{34}x_3) ; \end{cases} \quad 6) : \begin{cases} x'_1 = x_1 (1 + b_{12}x_2) ; \\ x'_2 = x_2 (1 - b_{12}x_1) ; \\ x'_3 = x_3; \\ x'_4 = x_4. \end{cases} \tag{3.6}$$

The form of Composition of these operators is

$$1) \circ 6) : \begin{cases} x'_1 = x_1 (1 + b_{12}x_2) (1 - a_{12}x_2 (1 - b_{12}x_1) - a_{13}x_3 - a_{14}x_4) ; \\ x'_2 = x_2 (1 - b_{12}x_1) (1 + a_{12}x_1 (1 + b_{12}x_2) - a_{23}x_3 - a_{24}x_4) ; \\ x'_3 = x_3 (1 + a_{13}x_1 (1 + b_{12}x_2) + a_{23}x_2 (1 - b_{12}x_1) - a_{34}x_4) ; \\ x'_4 = x_4 (1 + a_{14}x_1 (1 + b_{12}x_2) + a_{24}x_2 (1 - b_{12}x_1) + a_{34}x_3) ; \end{cases} \tag{3.7}$$

Lemma 3.3. *The following confirmations are satisfying for operator* $1) \circ 6)$*:*
i.There is fixed point other than vertices simplex I, P, H va D;
ii. Vertices I, P and H of operator $1) \circ 6)$ *are attractor;*
iii. Fixed point of operator on the edge Γ_{IP} *is saddle point.*

III)

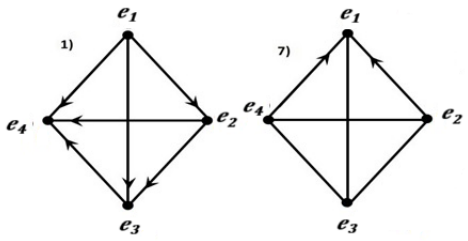

Figure 5. Complete oriented tournament and graph which two edge is oriented.

$$1): \begin{cases} x'_1 = x_1\,(1 - a_{12}x_2 - a_{13}x_3 - a_{14}x_4)\,; \\ x'_2 = x_2\,(1 + a_{12}x_1 - a_{23}x_3 - a_{24}x_4)\,; \\ x'_3 = x_3\,(1 + a_{13}x_1 + a_{23}x_2 - a_{34}x_4)\,; \\ x'_4 = x_4\,(1 + a_{14}x_1 + a_{24}x_2 + a_{34}x_3)\,; \end{cases} \quad 7): \begin{cases} x'_1 = x_1\,(1 + b_{12}x_2 + b_{14}x_4)\,; \\ x'_2 = x_2\,(1 - b_{12}x_1)\,; \\ x'_3 = x_3; \\ x'_4 = x_4\,(1 - b_{14}x_1)\,. \end{cases} \tag{3.8}$$

The form of Composition of these operators is

$$1) \circ 7): \begin{cases} x'_1 = x_1\,(1 + b_{12}x_2 + b_{14}x_4)\,(1 - a_{12}x_2\,(1 - b_{12}x_1) - a_{13}x_3 - a_{14}x_4\,(1 - b_{14}x_1))\,; \\ x'_2 = x_2\,(1 - b_{12}x_1)\,(1 + a_{12}x_1\,(1 + b_{12}x_2 + b_{14}x_4) - a_{23}x_3 - a_{24}x_4\,(1 - b_{14}x_1))\,; \\ x'_3 = x_3\,(1 + a_{13}x_1\,(1 + b_{12}x_2 + b_{14}x_4) + a_{23}x_2\,(1 - b_{12}x_1) - a_{34}x_4\,(1 - b_{14}x_1))\,; \\ x'_4 = x_4\,(1 - b_{14}x_1)\,(1 + a_{14}x_1\,(1 + b_{12}x_2 + b_{14}x_4) + a_{24}x_2\,(1 - b_{12}x_1) + a_{34}x_3)\,; \end{cases} \tag{3.9}$$

Lemma 3.4. *The subsequent confirmations are pleasing to the operator* $1) \circ 7)$*:*
i. There are fixed point other than vertices simplex I, P, H and D on the edges Γ_{IP} *and* Γ_{ID}*;*
ii. Vertices I, P and H of operator $1) \circ 7)$ *are saddle point and vertex D is attractor;*
iii. Fixed points of the operator $1) \circ 7)$ *on the edges* Γ_{IP} *and* Γ_{ID} *are saddle points.*

4. Conclusion

In the paper, according to [6]-[8], oriented and partially oriented graphs are given for $m = 4$ (they turned out to be 42, see Figure 1). All graphs are described by discrete Lotka-Volterra dynamical systems operating in a three-dimensional simplex. In [9], [10], the dynamics of the Lotka-Volterra operators are studied, and the works [1], [2], [4] are devoted to the study of the dynamics of the trajectories of the inner points of the composition of Lotka-Volterra operators operating in a two-dimensional simplex. In contrast to these works, this article examines four compositional Lotka- Volterra operators corresponding to some of the graphs in Figure 1 (see Figures 2-5), for $m = 4$. Fixed points are found for all considered compositional operators and their characters are investigated (Lemma 2.1-2.4).

Acknowledgements

We express our gratitude to R. N. Ganihodzhayev, professor of the National University of Uzbekistan named after Mirzo Ulugbek, doctor of physics and mathematics, who helped us closely with his recommendations in the preparation of this article.

Author's contributions

All authors contributed equally to the writing of this paper. All authors read and approved the final manuscript.

References

[1] D.B.Eshmamatova, F.A.Yusupov: *Dynamics of compositions of some Lotka–Volterra mappings operating in a two-dimensional simplex.* Turkish Journal of Mathematics, **48** (3), 2024, 391-406.

[2] D.B.Eshmamatova.,F.A.Yusupov: *Classification of fixed point mappings of the composition of the Lotka – Volterra operators.* Uzbek Mathematical Journal, **3**, 2024, pp 37-52.

[3] R.L.Devaney. Complex Exponential Dynamics. Elsevier, Vol. 3, Issue 2, 125-224 (2010).

[4] D.B.Eshmamatova: *Compositions of Lotka-Volterra Mappings as a Model for the Study of Viral Diseases*. AIP Conference Proceedings, 2024, 3085(1), 020008.

[5] D. B. Eshmamatova, Sh.J.Seytov, and N. B. Narziev: *Basins of Fixed Points for Composition of the Lotka–Volterra Mappings and Their Classification*. Lobachevskii Journal of Mathematics,2023, Vol. 44, No. 2, pp. 558–568.

[6] G. Chartrand, H. Jordon, V. Vatter, P. Zhang, *Graphs and digraphs* (CRC Press, New York, 2024). 364 p.

[7] J. W. Moon, *Topics on tournaments* (New York, Holt Renehart and Winston, 2013). 132 p.

[8] K. Koh, F. Dong, E. G. Tay, *Introduction to graph theory: with solutions to selected problems* (Singapore: World Scientific Publishing Company, 2023). 308 p.

[9] D. B. Eshmamatova, Sh. J. Seytov and N. B. Narziev *Basins of Fixed Points for Composition of the Lotka–Volterra Mappings and Their Classification*. Lobachevskii Journal of Mathematics, 2023, Vol. 44, No. 2, pp. 558–569.

[10] M.A.Tadzhieva, D.B.Eshmamatova, R.N.Ganikhodzhaev: *Volterra-Type Quadratic Stochastic*. Journal of Mathematical Sciences (United States), 2024, 278(3), pp. 546–556.

[11] R.N.Ganikhodzhaev, F.M.Mukhamedov, U.A.Rozikov: *Quadratic stochastic operators: Results and open problems*. Infin. Dimens. Anal.Quantum.Probab. Relat, 2011, 14(2), pp. 279-335.

[12] P.Szor: *The Art of Computer Virus*. (Research and Defense. Addison-Wesley, Reading 2005)

[13] N.Bacaer: *A Short History of Mathematical Population Dynamics* (Springer Science and Business Media, London 2011)

[14] R.N.Ganikhodzhaev: *Quadratic stochastic operators, Lyapunov function and tournaments*. Acad. Sci. Sb. Math, 1993. 76(2), p. 489-506.

[15] D.B.Eshmamatova: *Som Lotka-Voltrra mappings with a dgnrat skw-symmtric matrix, and thir rlation to pidemiological situations*. Uzbek Mathematical Journal. 2023, 67(2), pp. 39-48.

Affiliations

F.Yusupov
Address: Tashkent State Transport University, Tashkent. Uzbekistan.
e-mail: farrukhyusupovchambil@mail.ru
ORCID ID: 0000-0003-1909-6420

D.Ahmedova
Address: Andijan State University, Andijan. Uzbekistan.
e-mail: dilafruz.ahmedova.0695@gmail.com
ORCID ID:0009-0006-2409-5229

U.Shamsiyeva
Address: Tashkent State Transport University,Tashkent. Uzbekistan.
e-mail: nuriyashamsiyeva304@gmail.com
ORCID ID:0000 0001 5070 0919